MACHINE TOOL DESIGN VIA LIGHTWEIGHTING FOR REDUCED ENERGY CONSUMPTION

by

Matthew J. Triebe

A Dissertation

Submitted to the Faculty of Purdue University

In Partial Fulfillment of the Requirements for the degree of

Doctor of Philosophy

Environmental and Ecological Engineering

West Lafayette, Indiana

December 2021

THE PURDUE UNIVERSITY GRADUATE SCHOOL
STATEMENT OF COMMITTEE APPROVAL

Dr. John W. Sutherland, Co-Chair
Environmental and Ecological Engineering

Dr. Fu Zhao, Co-Chair
School of Mechanical Engineering
Environmental and Ecological Engineering

Dr. John A. Howarter
School of Materials Engineering
Environmental and Ecological Engineering

Dr. Hua Cai
School of Industrial Engineering
Environmental and Ecological Engineering

Approved by:
Dr. John A. Howarter

To my parents, Fred and Donna Triebe,
and to my wife, Beth Pletsch

ACKNOWLEDGMENTS

This work is supported in part by the U.S. National Science Foundation (Grant No. 1512217), and by the Covid Relief Fellowship provided by Environmental and Ecological Engineering at Purdue University.

I would first like to thank my advisors Dr. John W. Sutherland and Dr. Fu Zhao for their continued support, guidance, and encouragement over the past years. They have taught me much over the years and been a great source of wisdom and drive for excellence. I would also like to thank my committee: Dr. John Howarter and Dr. Hua Cai for their support and input. Their feedback has been invaluable to the shaping of my research.

I would also like to thank my colleagues and friends at EEE that have made my time there enjoyable. Thank you to Justin Richter, Ehsan Vahidi, Enze Jin, and Hongyue Jin for welcoming me into the office and providing insight. Thank you to Yue Wang, Wo Jae Lee, and Nehika Mathur for working through the PhD program with me together and the encouragement to keep going. I would specifically like to thank Yue Wang for reading all my papers, over and over, and providing invaluable feedback. Thank you also Gamini Mendes, Aihua Huang, and Zhongtian Li for your insight and feedback on my papers research. Thank you to the rest of the LSM office, Sidi Deng, Byung Gun Joung, Jesús Pérez-Cardona, Thomas Maani, Haiyue Wu, Xiaoyu Zhou, Jerome Perino, Daniel Luke, and Neha Shakelly for your encouragement throughout my time in the program.

I would like to thank my colleagues in China that assisted me throughout my PhD and for welcoming me on my travels over there. Thank you to Junkai Wang for meeting me at the airport in Shanghai and making sure I got on the train to Wuhan. Thank you also for your friendship and encouragement while at Purdue. Thank you to Dr. Choayong Zhang at Huazhong University of Science & Technology for welcoming me and providing hospitality when I visited. Thank you to Dr. Haihong Huang for welcoming me to Hefei University of Technology and to Dr. Lei Li for making sure I had everything I needed on my visit.

I would also like to thank those outside of Purdue that have helped me during my studies. Thank you to Nick Szczypiorski for answering all my questions on machine tools and providing so much information. Thank you to Adriana M. Muñoz Soto for all your help with gathering data for one of my papers.

I would like to thank my parents, Fred and Donna Triebe, for their continued support and love. Thank you for everything you have done for me. There are so many decisions and sacrifices you made that I will never know of but am deeply grateful for. Thank you as well to my father-in-law and mother-in-law, Roy and Sue Pletsch, for your support and welcoming me into your family.

Finally, I would like to thank my wife, Beth. Thank you for all your love and encouragement over the years. Thank you for your patience through this long process of graduate school. Thank you for encouraging me to pursue the PhD and making sacrifices so that we can stay in Lafayette after you graduated. Thank you for reading my work and listening to my presentations and letting me bore you with all my talk on sandwich panels. Thank you for being my best friend.

TABLE OF CONTENTS

LIST OF TABLES

LIST OF FIGURES

ABSTRACT

Machine tools are an important piece of manufacturing equipment that are widely used throughout many industries. Machine tools shape and form raw materials into desired products through processes such as grinding, cutting, bending, and forming, and when they perform these operations, they consume large amounts of energy. Due to the significant energy consumption, machine tools have a large environmental footprint. Addressing the environmental footprint of machine tools through energy reduction is important to addressing manufacturing and industry's footprint. One strategy with great potential to reduce machine tool energy consumption is lightweighting. Lightweighting is a design strategy that reduces the mass of moving components with a goal of reducing energy consumption. This strategy is effective since a greater mass requires more energy to move. Lightweighting has had great success in the transportation sector where lightweight materials and lightweight design strategies have been implemented. There has been some work to explore the potential benefits of lightweighting machine tools, however an in-depth study relating mass to energy consumption in machine tools along with exploring other potential concerns, i.e., impact on dynamics and cost, is required.

To explore the lightweighting of machine tools, a lightweighting application along with models are proposed to investigate the connection between mass and energy in machine tools and potential concerns associated with lightweighting, i.e., decreased dynamic performance and increased machine tool cost. First, a method to reduce the mass of a vertical milling machine tool table is proposed. This method will include the implementation of a sandwich panel for the table while optimizing the structure of the table to maximize its strength and minimize its mass. Following, to link mass to energy consumption, an energy model is proposed to quantify the energy required to drive the table throughout the use of the machine, including cutting and non-cutting moves. In addition to modeling energy, this model will explore the role of motor sizing in the energy consumption of the drive system. To address dynamic concerns resulting from lightweighting, a dynamic model is proposed. This model will provide insight into the dynamic performance of the table and explore the impact of lightweighting on machine tool performance. Finally, a cost model of machine tools is proposed to study the impact of lightweighting on cost.

Machine tool cost drivers will be explored along with the role that design complexity has on purchase price.

This dissertation provided a proof of concept for a lightweighting application through the sandwich panel design of the slide table. The energy model built considering the lightweight table provided a link between the mass and energy consumption in the machine tool. It was shown that more than 30% of the drive system energy could be saved by lightweighting the table. A 30% savings is substantial, especially if applied to multiple systems throughout the machine tool. The static and dynamic models showed that designing lightweight components can be accomplished without sacrificing performance. Various design tools, e.g., finite element analysis, can be used to address static and dynamic concerns. The cost model showed how lightweighting will not increase the cost of the machine tool and therefore will not discourage machine builders from implementing lightweighting to reduce energy consumption.

The contributions of this research are summarized as follows:

1. A shape optimization method to design the sandwich panel table, accomplished through a genetic algorithm. This provides a lower-cost lightweighting application.
2. A mechanistic model linking mass to energy consumption. This provides insight into design considerations required to implement lightweighting
3. Static and dynamic models of the milling machine slide table. These provide understanding of how lightweighting affects the performance machine tools
4. A cost model of milling machines. This provides insight into how lightweighting affects the machine tool cost

1. INTRODUCTION

Manufacturing plays an important role worldwide through providing the goods needed by consumers and industries. With an increased demand and a growing population, manufacturing will continue to play a significant role in the world's economy through meeting demand, contributing to wealth generation and job creation, and improving quality of life. In 2017 close to 25% of the global labor force was supplied by industry [1] and 30% of the global Gross Domestic Product (GDP) was attributed to industry with manufacturing being the dominant contributor to industrial activities.

Along with manufacturing's significant role, it has a considerable environmental burden through its waste and its non-renewable energy and resource consumption [2]. In 2016 industry worldwide accounted for 29.4% of the global greenhouse gas emissions [3] with 24.2% being attributed to energy consumption by industry. In 2020 the industrial sector in the U.S. consumed 36% of the end-use energy [4] while much of the electricity in the U.S. is generated by fossil fuels [5].

An important type of equipment within manufacturing is machine tools. Machine tools provide crucial services and highly advanced technologies for manufacturing and industries. Machine tools manufacture components by forming and shaping material into desired parts and products through operations such as forming, bending, grinding, and cutting. They are currently utilized worldwide with their demand expected to increase. Machine tool sales have grown from $119.7 billion in 2008 to $144.6 billion in 2018 and are expected to grow to $174 billion in 2023 [6]. Machine tools can vary greatly in size from filling a room to fitting on a tabletop. They also vary greatly in complexity and technology. Over the years they have grown in complexity and have become more powerful, automated, and accurate.

Along with their widespread use, machine tools have their own significant environmental footprint. Machine tools have a lifecycle like any other product: resource extraction, material processing, manufacturing, component assembly, use, and end-of-life. Due to the use stage being the longest of all the stages in the lifecycle and the conspicuous electricity consumption during the use stage, which can account for up to 80% [6] of the energy consumed through the life of the machine tools, the use stage is the most significant in terms of environmental impact and carbon footprint [6,7]. Energy consumption of machine tools directly relates to their environmental

footprint due to electricity being mostly generated from fossil fuels, especially in the US where over 80% of electricity generated from fossil fuels [3,4].

There are various types of machine tools which includes mills, lathes, boring equipment, drilling machines, presses, and grinding machines. Two commonly used machine tools are the milling machine and the turning machine. With the milling machine the workpiece is clamped to a table and the cutting tool, attached to the spindle, spins to cut the material. This is different from the turning machine where the material is attached to the spindle and the tool does not spin. An example of a milling machine can be seen in Figure 1.1(a) and an example of a turning machine can be seen in Figure 1.1(b). In Figure 1.1(a), the table moves in the x and y-directions while the cutter moves in the z-direction. In Figure 1.1(b) the cutter moves in the x, y, and z-directions while the workpiece, attached to the spindle, rotates.

Reducing energy consumption of machine tools is very important to reducing manufacturing's environmental impact. However, reducing energy can be difficult due to that a machine tool's power demand and energy consumption can be complicated, especially as more technology has been included in these machines [7]. An example of a milling machine power curve can be seen in Figure 1.2(a) and an example of a turning machine power curve can be seen in Figure 1.2(b). As can be seen Figure 1.2(a) and (b), much of the energy consumption comes from supporting systems, not from machining [8]. These systems consist of components and processes that support the machine tool but may not directly relate to cutting. Some of these systems and components include the cooling system, the chip removal system, and the automatic tool changer. Due to the complexity of power demand, no one method by itself will fully address machine tool energy consumption.

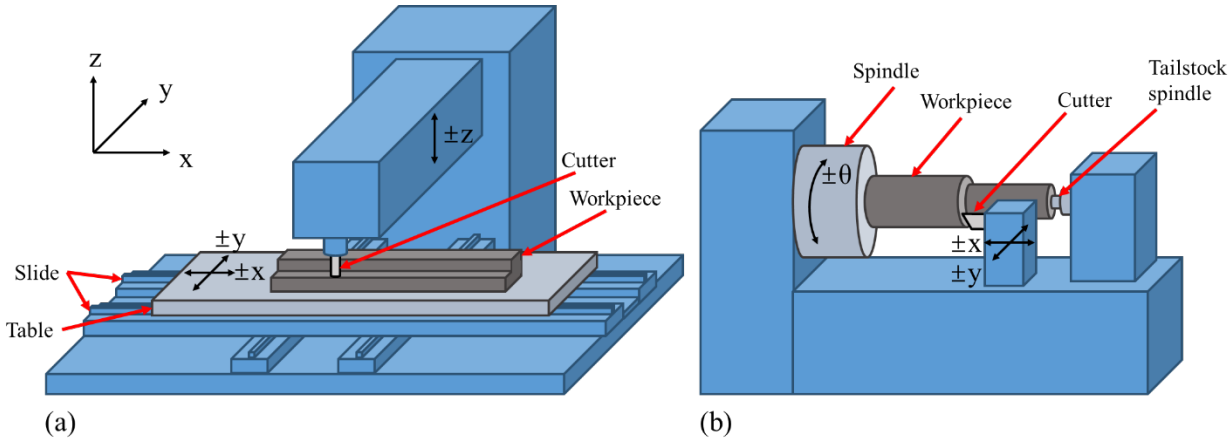

Figure 1.1. (a) An example of a milling machine, (b) an example of a turning machine

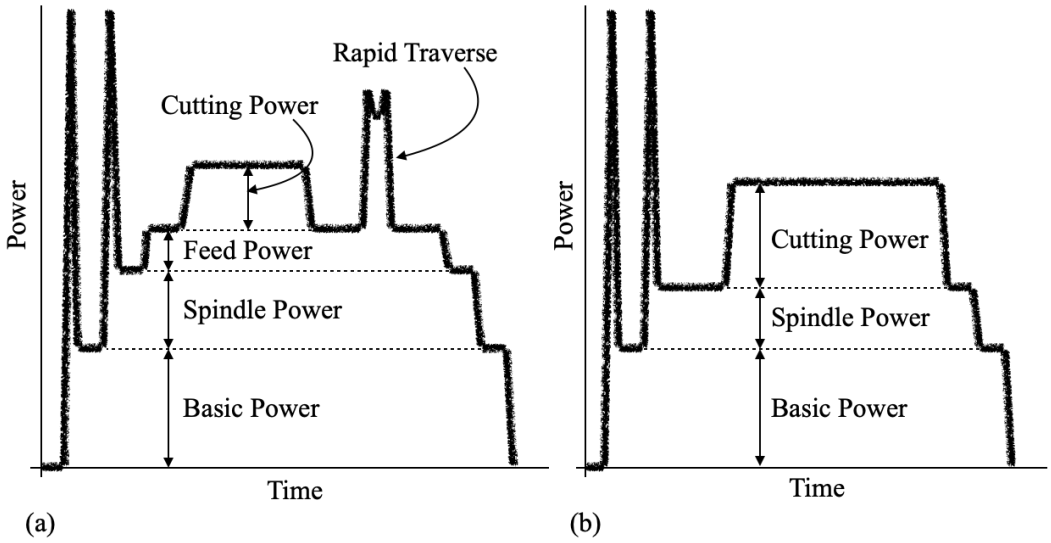

Figure 1.2 (a) Power profile of a milling machine (adapted from He et al. [9]), (b) power profile of a turning machine (adapted from Li et al. [10])

There have been a number of proposed strategies to reduce energy consumption. These include improvements to the use of the machines and improvements in the design of the machines. Use improvements include process design [11,12], process parameter selection [13,14], and scheduling of machines [15]. Design improvements include the use of energy efficient components [16], and design optimization [17]. A deeper dive of previous research regarding machine tool energy consumption can be found in Chapter 2.

A promising method for reducing energy consumption is lightweighting, i.e., reducing the mass of moving components. Energy reduction occurs due to a smaller mass requiring less energy to move. Lightweighting has had great success in the transportation sector with their widespread use of lightweight materials that includes composites and aluminum to reduce component weight and increase fuel efficiency [18]. Most lightweighting within the transportation sector adopts one of three approaches (some overlap between the three approaches): lightweighting accomplished through lighter materials, lightweighting accomplished through manufacturing, and lightweighting accomplished through product structure. While the third approach is specifically a design-oriented approach, the other two approaches will require design changes as well, e.g., differences in material properties requiring dimensional changes. Material lightweighting involves replacing a material with a lighter weight material, e.g., replacing steel with aluminum, or replacing a material with a stronger material while requiring less material, e.g., switching to high-strength steel. Lightweighting via manufacturing involves using manufacturing methods that reduces mass through lighter parts or assemblies. These methods include processes such as additive manufacturing, Tailor-rolled blanks, vacuum-assisted die castings, and extrusions. Lightweighting via product structure involves creating designs that are stronger but have a lighter structure or reduced number of components. This can be accomplished through fewer-sub assemblies and fasteners, and shell design instead of frame construction, topology analysis, and system optimization.

Lightweighting a machine tool can be accomplished through a number of methods. Some in the past include Lv et al. [19] who lightweighted the spindle on a computer numerical control (CNC) lathe through the use of an aluminum chuck. Sulitka et al. [20] reduced the mass of the crossbeam and columns of a gantry machine tool through composites and sandwich structures. Suh et al. [21] lightweighted the horizontal and vertical slides of a large CNC machine tool through the use of carbon fiber reinforced polymer (CFRP) composite sandwiches. Zulaika et al. [22] reduced the mass of the ram on a milling machine tool through additional and redundant guideways of the frame to increase its stiffness.

While there have been some attempts at lightweighting machine tools, there have not been any in depth studies that connect energy consumption while addressing lightweighting concerns, e.g., increase in cost of the machine tool and dynamic performance. These previous studies have the following drawbacks:

1. While previous studies have demonstrated energy savings there has been no mechanistic model linking the mass to energy consumption and providing insight into design considerations required to implement lightweighting.
2. There has been investigation into the dynamic performance of large machine tools in regard to lightweighting but no study of how lightweighting affects the static and dynamic performance of more common milling machines.
3. There has also been no investigation into how lightweighting with the intent to reduce energy consumption affects the machine tool cost.

This dissertation will address these shortcomings through a number of tasks outlined in Chapter 3. Addressing these three shortcomings together is important because lightweighting affects more than the energy consumption of the machine tool. Reducing the mass of the machine can affect its stiffness and natural frequencies which in turn affect the machine performance (static and dynamic). It is important to understand how lightweighting affects the static and dynamic performance and how design can improve the performance. Lightweighting can also affect the cost of the machine due to a potential change in design complexity. If the new design greatly increases the complexity of the machine, then the cost to manufacture the machine could significantly increase as well, which will drive up the cost to the customer. This cost increase may deter machine tool builders from incorporating lightweight designs and therefore the link between lightweighting and the cost of the machine should be investigated.

To address these shortcomings, first a lightweighting application for a common milling machine will be provided. Following, a mechanistic energy model demonstrating the energy savings from the lightweighting application will be presented. Then the static and dynamic performance of the milling machine will be investigated in regards to the lightweighting application. Finally, the concern of lightweighting's impact on cost will be explored through the construction of cost models.

This dissertation includes eight chapters and is structured as follows. Chapter 2 will review literature concerning past efforts to reduce the environmental footprint of machine tools. The focus will be mostly on energy consumption and will include a dive into where the energy is consumed within the machines. The review of past work regarding energy reduction will include applications relating to machine use, planning of multiple machines, and the design of machines.

Following the review, Chapter 3 will highlight and describe in detail the gaps found in the literature. Then to address these shortcomings, four tasks will be proposed. Chapters 4-7 will then describe the work accomplished regarding each task.

Chapter 4 will describe the lightweighting application, i.e., a lightweight slide table for a three-axis milling machine. The slide table was chosen for lightweighting due to the table moving throughout the use of the machine. Lightweighting is applied through a sandwich panel design and the sandwich panel structure is optimized through a genetic algorithm.

In Chapter 5, a mechanistic energy model of the table drive system is presented. This model provides insight into how the mass of the table affects the energy consumption of the drive system and provides understanding into the design consideration required to implement lightweighting of the table, i.e., motor sizing. Energy is modeled for two drive systems: one consisting of a standard table and one consisting of a lightweight table. Motors are sized for both drive systems and energy is modeled based on two different workpieces.

Chapter 6 will explore the dynamic and static performance changes due to lightweighting. Finite element models are constructed for the standard table and three lightweight table designs. The natural frequencies and mode shapes are compared across the table designs along with the change in stiffness.

In Chapter 7, the impact lightweighting has on the cost of the machine tool is explored. Data of features from a wide variety of vertical milling machines are collected. Then empirical cost models are fitted to the data to provide insight into the cost drivers of the machines. Complexity of design is also explored to further investigate how lightweighting will affect the cost of the machine tool.

Chapter 8 will then summarize the contributions of this dissertation and provide a brief discussion of future directions.

2. LITERATURE REVIEW

2.1 Manufacturing

Manufacturing produces much of the goods needed today. It converts raw materials into finished products for customers. Manufacturing is very important for the global economy and individual people. In 2017, 30% of the global Gross Domestic Product (GDP) was attributed to industry [1], in which manufacturing is the largest portion of industry's activities. Further, manufacturing supplies employment for nearly 25% of the global labor force of 3.43 billion people [1].

There are many types of manufacturing: chemical, pharmaceutical, electronics, food, metal working, and so on. Metal working, specifically machining, is of great importance. Machining is a form of subtractive manufacturing. A block of metal is formed through casting or forging or other methods and then machining cuts out the desired shape.

With manufacturing's significant role in the world, it also has a large environmental footprint. This is partly due to its energy consumption and its production of waste streams: solid, liquid, and gas [23]. For example, industry is responsible for about 35% of the global greenhouse gas emissions, 11.6 $GtCO_{2eq}$, in 2018. When looking specifically at machining, it also has a large impact. With machining being a form of subtractive manufacturing, there is inherently waste due to material being removed to make the part. This material is normally recycled; however, additional energy is required to reuse the material. A significant portion of machining's environmental impact comes from its energy consumption. There are other impacts too such as from the use of cutting fluids.

2.1.1 Metal cutting, importance and portion of manufacturing

Metal cutting plays a large role within manufacturing because of its importance and size of operation. Much of metal cutting is done by machine tools (MTs). A MT is a piece of manufacturing equipment used for shaping or forming metal or other materials. These forming or shaping processes are normally accomplished by grinding, shearing, cutting, boring, or other forms of deformation. There are many types of MTs. These consist of lathes, mills, planers, and others.

MTs also significantly vary in size ranging from a tabletop machine to ones that can fill a room. MTs also vary in complexity and technology. Over the years MTs have become more automated, faster, and more accurate.

MTs have become very widespread as manufacturing has grown significantly since the industrial revolution. With this growth, the MT's environmental impact has grown too. The world MT demand in 2018 was $144.6 billion with a projected demand in 2023 of $174 billion [6]. With this great size and contribution to manufacturing, it is expected for MTs to play a significant role in manufacturing's environmental burden.

2.1.2 Machining's environmental burden: energy consumption

To perform the required shaping and forming, large amounts of energy is required. Therefore, when the machine is operating, it consumes a significant amount of energy. Due to the use stage of the MT's lifecycle being the longest of any other stage (see Figure 2.1), and due to the machines operating for a significant portion of the day and consuming large amounts of energy, the environmental burden of a MT is mostly attributed to their energy consumption. Diaz et al. [24] conducted a lifecycle assessment (LCA) of a MT and verified that the use phase of MTs indeed does have the greatest impact (see Figure 2.2). The authors included HVAC and lighting in the LCA but the energy from manufacturing parts was shown to have a significant impact. When looking strictly at energy consumption, it can be seen as to why the use phase has such an impact. Both in the US (2019) and worldwide (2017), over 80% of the electricity was generated from fossil fuels [25,26]. Due to the impact of energy consumption, the use phase of MTs has a great impact on the environment; the more energy consumed, the more pollutants released into the environment. To reduce the environmental impact of MTs, the use phase should be focused on.

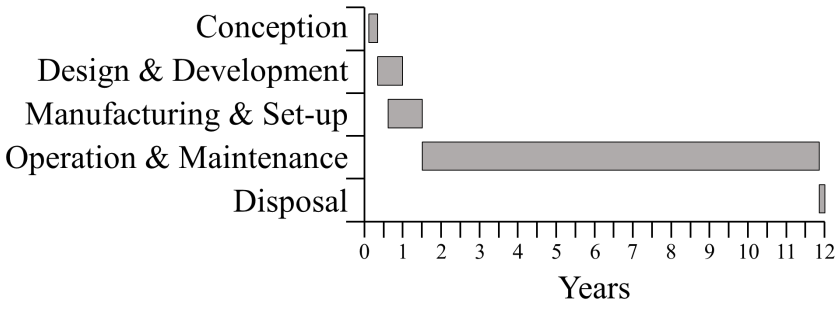

Figure 2.1 Machine tool life phases, adapted from Enparantza et al. [27]

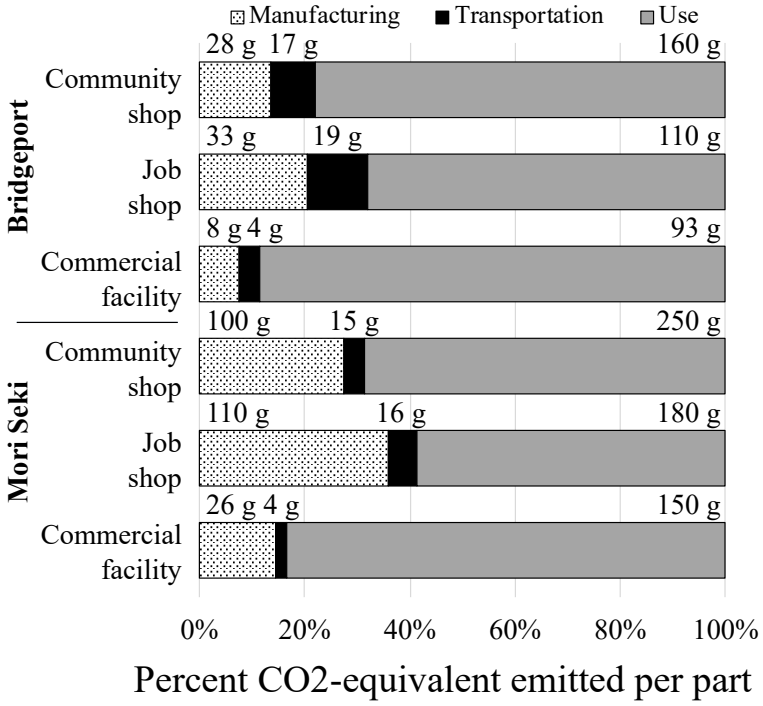

Figure 2.2 LCA of a Mori Seki and a Bridgeport MT, adapted from Diaz et al. [24]

2.2 Energy Consumption and Energy Mapping

2.2.1 Power and Energy Profile

To reduce the energy consumption of MTs, it is important to know where the energy is consumed in the MT. From previous studies of MT energy consumption, it has been found that much of the energy consumed is not attributed to cutting but to other systems [8]. Dahmus and

Gutowski [8], and Kordonowy [28], showed that auxiliary systems, or supporting processes, can consume the majority of the energy. Dahmus and Gutowski [8] examined a number of machine tools and found supporting systems can consume a large portion of the energy consumption (see Figure 2.3). Zein [7] has shown how over time with the implementation of automation and progression of technology the power demand for a MT became more complex (see Figure 2.4). Zein similarly showed that machining still consumes but a portion of the total energy consumption. When a machine is cutting, many systems can be running in addition to the cutting spindle. This can include cutting fluid, feeds, and coolant. This will vary based on machine type, technology level of the machine, and others. This can be seen by the various work of mapping and modeling energy consumption in MTs [7,8,36,28–35].

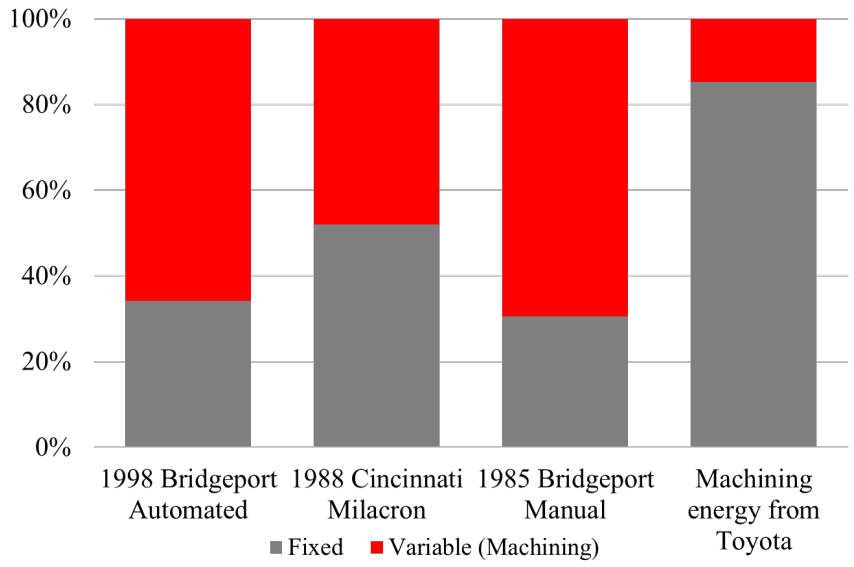

Figure 2.3 Fixed and variable (machining) energy for various MTs, adapted from Dahmus and Gutowski [8]

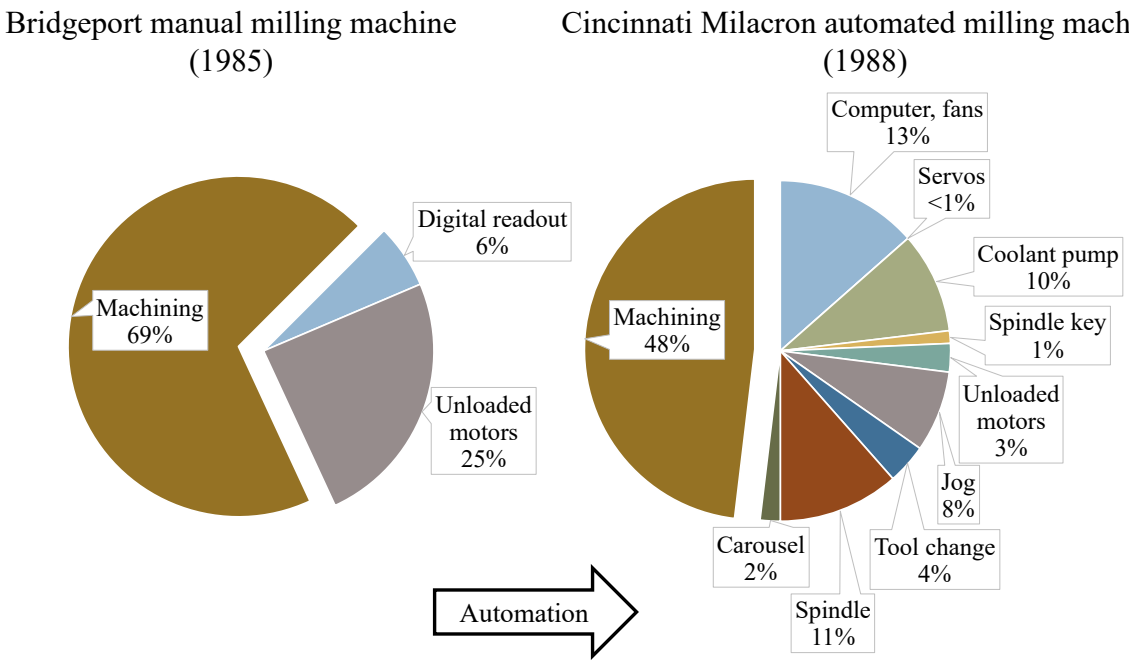

Figure 2.4 Automation's effect on power demand. Adapted from Zein [8] and Dahmus and Gutowski [7].

There has been much work since over characterizing a MT's energy consumption. Zhou et al. [29] among many others created a power profile of the milling process to show how the different systems contribute to the overall power and energy consumption. To provide a visual, two common MTs, a milling machine and a turning machine, are found in Figure 2.5 with examples of their power profiles in Figure 2.6. For the milling machine shown in Figure 2.5(a), the table moves in the x and y-directions to cut the workpiece while the ram moves in the z-direction. For some milling machines the ram will move in all three directions or even in more directions (4 or 5-axis machines). For the turning machine in Figure 2.5(b), the cutter moves in the x and y-directions. For milling the tool rotates to cut the material while in turning the workpiece rotates and the tool does not. Understanding the basic movement of the milling machine and turning machine, let us turn our attention to their power consumption as shown in Figure 2.6. Both power profiles have similar components but understanding the movement of the machines will help understand their differences. For both when the machines are turned on there is a power spike and then the power settles at a steady-state; this steady-state is the basic power which consists of systems that are always running, e.g., fans, computers, and the control system. Then, for both machines, when the spindle is turned on the power spikes again and then settles at another steady-state called the

spindle power. During this power state the spindle is turning but no cutting is occurring. Next, the feed drives are engaged. For the turning machine the feed power is minimal and therefore not shown in Figure 2.6(b). For the milling machine the feed power is shown as another steady-state level. Once the tool engages the workpiece cutting begins and the power increases to the cutting power state. Once cutting finishes, the power drops back down. For the milling machine, the workpiece is repositioned between cuts. This normally occurs at a high speed called rapid traverse. During this movement the power increases greatly due to a high acceleration and speed. This power increase is part of the feed power since it is attributed to the feed drives. Once cutting is complete, the feed drives are turned off and the power drops down to the spindle power level. Then the spindle is turned off and the power drops again. Finally, the machine is turned off and the power drops to zero.

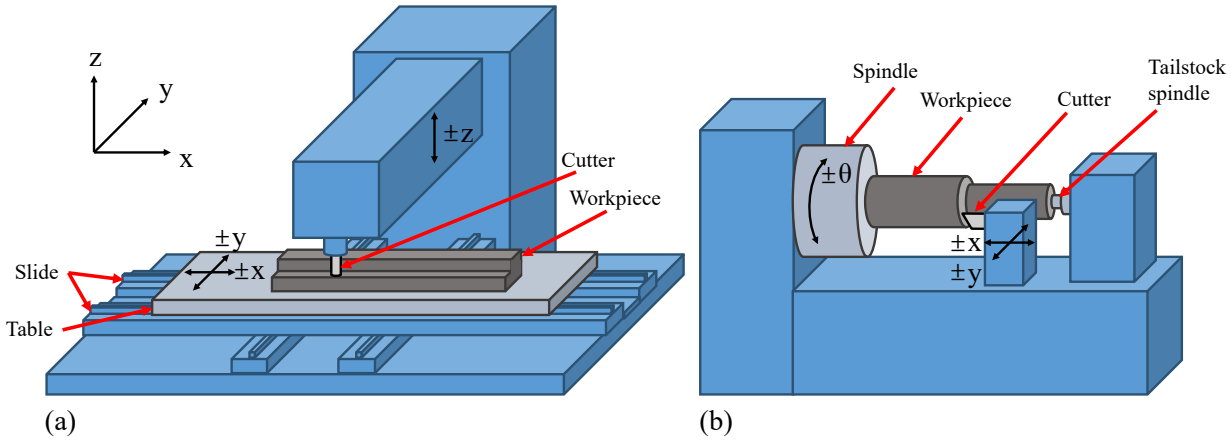

Figure 2.5 (a) An example of a milling machine, (b) an example of a turning machine

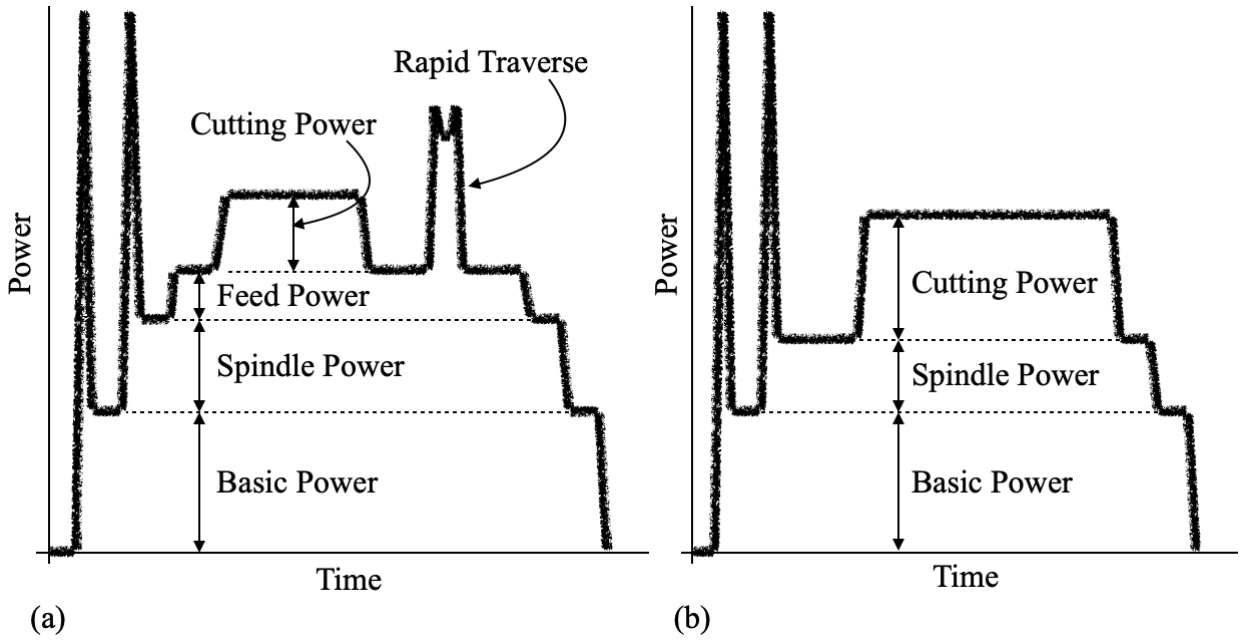

Figure 2.6 (a) Power profile of a milling machine (adapted from He et al. [9]), (b) power profile of a turning machine (adapted from Li et al. [10])

Others have explored the energy consumption of the different systems that make up the power levels in Figure 2.6. Zein [7] created a Sankey diagram of the energy consumption for a grinding machine to further characterize how the energy is consumed. Beck et al. [30] showed the overall energy flow of a MT. Behrendt et al. [31] monitored the energy consumption of multiple milling machines. Denkena et al. [32] created power distributions for various MTs to investigate strategies for lowering power consumption. Peng and Xu [35] show a power distribution of a MT with the intent of finding energy efficient strategies. Warsi et al., [34] create an energy consumption map for the high-speed machining of Al 6061-T6 alloy.

Some authors created models of energy and power consumption for MTs to find energy reduction strategies. Moradnazhad and Unver [33] created a generic energy prediction model for turning. Yoon et al., [36] created an empirical power-consumption model for material removal.

2.2.2 Auxiliary Components

As stated earlier, machining does not consume the majority of the energy. Depending on the state of the MT, the supporting or auxiliary systems can consume the most energy. These systems may be running always.

In Behrendt et al. [31] the authors broke up the power consumption of a MT, NH8000, into many of its systems. They broke up the systems into two categories: constant and variable. The constant power consuming systems would be classified as auxiliary. In Behrendt et al., these would consist of the main switch, CNC monitor, hydraulics and servos, door, and lighting. Other support systems that may not necessarily be on all the time include the automatic tool changer, coolant cooling system and chip conveyor.

These components can consume a majority of the energy. This is shown in Behrendt et al. [31]. Zein [37] showed that the process energy of a grinding process is less than 10% of the entire machine energy. Peng and Xu [35] showed cutting could consume only 25% of the power while idle running consumes 20%, process losses 10%, motor losses 15%, and infrastructure 30%.

2.2.3 Consumption during Cutting

Energy consumption during cutting is not only due to the main spindle. This can include the feed, cutting fluid, and coolant. The feed positions the workpiece or the tool for removing material. Cutting fluid has a number of uses. These include chip removal, lubrication, and tool and workpiece cooling. Cutting fluid can consume a large portion of the energy. Jedrzejewski and Kwasny [38] found the cutting fluid system consumed 24% of the DMU 340 P electrical power. The coolant will keep components of the MT cool in order to increase precision. In the DMU 340 P [38], the authors found the cooling system to consume 27% of the power. The feed systems position the workpiece or the cutting tool. The feed system must overcome friction, inertia, and cutting forces. In the DMU 340 P, the authors found the feed system consumes 4% of the electrical power. The main spindle does the cutting. In a milling machine, it spins the tool. In a turning machine, it turns the workpiece. In the DMU 340 P, a milling machine, the main spindle consumes 21% of the power.

2.3 Energy Saving Methods

Due to the complexity of the energy consumption in MTs, there are many areas to explore in reducing energy consumption with much having been done work exploring different techniques. Duflou et al. [23] and Sutherland et al. [39] introduced some of these potential areas of investigation. These include the modeling of energy consumption for better use and design. These

also include methods to reduce energy during the use of machines, e.g., turning off devices and systems when not needed, reducing idle production times, and optimizing process parameters. Redesign is also a very important method of reducing energy consumption. This section will introduce some of the methods investigated by researchers over the years to reduce MT energy consumption.

2.3.1 Assessment and Modeling

There has been a large body of work on modeling of MT energy consumption. Some have created empirical models for specific portions of the energy, e.g., fixed energy and specific cutting energy, while others modeled total energy for a specific machine. The goal of assessment and energy modeling of MTs and manufacturing processes is to find opportunities to reduce energy consumption. This section will attempt to cover a large portion of the work completed on energy modeling of MTs.

Fixed energy

The power and energy profiles of MTs have a fixed component, as shown earlier in Dahmus and Gutowski [8] and Zhou et al. [29]. This power component is called the basic power in Figure 2.6. Since this portion of energy consumption is significant, there have been some who tried to quantify and model it. Li et al. [10] broke down the fixed energy by components and systems and modeled the fixed energy for various MTs. Verl et al. [40] presented a method to model a MT through modular modeling of systems that contributed to the fixed energy. The authors displayed the capability of the model through modeling the auxiliary systems. Similarly, Dietmair and Verl [41] modeled discrete systems to build a larger model. The authors started with the auxiliary and expanded their model to include other systems.

Specific Cutting Energy

A method of modeling that many have looked at is the building empirical equations to model the MT. There have been many different approaches, some modeling an entire MT and others modeling systems of the machine. One method that has been looked into extensively is the

modeling of specific cutting energy (SCE). SCE is the amount of energy consumed per amount of material removed (J/mm^3). The energy within the SCE is not a portion of the energy allocated to cutting but the total energy during cutting. Understanding SCE is important since it allows for an easy understanding of cutting methods that require more energy. Specific cutting energy depends on the material being cut and the material removal rate (MRR), plus other factors. MRR is equal to the depth of cut times the width of cut times the cutting speed (volume of material per time).

Budinoff et al. [42] modeled SCE by measuring energy consumption through machining five different parts. The authors found using chip thickness as a parameter allows for a more accurate prediction of energy consumption. Deng et al. [43] investigated SCE and the effects various cutting parameters have on it. A model of SCE has been created based on experimental data. Kara and Li [44] also investigated the relationship between SCE and cutting parameters. The authors found a strong indirect relationship between SCE and MRR. Li and Kara [45] continued the work from [44] by exploring more of the relationship of SCE and cutting parameters but looked more into how materials change the SCE. Li and Kara found as MRR increases SEC decreases. This shows it is better to have a larger or faster cut to reduce energy consumption.

Modeling systems and components, bottom-up approach

Another approach to building a model of a MT is to model the different components of the machine and build a larger model based on the individual models. The previous approach, modeling SCE, which is based on the total energy consumed during cutting. This method attempts to break up the energy and allocate it to different systems within the MT, similar to some of the work in the fixed energy section. This allows for greater understanding of how the energy is consumed and where improvements can be made.

Verl et al. [40] and Dietmair and Verl [41] built models in this manner. They applied their methods to the constant energy consuming systems but their models can be applied to the whole MT. Eisele et al. [46], built a model that simulated the energy consumption of MTs by modeling the energetic interactions of the components in the MT. The authors applied this method to the coolant system and built the model based on the components within the coolant system. Bech et al. [30] created models for individual systems to find opportunities for improvement in efficiency. The authors use their model to find efficiencies in manufacturer's data. Abele et al. [47] modeled

a spindle through its individual components in order to find efficiency potential. Schudeleit et al. [48] built a generic power map of a MT. The authors investigated the behavior of each component and then aggregated the information to build the overall power map. Narita et al. [49] built a model based on cutting parameters to predict the CO_2 emissions. CO2 is calculated from energy consumption, coolant quantity, metal chip quantity, and other factors. Bi and Wang [50] built an energy model based on the kinematic and dynamic behaviors of a MT. This model helps connect design variables to the energy consumption through the relationship with the manufacturing processes. Flum et al. [51] discussed in their book chapter how to apply this idea to build a digital twin. This tool was developed for planning of energy-efficient MT configurations. The authors also state the model can be coupled with an optimization tool. Yoon et al. [36] created an equation-based model to better understand the relationship between cutting power and process parameters. The authors included wear of tool into the model in addition to parameters such as feed and speed.

Entire machine, top-down

Another approach to modeling the MT is to take a top-down approach instead of a bottom-up approach. There are researchers that model the MT as a whole instead of modeling smaller systems and building up to the entire machine. Herrmann et al. [52] built a holistic view of MT through modeling the inputs and outputs, not just energy; this includes raw material, coolant, and cutting tools. The authors modeled the inputs and outputs for different processes and systems within the MT. Xue et al. [53] presented a method that forms combined material input-output models for manufacturing systems. This method aggregates process-level input-output material models. The overall model serves as a link between unit-level changes and the broader system. Kuhrke et al. [54] created a model that informed customers as to which energy efficient components of MTs would provide the greatest benefit to their application. The authors considered the MT's use, length of use, downtime, and how long it would not be in use. Götze et al. [55] presented an integrated method for the measurement of energy consumption, modeling of energy flows, and analysis of energy saving potentials. This method includes a lifecycle cost. Schmitt et al. [56] presented a model of a MT that allows for self-optimization. The authors classify components based on a hierarchy to show better show the flow of energy. With this classification the authors can identify an energy supply excess in order to stop that excess.

Empirical based models

Other researchers took a different route to create a model which includes creating empirical models. Wu et al. [57] constructed an energy model of both a turning a milling CNC machine during the cutting of an impeller. The authors explored the impact varying cutting parameters had on SCE. Depth of cut was found to have the largest impact on cutting energy. Kant and Sangwan [58] created an artificial neural network (ANN) model for predicting energy consumption. The ANN was built based on experimental data with the results showing it is capable of predicting energy consumption. Avram et al. [59] built a software model to evaluate the use phase of a MT based on technical, economical, and environmental criteria. These criteria consist of tool life, cutting power, surface roughness, and more. The authors use a ranking criteria to rate strategies. Bhinge et al. [60] presents a Gaussian process (GP) to predict the energy consumption of a MT. The authors use training datasets to construct the model through machine-learning. The method is tested with a milling MT.

Monitoring

One last method for assessment and modeling is the monitoring of energy consumption. Research was completed in this area to provide methods of organizing and visualizing energy data to assist in decision making. Mohammadi et al. [61] proposed a visualization method to monitor energy consumption in a MT. The method created a Sankey diagram showing the flow of electrical, mechanical, thermal, and fluidic power. The machining processes were classified into drive train, machine cooling, process cooling, and hydraulics. Zampou et al. [62] examined two case studies to identify characteristics of energy-aware information systems in manufacturing. The authors found these information systems combine at a system level energy monitoring with energy-aware analytics. To deploy these systems, the authors present an approach that integrates energy and operational information flows. Vijayaraghavan and Dornfeld [63] presented an automated energy monitoring system that uses event stream processing techniques. Event streams are ordered sequences which correspond to time series events. The authors discuss method to identify patterns. Verl et al. [64] presented a method for multilevel energy monitoring. The method monitors at component, machine, production line, factory, and production system level. This method implements learning at the component, machine, and factory level so that these systems can self-

optimize. Seevers et al. [65] proposed a monitoring method that detects patterns from energy consumption data. The monitoring method detects when the energy consumption varies from standard operation to allow for investigation into the cause of the change.

2.3.2 Cutting fluid

As stated earlier, cutting fluid has a number of uses: chip removal, lubrication, and tool and workpiece cooling. Cutting fluid can have a significant environmental impact through health concerns, pollution, and energy consumption. To reduce the environmental impacts of cutting fluid there are a number of steps that can be taken. Reducing and eliminating cutting fluids is one step [66,67]. To reduce, this can be accomplished through minimum quantity lubrication (MQL). MQL is the use of a spray of lubrication instead of a constant flow. Standard flood coolant can be seen in Figure 2.7(a) and MQL can be seen Figure 2.7(b) Dry cutting is also another method of reducing cutting fluid. This is by, as the name suggests, using no cutting fluid. This is not possible for all applications. There are also other methods such as cryogenic cooling. Adler et al. [67] suggested MTs can be designed to incorporate less use of cutting fluids. Debnath et al. [66] suggested the use of vegetable based cutting fluids to reduce environmental harm.

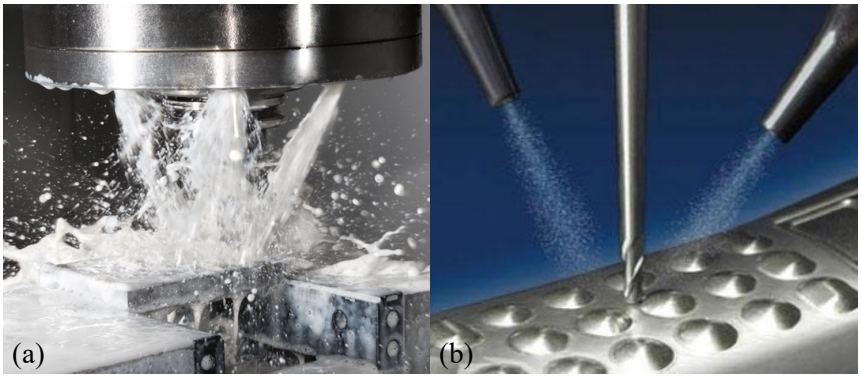

Figure 2.7 (a) Flood coolant [68], (b) MQL [69]

2.3.3 Tool Path

Another method investigated to reduce energy consumption is through optimizing the tool path. Diaz et al. [70] found that longer tool paths correlate to larger energy consumption due to the

relationship between processing time and energy consumption. Kong et al. [71] found that different tool paths had different energy demands (see Figure 2.8). Li et al. [72] presented a methodology to optimize tool path for low energy consumption and carbon footprint in the milling process.

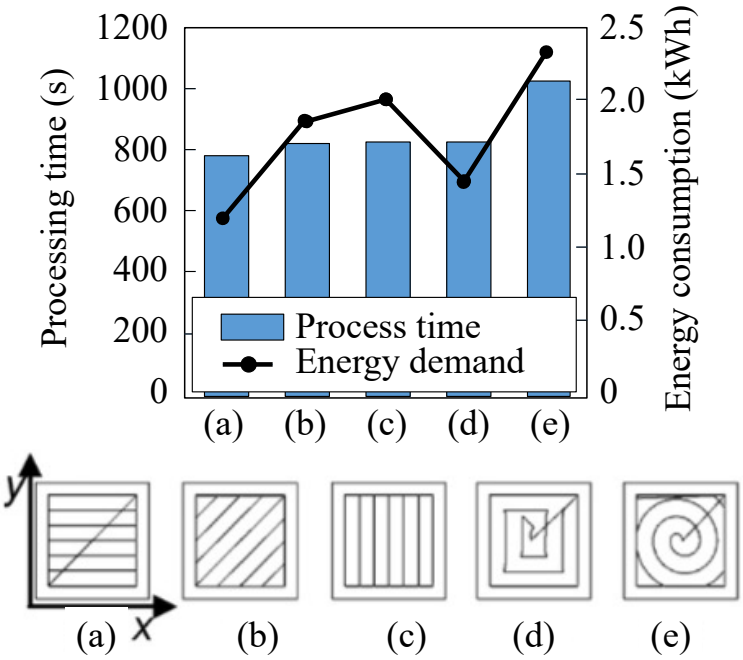

Figure 2.8 Processing time and energy consumption of various tool paths, adapted from Kong et al. [71]

2.3.4 Control

Better control over the processes in the MT can also help. Currently machines are designed for performance with less focus on environmental issues. Denkena et al. [32] found that some peripheral subsystems are nearly self-contained and are controlled independently. No information is exchanged with the machine control and there can be no change based on a machine's state. To improve this, Denkena et al. proposed allowing peripheral subsystems to be controlled by the machine control and to implement requirement-oriented control. This will allow for the adjusting of subsystems based on machine state. Similar to Denkena et al., Schlechtendahl et al. [73] designed a control system to change the state of systems and components in the MT, to reduce energy consumption. The control system would change the state to a lower energy consumption state if possible.

2.3.5 Scheduling

One method to reduce energy consumption of MTs is to create a schedule that optimizes machine usage based on the parts being made. In the past, schedules have been made to improve throughput. However, this may not always be the most energy efficient. There has been some work on scheduling MTs with the goal of reducing energy consumption. Fang et al. [15] built a model to consider carbon footprint, energy consumption, peak power load, and cycle time. Fang et al. [74] continued with the work of scheduling to reduce energy consumption but considered more restrictions on peak power consumption. Zhang et al., [75] presented a method that identified manufacturing schedules with a goal of minimizing both carbon footprint and electricity cost while considering time-of-use tariffs. These schedules did not sacrifice production throughput. Fang et al., [76] considered scheduling jobs on a single machine under time-of-use tariffs. Similarly Sharma et al. [77] and Yin et al. [78] considered the economic and environmental aspects under time-of-use tariffs. Liu et al. [79] proposed a fruit fly algorithm to schedule flexible job-shops with a goal of reducing manufacturing carbon footprint. Dai et al. [80] applied genetic algorithm (GA) to determine if a MT should go into idle. Morad and Zalzala [81] created a GA based method that schedules machines while considering process capabilities, tolerance limits, and processing costs in addition to the time. The authors were able to minimize makespan, number of rejects, and the total cost of production. Biel et al. [82] developed an optimization procedure that computes a production schedule based on the availability of on-site renewables.

2.3.6 Flexible Manufacturing Systems

Flexible manufacturing systems (FMS) is a group of MTs with automated guided vehicles (AGV) that can produce various types of parts. The goal of an FMS is to be able to produce various types of parts and allow for customization. In FMS there is the potential for reducing the environmental impact due to their flexibility in how and when parts are made. Li et al. [83] developed an optimization method for energy-conscious production in FMS. Rossi and Dini [84] created a real-time GA to optimize production plans for FMS. The authors were able to reduce makespan and the time to produce production plans.

In FMS, machine selection is a problem that has been worked on by researchers. Rai et al. [85] applied fuzzy goal-programming based GA to address MT selection and operation allocation

in FMS. The objectives included cost of machining operation, material handling, and set-up. Bensmaine et al. [86] addressed MT selection within reconfigurable manufacturing systems. The authors used an adapted version of the non-dominated sorting genetic algorithm (NSGA-II). Objectives were minimization of the total cost and the total completion time. Kumar et al. [87] applied constraint-based genetic algorithm (CBGA) to FMS. The authors showed the potential of CBGA in a standard FMS-loading condition to manage a variety of constraints and variables. He et al. [88] proposed an optimization method to reduce energy consumption that considered MT selection and operation sequence.

2.3.7 Process Plans

A product is manufactured through a set of operations and processes. The ordering and plan for implementation of the operations and processes is the "process plan" [12]. When developing a process plan, normally those that make the plans look for ways to shorten production time and lower costs without compromising quality. In addition to costs and time, environmental performance can be an objective of the process plan. To do this, Jiang et al., [12] developed a method to evaluate a process plan's environmental performance. Zhao et al. [11] proposed a method to include environmental conscious into process planning. This method evaluates process plans by identifying impactful steps and the design features associated with the steps. This method identifies the steps in terms of environmental impact and manufacturing cost.

2.3.8 Process parameter improvement

Process parameters are variables that affect the production process. These are controllable parameters in which it is desired to control them. Controlling process parameters allows for a more controlled product. In metal cutting, process parameters include feed rate, cutting speed, and depth of cut. Normally process parameters are controlled to increase the quality of the product without considering environmental impacts. However, there has been some work into reducing energy consumption and other impacts.

There have been a number of researchers who looked into process parameter improvements to reduce energy consumption and other environmental impacts. Winter et al. [89] examined the grinding process. They optimized cutting fluid use and a number of process parameters based on

surface roughness and carbon footprint. Process parameters, specifically the effect of MRR on specific cutting energy, was examined a number of times [14,70,90]. A common result in the studies is how as MRR increased, specific cutting energy decreased. Jiang et al. [91] the relationship between process parameters, cost, and cutting fluid in turning. The goal was to reduce the use of cutting fluid. Oda et al. [92,93] examined cutting conditions during milling, such as tool angles and cutting speeds, with focus on reducing energy consumption. Mori et al. [13] presented a method that would apply to drilling, face/end milling, or deep hole machining. The authors synchronized the spindle acceleration with the milling feed system through a control method in order to reduce the milling machine energy consumption.

There has also been a number of researchers to investigate improving process parameters through the use of genetic algorithm (GA). Yildiz [94] used a cuckoo search algorithm to optimize cutting speed an feed rate. Suresh et al. [95] applied GA to grinding to optimize surface roughness. Sardiñas et al. [96] implemented multi-objective optimization to select cutting parameters during turning. Cus et al, [97] implemented particle swarm optimization (PSO) for cutting parameters during milling. Oktem et al. [98] created a feed forward neural network model of surface roughness from experiments with a goal of minimizing surface roughness.

2.3.9 Remanufacturing

Remanufacturing returns a worn-out or broken-down product to a “new” condition. It applies manufacturing to returning the product to a “new” condition. Remanufacturing can not only be profitable but also a method to reduce the environmental impact of products at the end of their life [99]. Du & Li 2014, [100] investigated the benefits of remanufacturing MTs by the original equipment manufacturer (OEM). The authors found remanufacturing can help OEM’s reduce energy consumption in addition to lowering costs. Du et al. [101] and Gontarz et al. [102] investigated methods to determine if a machine is can be remanufactured. Jiang et al. [99] presented a method for remanufacturing planning that considers both economic and environmental criteria. Cai et al. [103] investigated designing machines to be remanufactured at the end of their life.

2.3.10 Design for Environment

Possibly the most beneficial method for reducing the environmental impact is through design. This is due to the fact that most of the impact of a product is determined during the design phase [104]. Yoon et al. [105] a hierarchical approach to reducing energy consumption in MTs and placed design for the environment at the top for that very reason. All other methods, e.g., software and hardware-based optimization, and cutting improvements, are all limited by the design of the machine. The design increases the optimal running. This section will highlight research over designing for the environment.

LCA

To design for the environment, a lifecycle mindset must be incorporated. A lifecycle mindset allows the designers to look beyond the use phase for environmental impacts and see when a product will have the greatest impact. For electronics, their impact is normally high during the extraction and manufacturing phase. Automobiles have their greatest impact during their use. Applying this mindset to MT design will help find the greatest opportunities for reducing their lifecycle impact.

Santos et al., [106] performed a full LCA on an all-hydraulic press brake. When looking at the full lifecycle, the authors found the MT structure contributed 40% of the overall impact while electricity consumption during the use phase contributed 46%. This contradicts published results where they say energy consumption dominates the lifecycle impacts while all other stages contribute only minor impacts. This LCA provides information for redesign strategies.

Azevedo et al. [107] presented results of a comparison between a simplified, Direct Method, and detailed, Detail Method, LCA of a MT commercial CNC press-brake. The goal was to see whether the most detailed information allowed for better design decisions in terms of environmental performance during a redesign. The authors found the Direct Method did reveal the same priorities as the Detailed Method but did not properly account for the contributions of the main life cycle stages.

Machine design

Redesign of the MT is a very important step to reducing their environmental impact. There has been a number of works on the topic of machine design for the environment. Weinert et al. [108] investigated the benefits of dry machining and MQL. The authors looked beyond the benefits and proposed methods for design of machines and parts to use dry machining and MQL. Diaz et al. [70] explored the potential energy savings found in kinetic energy recovery systems (KERS). These systems recover energy from the deceleration of motors, similar to hybrid vehicles. The authors found a power savings of up to 25% from the implementation of KERS on a MT's spindle. Albertelli [16] compared a classical solution gearbox based spindle system to a direct drive spindle system. The author found energy improvements through direct drive by there being no gearbox, no chiller for oil, and no pump for oil. However, the electrical motor efficiency would be lower.

Devoldere et al. [109] investigated a press brake and a multi-axis milling machine to find potential design improvements. The authors quantified the economic and environmental impacts of these potential energy saving design improvements. Neugebauer et al. [110] discussed and analyzed potential design improvements of MTs and production systems. The authors investigated mobility, miniaturization, autonomy, and adaptivity.

Design of products, not necessarily machines

Since most of a product's environmental impact is determined during the design phase [104], it would stand to reason that including lifecycle thought in the design phase would greatly improve a product's impact. One method to reduce manufacturing impact is to design the products, in addition to the machines, to have lower impacts during the manufacturing stage and the rest of the lifecycle (see Figure 2.9). Design of the MTs is very important but there is also great potential in incorporating a lifecycle mentality into the design phase of the products. Ramani et al. [111] investigated eco-design tools with integrated life cycle data to achieve sustainable product development. The authors reviewed related research to provide a framework that merges sustainable thinking with traditional design methods and that encourages research collaboration. Similarly, Umeda et al. [112] proposed a framework of lifecycle planning to reduce the lifecycle impacts of products. The framework integrated design with lifecycle flow design to reduce resource consumption and other environmental impacts. Jayal et al. [113] reviewed recent trends

in addressing sustainable manufacturing. Some of these trends included modeling and optimization at the product, process, and systems levels. The main them was a holistic approach that spans the entire lifecycle. The focus was on dry, near-dry, and cryogenic machining. Seow et al. [114] proposed a design for energy minimization (DfEM) approach. This approach intends to provide transparency in regards to energy consumed during manufacturing to inform design. The authors then built an energy simulation model to aid designers. Huang et al., [115] presented a multi-criteria decision making (MCDM) model to assist in environmentally minded design. The model was to address the problem of selecting environmentally friendly material. The model incorporated a lifecycle view, environmental impacts and costs of materials, and uncertainties of the lifecycle scenario.

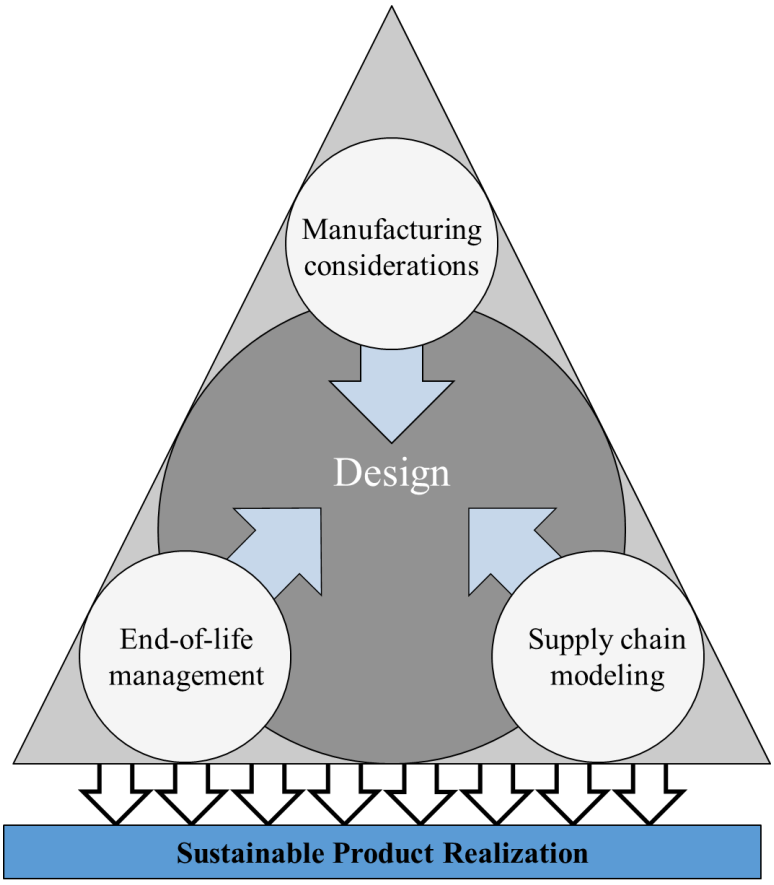

Figure 2.9 Design should be impacted by the product's lifecycle, adapted from Ramani et al. [111].

Motors

Electric motors have a very broad use throughout industry. They are used for heavy duty use in machinery and for lighter applications such as for a fan in a computer. Saidur [116] stated they have a significant share of the energy consumption in industry in the EU. Their share is 36%. With the widespread use, their design is very important. If a motor is not designed well for an application, it can become inefficient. Figure 2.10 shows an example of a relationship between a motor's loading and its efficiency. As the load drops from the motor's designed load, its efficiency drops. The desired operating range is 60% to 90% of full load [116]. Saidur stated that 75% of all motors have load factors less than 60%. Capehart et al. [117] said one of their authors audited over 100 medium-sized manufacturing companies and found motor load factors on average to be around 30% to 40%. Zein [37] had similar findings from his review. He found energy efficient motors had a high potential of improving energy efficiency in MTs.

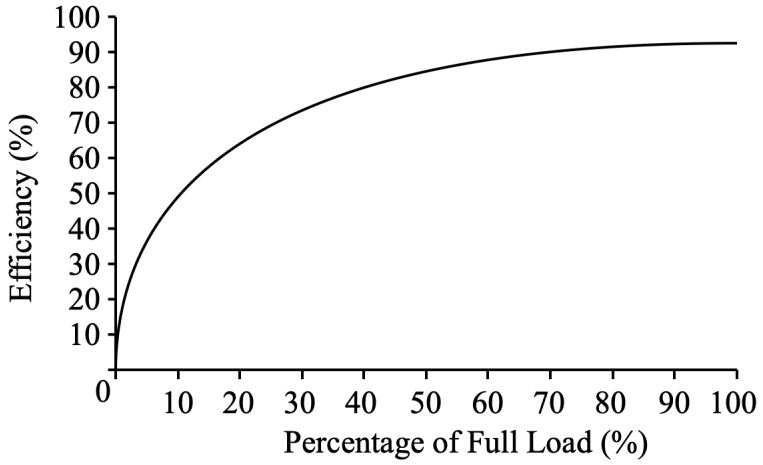

Figure 2.10 Relationship between motor loading and efficiency, adapted from Saidur [116]

Factory Layout

Hicks [118] applied GA to designing manufacturing facilities to reduce their environmental footprint. The author's goal was to minimize material movement for a given schedule of work. Geometric information and building constraints were included. The method can work for both brown-field and green-field layout design problems.

2.4 Lightweighting Potential

Another potential for reducing energy in MTs is lightweighting. The transportation sector has benefited greatly from lightweighting. Reducing the mass of the vehicle has reduced fuel consumption and still has potential in the sector [18]. The potential energy savings of lightweighting vehicles can be found in Figure 2.11 and the materials used in lightweighting automobiles can be found in Figure 2.12. This reduction in fuel is due to reducing the power required to move the vehicle. The mass of the vehicle ties directly to power. With force equally mass times acceleration, power equaling force times distance, and energy equaling power multiplied by time, it is clearly seen mass' role in energy consumption.

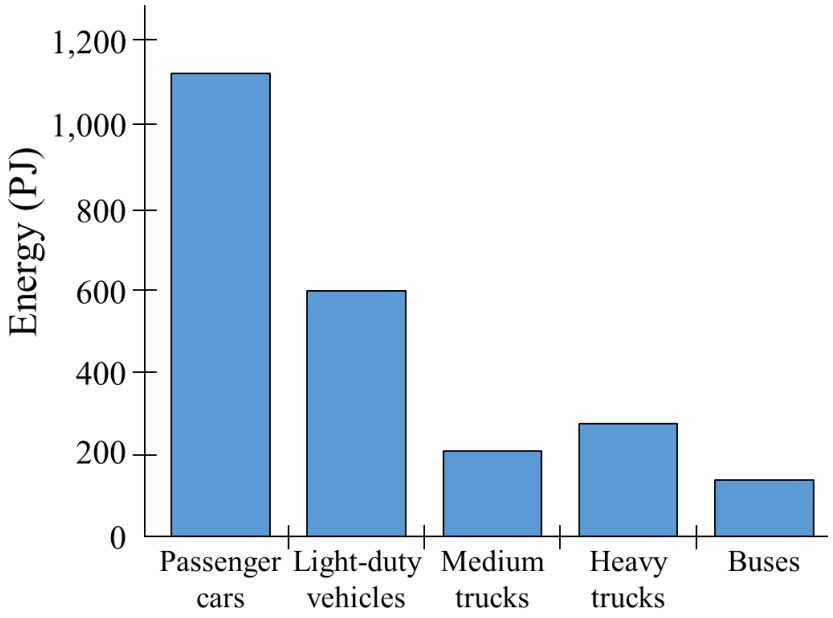

Figure 2.11 Potential global annual primary energy savings by lightweighting automobiles, adapted from Helms & Lambrecht [18]

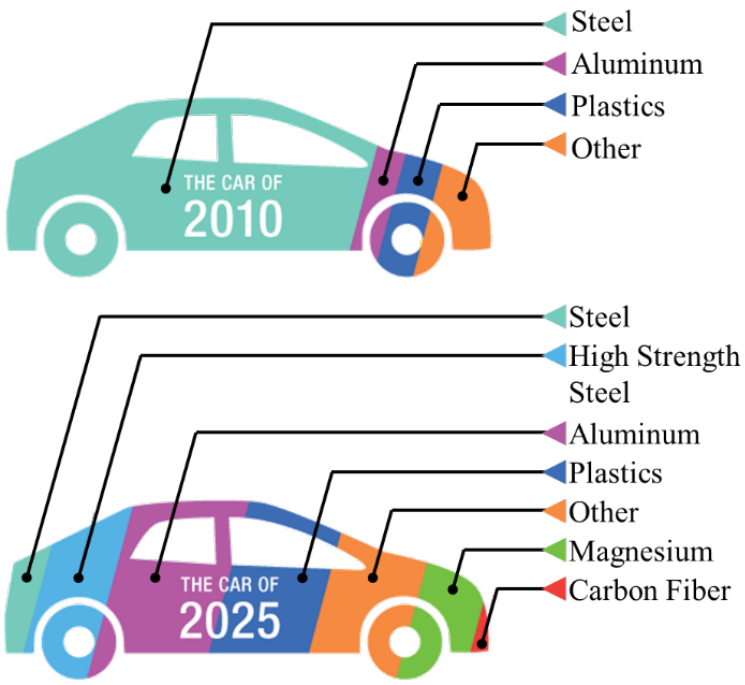

Figure 2.12 Lightweight materials used in automobiles to reduce their mass, adapted from Auto Lightweighting [119]

There has been some work already in reducing the mass of MTs. Kroll et al. [120] investigated the benefits of mass reduction in MTs. The authors summarized the benefits as being a decrease in reactive energy and friction power, and an increase in acceleration capability, process stability, and guide bandwidth. The authors modeled motor energy loss based on acceleration and mass. They showed mass relates directly to energy loss in motors. The authors summarized the potential for various types of MTs. Herrmann et al. [121] explored the energy reduction potential of light weight structures through a literature review. This review focused on both the successes of other industries to lightweight components and save energy and the potential material reduction. The authors investigated the impact of lighter weight materials during their manufacturing stage and the length of time the product should be used to overcome those initial impacts. They also looked into various recycling rates of the lightweight materials. Dietmair et al. [122] investigated mass reduction in MTs and found it is possible to reduce energy consumption while maintaining productivity. The authors presented a lightweighting method that encompasses mechanical and electrical systems, along with control and manufacturing processes. This method addressed vibration and other concerns that are associated with lightweighting. Aggogeri et al. [123]

investigated lightweight materials in MT structures in regards to vibration. The authors found some materials, e.g., aluminum foam sandwiches and aluminum corrugated sandwiches, can improve machining performance and increase damping.

Li et al. [124] designed a lightweight, stiffer grinding machine column. The authors used the branching pattern of leaf venation as inspiration. The maximum deformation was reduced by 23.60% and weight reduced by 1.31%. Zhao et al. [125] used a structural bionic method to design a tool column that improves static and dynamic performance. The design was based on configuration principles from bone and plant stems. The authors were able to decrease mass and deflection by 6.13% and 45.9% respectively. Triebe et al. [126] developed a method to reduce the mass of the working table in a MT through GA. The solid table design was changed to a sandwich panel and the method optimized parameters of the sandwich design, such as thickness of cell wall and height of core. The authors created a Pareto Front for two different designs, honeycomb core and foam core, and compared it to a solid plate.

Zhao et al. [127] were able to accomplish lightweighting through bio-inspired techniques. Zhao et al. [127] designed a lightweight milling slide table. Three different bio-inspired construction methods were employed: hollow stem, sandwich node, and radial root. Fuzzy assessment was used to assist in choosing when to employ which. Suh and Lee [21] proposed the use of composites for slides in MT structures to allow for rapid acceleration and deceleration. From implementing composites, the authors decreased the weight of the horizontal and vertical slides by 26% and 34%. The damping was also increased by 1.5 to 5.7 times without sacrificing stiffness.

3. VISION AND MOTIVATION

3.1 Research Gaps

It is clear there is a connection between mass and energy consumption of moving components and systems. This is seen by the simple work equation of energy equaling force times distance and force equaling mass times acceleration plus the coefficient of friction times mass times gravity (see Eqs. (3.1) & (3.2)).

$$E = Fx \tag{3.1}$$

$$F = ma + \mu mg \tag{3.2}$$

However, in machine tools there are many factors to consider that can affect energy consumption, e.g., friction and sizing of motors. Therefore, when implementing a design change, it is imperative to understand and consider the various systems and components that will be impacted by the change. While it is clear the previous work regarding energy consumption of machine tools has been substantial, there has not been a study to directly connect mass reduction to energy savings of a system within a machine tool while considering additional changes required to implement the lightweight design. There have been applications of lightweighting and demonstrations of energy savings but no thorough study to connect the two. A comprehensive study will support the implementation of lightweighting throughout the machine tool through a better understanding of the required design considerations and their impact on the final energy savings.

When implementing any design change of a machine tool, especially when reducing the mass of moving components, it is important to consider how these changes will affect the dynamic and static performance of the machine tool. A machine tool needs to have a large enough stiffness so as to reduce vibrations and allow for high quality cutting. There have been studies regarding the impact of lightweighting on the static and dynamic performance of machine tools. However, the machines studied were less common, very large machines. These include Zulaika et al. [22] who investigated the lightweighting of large conveyor milling machines and Sulitka et al. [20] who investigated the lightweighting of a large gantry style machine. There also has been investigation

into improving dynamic performance of machine tools through stiffening the structure of the machines. However, these did not explore design improvements to reduce energy consumption.

Another concern that arises when implementing lightweighting is the potential for a cost increase. Lightweighting can reduce the amount of material used to manufacture the machine tool, which can lead to a lower cost, but lightweighting can also lead to a more complex machine. Machines with greater complexity can be more difficult to produce and therefore more costly to manufacture. Currently there has been no study investigating the impact lightweighting has on machine tool cost. There have been many studies regarding lifecycle costing (LCC), total cost of ownership (TCO), and machining costs. There even has been some investigation into costs to manufacture large equipment including heavy construction equipment, automobiles, and one study regarding machine tools. However, none of these studies, including Ciurana et al. [128] who investigated the cost to manufacture machine tools, did not explore how lightweighting design changes, i.e., material and complexity changes, affect the cost to produce the machine.

The shortcomings found in the literature can be summarized as follows:

1. There has been no mechanistic model linking mass to energy consumption while providing insight into design considerations required to implement lightweighting.
2. No study currently exists of how lightweighting affects the static and dynamic performance of common milling machines.
3. There has been no investigation into how lightweighting with the intent to reduce energy consumption affects the machine tool cost.

3.2 Objectives and Research Approach

Energy reduction of machine tools is an important step to reducing manufacturing's environmental impact and lightweighting has great potential for doing that. To address the gaps outlined in the previous section, four tasks have been proposed.

First, a lightweighting application is proposed to reduce the machine tool energy reduction. This application will provide a proof of concept and allow for carrying out the rest of the tasks to demonstrate lightweighting is effective and can be accomplished in a manner that will not compromise quality. This application will include redesigning the table of a vertical milling machine to reduce its mass by replacing the solid design with a lightweight sandwich panel design.

A genetic algorithm will be implemented to optimize the mass of the table while preserving its strength.

To demonstrate the effectiveness of lightweighting, an energy model for a vertical milling machine is proposed. This model will quantify the energy consumption of the table drive system under various cutting conditions. The mass of the table, workpiece, and cutting forces will be considered to model the energy consumption. Since motors play a significant role in the energy consumption due to their efficiency, motors will be chosen to match the requirements of the table drive system. The proposed model will be constructed for both a standard table design and the lightweight table design proposed in task 1. The model will explore whether the motors can be resized to better match the system requirements of having a lighter weight table. These two energy models will provide a direct connection between mass and energy consumption and will provide insight into design considerations when lightweighting a machine tool.

A concern when reducing mass of machine tool components is dynamic performance and loss in stiffness. Therefore, a dynamics model and a stiffness model of the table are proposed. In the past the general thought was to increase mass to reduce vibrations. However, there are other methods to reduce vibrations, e.g., increase stiffness. The dynamic model will provide insight into the dynamic performance of a lighter weight machine. These models will provide insight into whether lightweighting affects a machine tool's performance and what can be done to improve its performance. The dynamics model will provide insight into the natural frequencies of the standard and lightweight tables.

The design changes required to reduce the mass of the machine may reduce the amount of material to build the machine which can lead to a lower cost to produce the machine. However, lightweighting may also increase the complexity of the machine which can also increase the cost to manufacture the machine. If the cost to manufacture the machine increases significantly, machine tool builders may be hesitant to incorporate environmentally minded design changes, i.e., lightweighting. To address this concern, a machine tool cost model is proposed to explore the cost drivers associated with building a machine tool. To construct this model, it is proposed to collect machine tool feature data from a wide variety of machines. Then empirical cost models can be fit to this data. Since manufacturing cost data is not available it is assumed the cost to manufacture a machine tool is linearly related to the purchase price.

The four proposed tasks are summarized as follows:

1. Create a lightweighting application through the design of a sandwich panel slide table for a vertical milling machine.
2. Build a mechanistic energy model to provide insight into how the mass of the table affects the energy consumption of the drive system and provide understanding into the design considerations required to implement lightweighting of the table.
3. Construct dynamic and stiffness models to determine the impact of lightweighting on the performance of the machine tool.
4. Make an empirical cost model for vertical milling machines to determine the effect of lightweighting on machine tool cost.

4. GENETIC OPTIMIZATION FOR THE DESIGN OF A MACHINE TOOL SLIDE TABLE FOR REDUCED ENERGY CONSUMPTION

Reprinted with permission (portions enhanced/adapted) from Triebe, M. J., Zhao, F., & Sutherland, J. W. (2021). Genetic Optimization for the Design of a Machine Tool Slide Table for Reduced Energy Consumption. *Journal of Manufacturing Science and Engineering*, 143(10), 101003

4.1 Introduction

Manufacturing plays a vital role in our lives. It provides the goods needed by consumers and industries worldwide for global development and for improving the quality of life. It contributes to wealth generation and job creation. In 2017, 30% of the global Gross Domestic Product (GDP) was attributed to industry [1], and manufacturing represents the largest portion of industrial activities. Further, manufacturing supplies employment for nearly 25% of the global labor force of 3.43 billion people [1].

However, along with its benefits, manufacturing does create an environmental burden through non-renewable resource and energy consumption/depletion, and waste streams. For example, in 2019 among all end users, industry accounted for 26.4% of the energy consumption in the US [129], with much of the electricity being generated from fossil fuels [25,26] . Without action, the environmental burden of manufacturing is expected to grow unabated as the world population and standard of living continue to increase.

One major class of equipment used to manufacture components are machine tools (MTs), and MT sales in 2018 were $144.6 billion with projected sales in 2023 of $174 billion [6]. MTs, e.g., lathes, milling machines, and drill presses, are often used to undertake machining operations, and when MTs perform these operations, they consume large amounts of energy and create a substantial environmental impact. Like any product, a MT has a lifecycle: extraction of resources, materials processing, manufacturing and assembly of components to create the MT, use, and end-of-life. The longest lifecycle stage for a MT is its use stage, and because of conspicuous electricity consumption during its use, which can be up to 80% [24] of the energy consumed throughout its lifecycle, the use stage is the most dominant in terms of carbon footprint and environmental impact [24,27]. This is the case since electricity used by MTs is largely generated from fossil fuels, especially in the US with over 80% produced from fossil fuels [25,26].

One potential approach falling under the structural optimization category for reducing the energy consumed during the use stage of a MT is lightweighting (LW) [120,121]. As is the case for automobiles [18], the greater the MT mass the more energy is required, especially for MT elements that move during the use of the MT. Kroll et al. [120] explored the potential of LW to reduce a MT's energy consumption along with other benefits such as increased acceleration capability and process stability. Hermann et al. [121] further examined LW potential by showing how the reduction in energy consumption during the use stage as a result of LW can offset any potential impacts during other lifecycle stages. To effectively reduce energy consumption through LW, it must be implemented through design, which as noted by Yoon et al. [105], has the greatest potential for energy reduction. Because of the influence of design on energy consumption, optimal design should be employed to take advantage of energy savings opportunities.

To effectively apply LW to MTs, it is important to have an understanding of where energy is consumed. The focus of this chapter will be over vertical milling MTs due to the significant number of vertical mills currently being used and the projected market growth being $8.77 billion in 2026 from $6.91 billion in 2018 [130]; see Figure 4.1(a) for a schematic of a vertical mill. Figure 4.1(b) shows a "standard" power profile for a vertical milling machine; the area under the power curve is the energy consumed. As is evident, the profile can be decomposed into four components. When the MT is turned on, the power consumption spikes and then quickly falls to a steady-state; this steady-state is the first component: basic power. Basic power is associated with devices and systems that are switched on when the machine is powered, e.g., computer, fans, lubricant system, and the control system. Then, the spindle and table feed drives are engaged, the feed drives move the table in the x and y-directions (see Figure 4.2). Another spike in the power occurs associated with the spindle start-up (often the spindle is started before the table drives are engaged). The power quickly drops down to another steady state which is the second component, the spindle rotation and feed power. A third component of the power profile occurs when the cutting tool engages with the workpiece: cutting power. This power is associated with moving the table while the workpiece material is being cut. When cutting ends, the cutting power component is eliminated. A fourth power profile component often occurs, fast feed power. This is associated with the table moving quickly during rapid traverse. After cutting is completed and the table is moved back to the starting position, the spindle rotation and feed power are eliminated. Then, when the machine is turned off, the basic power component is also removed. From this figure, it can be seen how the

speed of the table can greatly influence the MT's energy consumption, see power component 4, fast feed power. With the desire of faster throughput, faster feeds will be used, and therefore greater energy consumption and greater potential for LW to reduce energy consumption.

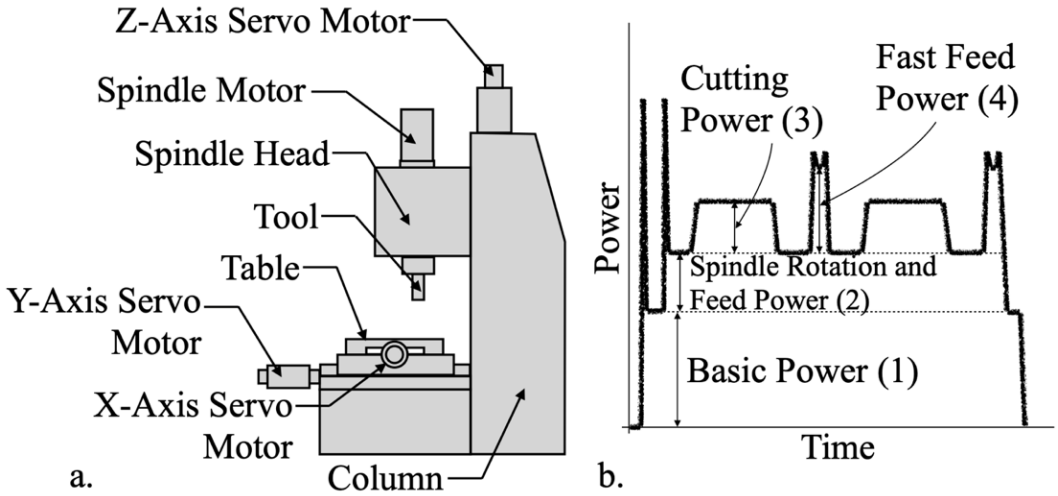

Figure 4.1 (a) Schematic of a vertical milling MT, adapted from Triebe et al. [131], and (b) power profile of a milling machine, adapted from He et al. [9]

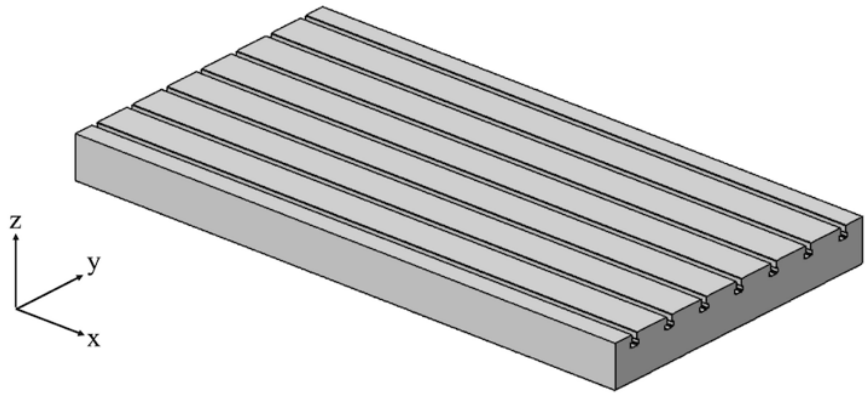

Figure 4.2 Slide table

To seize upon the benefits offered by optimal design and LW, the objective of this chapter is to establish a method that may be used to minimize the energy consumption of a MT through mass reduction. This is accomplished by replacing a solid MT slide table with a sandwich structure (the proposed method will optimize the structure). A representative slide table is shown in Figure

4.2. The table was chosen for LW for the reasons stated above. In many vertical milling MTs the table moves throughout the use of the MT which contributes to power components 2, 3, and 4 in Figure 4.1(b); to cut in the x and y-directions the slide table moves. Therefore, a reduction in mass of the slide table will reduce the power of these three components and energy attributed to them. However, mass reduction often leads to a loss of stiffness. Therefore, both mass and stiffness must be considered. To design the lightweight table, the proposed method optimizes the shape of the sandwich structure core with the goal of minimizing mass and maximizing stiffness. To accomplish this multi-objective optimization, a Non-Dominated Sorting Genetic Algorithm (NSGA-II) proposed by Deb et al. [132], is used to find the optimal core shape. NSGA-II was chosen for its ability to accommodate multiple objectives, preserve the diversity of the population (wide range of solutions), and search various regions of the solution space simultaneously.

Given this brief introduction, the remainder of the paper is structured as follows. First, an overview of LW will be given. Then, the optimization method will be described including assumptions made, how the core is generated using a genetic algorithm (GA), and the different objectives considered. Next, the results from the GA will be shown and discussed. Finally, the paper will summarize and state conclusions.

4.2 Literature Review

This chapter explores the use of LW to reduce the energy consumption of a MT. With this in mind, this section briefly reviews past efforts related to LW in several product design contexts. In particular, this section will review LW methods in the transportation sector and with respect to MTs.

4.2.1 Overview of Lightweighting in the Transportation Sector

LW has had success in the transportation sector due to the direct connection between mass and fuel consumption. Due to the clear successes of LW in automobiles and aircraft, literature where LW has been applied to automobiles and aircraft is reviewed, with an eye toward MT applications. Most LW design strategies for automobiles and aircraft adopt one of three approaches, where it is to be noted that there is some overlap among these approaches: lighter materials, LW via manufacturing, and LW via product structure. While it is evident that the third approach is

design-oriented, the other approaches often require design changes as well, e.g., dimensional changes due to differences in material properties. Material LW seeks to replace a current material with a lighter weight (lower density) material. Manufacturing LW encompasses manufacturing methods that help reduce mass through lighter parts or assemblies. LW through structural changes involves creating a design that reduces mass through a stronger but lighter structure or a reduced number of components.

Materials:

There are a number of materials-focused design strategies that may be pursued with respect to LW. These include the use of high-strength steel (HSS) [120,133–135], aluminum alloys [135,136], magnesium [135,137], and polymers and composites [121,135,138]. The use of these alternative materials allows for either less of similar material to be used, i.e., HSS, or a lighter material that provides similar strength. For example, although HSS is not a lightweight material, it still can achieve weight savings of 15 to 26% [135]. In the case of automobiles and aircraft, materials-focused strategies can be accomplished through a number of areas. For example, in automobiles, thinner walls can be achieved in the outer skin, floor panels, frame, chassis beams, and seat rails [134]. Aluminum can be used in areas of the automobile such as the roof, door, floor, and structural components like knuckles [135]; often, cast aluminum alloys are replacing ferrous alternatives. For aircraft, aluminum alloys are widely used [135]. For example, aluminum lithium alloys are being used in airframes of aircraft [135]. In automobiles, magnesium has potential in applications such as engine block, steering column, steering wheel, door inners, seat frame, and instrument panels [135,137]. In aircraft, magnesium alloys are used in castings to reduce weight. Titanium alloys are used in aircraft structures, fasteners, structural forgings, and fittings. Composites are another lightweight engineering material commonly used in automobiles and aircraft (e.g., Boeing 787) [121,135,138]. In automobiles, composites have been used in supporting roof pillars, door frames, chassis, body panels, fenders, and wheel houses [135]. In aircraft, focus has been on replacing secondary structures, structures that are not load bearing and not directly critical to flight, with composites [138]. This includes panels for the fuselage, clips, brackets, seat backs, window panels, and cockpit floor. It should be noted that use of alternative/lighter materials

is not a “one-to-one” replacement. Other design changes, such as dimensional changes, must be implemented due to the difference in the properties of the original and replacement materials.

Manufacturing:

Manufacturing provides multiple design strategies for LW automobiles and aircraft [133,135,139]. These include the use of Tailor-rolled blanks, hydroforming, hot forming, vacuum-assisted die castings, semisolid thixo-forming, extrusions, high pressure die casting, and additive manufacturing (AM). Tailor-rolled blanks allow for variation in sheet thickness to reinforce where needed and reduce weight where thickness is not needed. Hydroforming uses hydraulic fluid to press metal into a desired shape. This method allows for complex, structurally strong shapes and helps reduce the number of parts. Hot forming allows for the forming of high strength materials in which their formability increases significantly at high temperatures. Vacuum-assisted die castings allow for the integration of several parts with good dimensional accuracy, surface finish, and mechanical properties. Thixo-forming is a semi-solid processing method that can produce complex shapes at low temperatures. The extrusion process enables the mass production of complex designs. High pressure die casting is a cost-effective process that allows for the production of high-volume metal parts with tight tolerances. AM allows for novel geometries that could not be accomplished with traditional manufacturing methods. Other manufacturing methods more common in aircraft production include integral milling of pockets, cutouts and lightening holes, and local thinning by chemical milling [135]. Similar to material changes, the use of different manufacturing methods usually requires other design changes due to the differing capabilities of the methods and the differences in the geometries of the new parts.

Product structure:

LW via product structure in automobiles and aircraft can be accomplished through a number of methods which include topology analysis [121,133], system optimization [135], shell design instead of frame construction [121], and fewer sub-assemblies and fasteners [135]. Topology optimization can provide an initial structure to analyze and design from. System optimization reduces the number of parts and fasteners in an assembly or system. This can be accomplished through the use of various manufacturing methods including AM, bonded structures, co-cure co-

bonded composites, and single molded large structures. Shell designs replace frame constructions to reduce mass and are accomplished through the use of manufacturing techniques as stamping and welding [121].

An example that incorporates these three LW design techniques for the LW of automobiles is the 2015 Ford F-150. This vehicle used more lightweight materials with design changes to reduce the mass by 300 kg [135]. An example for LW aircraft is the design of the Boeing 787 which the primary structure is made up of as much as 50% composite while a previous model 777 was made up of only 12% composite by weight [140]. Because of this use of composites to reduce mass, the aircraft is up to 20% more fuel efficient.

4.2.2 Lightweighting in Machine Tools

LW of MTs has potential to reduce their energy consumption along with other benefits. Kroll et al. [120] summarized the benefits of LW as being a decrease in reactive energy (related to inertial forces) and friction losses, and an increase in acceleration capability, process stability, and responsiveness. The authors modeled motor energy loss based on acceleration and mass and showed a reduction in mass leads to a reduction in motor energy loss. The authors also summarized the LW potential for various types of MTs with laser cutting equipment having the greatest potential and a grinding machine having the least. Herrmann et al. [121] reviewed the lifecycle impacts of lightweight structures including the potential impact reduction during the use stage. The authors stated that the increase in energy efficiency, when applied to moving masses, can offset potential increased impacts during material extraction and manufacturing.

To accomplish LW in MTs, there have been a number of design strategies. One of these strategies includes the use of composites. Möhring [141] gave an overview of design and application of composite materials in MTs. One application covered was the use of composites in spindles and tools to reduce the inertia (I) of the spindle rotors and tool bodies, and reduce their thermal growth and improve their dynamic behavior. The author also examined the application of composites for slide structure and clamping systems. Neugebauer et al. [142] looked at a hybrid carbon fiber reinforced polymer (CFRP) ball screw drive; the ball screw drive had a lower inertia (I) that translates into lower electrical losses and higher drive dynamics. It also has about 10 times lower thermal expansion than a conventional metallic ball screw. Suh et al. [21] constructed

composite slides for a large CNC MT through bonding high-modulus CFRP composite sandwiches to welded steel structures. These composites reduced the mass of the horizontal and vertical slides by 26% and 34% respectively and increased damping by 1.5 to 5.7 times without sacrificing stiffness. Sulitka et al. [20] applied composites and sandwich structures to the crossbeam and columns of a gantry MT. The total x-axis moving mass was reduced by 35% and the total crossbeam and columns mass was reduced by 52.3%. Because of this reduced mass, the authors were able to employ a smaller motor that used 20% less power. Merlo et al. [143] substituted electro-welded steel structures in the column and ram with a hybrid sandwich structure made of steel facing plates with a core of CFRP and aluminum honeycomb. Damping was increased by up to 3 times for the ram and 8 times for the column while mass was reduced by 20% for both. For a second case study the authors substituted the steel ram with one made of a hybrid material structure. The skin was thin steel plates that were glued on an internal tube fabricated through filament winding technology. Mass was reduced by 40% and damping increased by 2.5 times.

In addition to the use of CFRP, mass can be reduced through the use of other lightweight materials. Lv et al. [19] explored reducing the inertia (*I)* of the spindle by reducing the mass of the chuck through an aluminum design that reduced the mass by up to 60%. The authors chose to focus their efforts on the chuck instead of the spindle in order to retain stiffness in the spindle. The authors found the inertia (*I)* of the spindle system dropped from 0.3354 to 0.2380 kg-m^2 which reduced peak power and energy consumption by 21.2% and 20.6% respectively. Dietmair et al. [122] redesigned a milling machine by employing steel and aluminum foam sandwiches to reduce the mass of the ram. The mass was reduced by 15% and the structural damping coefficient was increased by 250% while the static stiffnesses in the x and z-directions were sacrificed by 10%. The authors also investigated reducing weight of the milling head by replacing the steel with aluminum which reduced its weight by 27%. Other design changes the authors explored included reducing the inertia of the drive chain, lower power motors and converters, and advanced instrumentation and control. With all these changes the authors were able to reduce the moving mass in the Y and Z axes by 16% and 18% respectively and reduce the motor power in both axes by 40%.

Other LW methods include structural design changes. Zulaika et al. [22] explored reducing the mass of the ram through thinner wall thickness while increasing stiffness via additional/redundant guideways in the vertical guiding system of the frame. The authors

redesigned the ram based on modeling the interactions between the representative milling operation and the machine dynamics. Li et al. [124] designed a new grinding machine column with a focus on enhanced stiffness and decreased weight using a branching pattern of leaf venation as inspiration. The maximum deformation was reduced by 23.60% and weight reduced by 1.31%. Zhao et al. [125] designed a tool column with improved static and dynamic performance using a structural bionic method. This design was based on configuration principles from bone and plant stems and was able to decrease mass and deflection by 6.13% and 45.9% respectively. Zhao et al. [127] designed a lighter working table of a MT using three construction types: hollow stem, sandwich node, and radial root. Fuzzy assessment was used to decide when which method should be used. Triebe et al. [126] also developed a method to reduce the mass of the working table in a MT through GA. The solid table design was changed to a sandwich structure and the method optimized parameters of the sandwich design, such as thickness of cell wall and height of core. A Pareto front (PF) was made for two different designs, honeycomb core and foam core, and compared it to a solid plate. Li et al. [144] designed a lighter weight and stiffer MT bed through topology. The authors developed a simplified spring model composed of shell and matrix elements to simulate a real bed structure. The finite element method was employed to identify the load bearing topology. The final design reduced the maximum deformation by 19% and the transverse stiffness was improved by 7.82%.

Having provided background on LW strategies employed with automobiles, aircraft, and MTs, this chapter will now shift to the proposed method of LW and design optimization. The following section will describe the application of GA to reduce the mass of a MT.

4.3 Application of GA to Table Design

With an understanding of past efforts relating to MT energy consumption and LW design strategies for reducing mass and thus energy, attention now shifts to applying the LW concept to a MT table. An example of a slide table can be found in Figure 4.2. Drawing on successes from LW in transportation and previous MT research, a sandwich structure design will be explored to replace the solid table construction shown in Figure 4.2. A sandwich structure has been chosen due to its lightweight yet strong characteristics. The sandwich structure will draw from manufacturing advances covered in Section 4.2 by using a single row of cells for the core structure

that have the potential of being economically manufactured, see Figure 4.3 for an example. Figure 4.3 shows a sandwich structure consisting of square cells along with other potential cell shapes. These various cell shapes will change the properties of the table and therefore should be investigated.

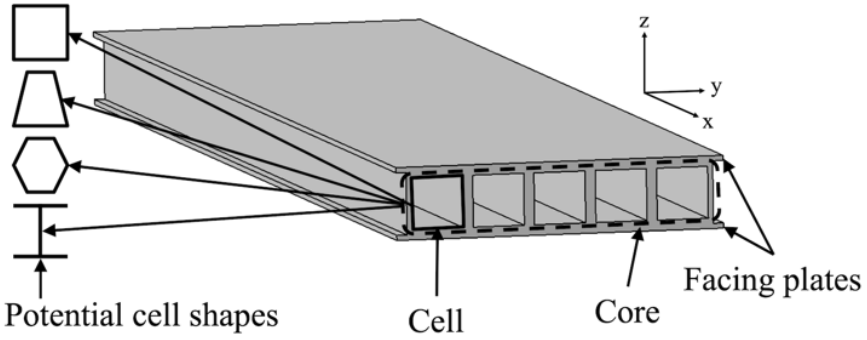

Figure 4.3 An example of a sandwich structure configuration

To design the sandwich structure, a biologically inspired optimization method, GA, will be utilized. This specific algorithm to be employed is NSGA-II. GA will allow for the optimization of the core with respect to multiple objectives (more description on the method can be found in Deb et al. [132]). GA allows for the finding of multiple optimal solutions, as opposed to a single solution, and reduces the chance of getting stuck at a local optimum. This particular algorithm, NSGA-II, better maintains a diversity of solutions instead of congregating at one end of the optimal spectrum. The main goal for this GA is to reduce the mass of the table, however, with reducing mass there is the potential of reduced strength. Therefore, strength will be a second consideration in the optimization procedure. The core is optimized through the shape of the cells that affect the mass and strength of the table. NSGA-II will choose optimal shapes for the cells to reduce mass but maintain strength of the sandwich structure. The profile of the cells along with the wall thickness will be chosen.

An illustrative example will be considered to demonstrate an application of the GA method. This will be accomplished through a model of the table slide for a vertical milling machine, e.g., Hurco VMX64i. The table dimensions are 889 by 1676 by 89 mm (width x length x height) with the core height being 76 mm and both of the facing plates having a thickness of 6.4 mm. The material of the table is steel, ASTM-A36. For simplification, T-slots were not included in the analysis.

4.3.1 Generation of cell shapes

Since the shape of the cells are being optimized, the chromosomes were defined as the cell shape. The chromosomes are made up of y and z coordinates of each individual point of the cell profile (20 points total) and the thickness of the profile. An example cell profile can be found in Figure 4.4(d) with an explanation of chromosome generation to follow. To form the shape, the points are arranged in a counterclockwise fashion with each point being connected to the next in the chromosome, i.e., the first is connected to the second which is connected to the third and so on. The final y-z coordinate is connected to the first, which produces a closed shape. The final value in the chromosome is the thickness of the profile which ranges from a solid cell to a wall thickness of 2.5 mm. To generate each shape, the following procedure is used, see Figure 4.4 for more detail (Figure 4.4 shows a total of 14 points (n=14) instead of 20 for ease of viewing):

1. First, four fixed points are generated creating a rectangle. The generated rectangle has a width of 13 mm and a height of 76 mm, matching the core height. This creates flat areas to which the upper and lower plates can be attached. These four points are always 1, n/2, n/2+1, and n (see Figure 4.4(a)) and will never move throughout the generations.
2. The next points generated are immediately to the right of points 1 and n/2 (2 and n/2-1) and to the left of n/2+1 and n (n/2+2 and n-1, see Figure 4.4(b)). These points determine the width of the top and bottom of the cells. These y-value coordinates of these points can be in the range of 6.5 mm from the center (location of the first 4 points) to 51.5 mm from the center (the maximum width of the shape). The z-value coordinates are 0 mm for bottom two points and 76 mm for the top two points. During recombination and mutation, these points can move horizontally, but not vertically, between these two boundaries.
3. The rest of the points are generated randomly horizontally between the maximum width and the minimum thickness; however, their vertical, z-direction, positions are predetermined, see Figure 4.4(c). The vertical position of each point is based on where the point lies in the chromosome. Throughout the generations these points can move horizontally between these boundaries.
4. Once all points are generated, they are connected from 1 to 2, 2 to 3, and so on till n with point n being connected to 1 to create a closed shape. This can be seen in Figure 4.4(d).

5. Finally, the inner profile is made using the outer profile and the thickness value, labeled as t in Figure 4.4(e), within the chromosome. The thickness is initially a random value between 2.5 and 50 mm, which creates a solid cell, for each shape. During recombination the thickness is averaged between the two parents and during mutation the thickness is modified by a random number between the +/- mutation distance divided by 2.

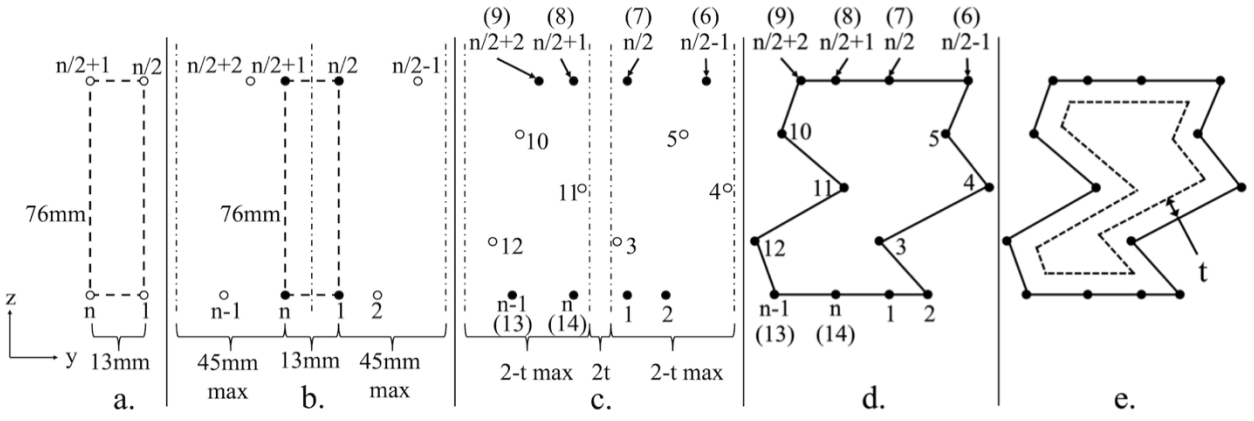

Figure 4.4 Shape generation procedure (14 points shown instead of 20 for ease of viewing) described in steps 1-5 of Section 4.3.1

4.3.2 Objective functions

The first of the objective functions is mass of the sandwich structure table. To calculate the mass, the area of a single cell is found through the profile and thickness and then multiplied by its length and by the density of the material, ASTM-A36. The mass of a single cell is then multiplied by the number of cells required to fill the core horizontally. This can change depending on the width of the cells. Finally, the mass of the outer plates is included.

Two objective functions were created to consider strength of the table: an expression for the moment of inertia, *I*, and an equation for the polar moment of inertia, *J*. These objective functions relate directly to bending, along the x-axis, and torsion, around the x-axis, of the table, which are two indicators used for measuring strength of the sandwich structure in this chapter; the larger *I* and *J* are, the less bending and torsion in the table, respectively. From looking at a free body diagram of the table, shown in Figure 4.5, it is seen how the forces applied by the drive system (e.g., lead screws) along with the cutting forces and force due to gravity can produce bending and

torsion in the table. *I* and *J* of the table were calculated about its centroid. The centroid can be found through integrating across the area (A) using Eq. (4.1). Once the centroid is found, *I* and *J* may be calculated. *I*, in this case is equal to the moment about the y-axis, is calculated by Eq. (4.2), while *J*, found by Eq. (4.3), is equal to the moment about the y-axis, Eq. (4.2), plus the moment about the z-axis, Eq. (4.4).

$$\bar{y} = \frac{\int_A y \cdot dA}{\int_A dA} \quad \bar{z} = \frac{\int_A z \cdot dA}{\int_A dA} \tag{4.1}$$

$$I_{\bar{y}} = \int_A z^2 \cdot dA \tag{4.2}$$

$$J = I_{\bar{y}} + I_{\bar{z}} \tag{4.3}$$

$$I_{\bar{z}} = \int_A y^2 \cdot dA \tag{4.4}$$

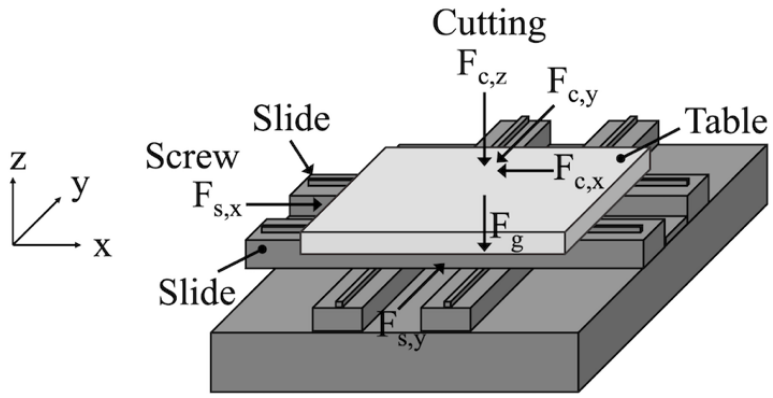

Figure 4.5 Free body diagram of the slide table

The fitness objectives for the GA include the mass and the values for *I* and *J*. *I* and *J* were modified because I_z was naturally much larger than I_y due to the table being a long rectangle. Therefore, *I* was modified by multiplying I_y by 100 to provide similar scaling in the optimization procedure to I_z, see Eq. (4.5). *J* was also modified by multiplying I_y by 100 to provide similar scaling, see Eq. (4.6). These two modifications ensure that the different objectives have comparable values in the GA fitness function. To summarize, the objective functions include the mass of the table, I_{mod} Eq. (4.5), and J_{mod} Eq. (4.6).

$$I_{mod} = 100I_{\bar{y}} \tag{4.5}$$

$$J_{mod} = 100I_{\bar{y}} + I_{\bar{z}} \tag{4.6}$$

4.4 Results from GA

The GA was run for 100 generations (not much improvement was seen after that) and the values for mass, *I*, and *J* were recorded for all the solutions in the final population. I_{mod} and J_{mod} were not recorded since they were needed only during the optimization process and do not represent the true moment of inertia and polar moment of inertia. These members of the population establish the PF shown in Figure 4.6. This figure shows how the population approached an optimal front. To further show the convergence of the population, the GA was run for 500 generations to build an equation representing the optimal PF. Then to represent a fitness value for each generation, the average distance of the whole population to the PF representation was found. This was accomplished by finding the distance of each point to the representative PF and taking the average for each generation. This average distance was plotted for all 500 generations, see Figure 4.7. Using this method to visualize the fitness, it can be seen that at generation 100 the population converged to the representative PF front with little improvement seen in later generations. In all cases the cell shapes converged to a cross-section that resembles an I-beam, a set of I-beams that form the table. This is not unexpected since I-beams handle bending very well. The points with the large mass in Figure 4.6 tend to be bulkier but have better stiffness than the ones with the smaller mass. Examples of how these shapes will work in a MT table is shown in Figure 4.8.

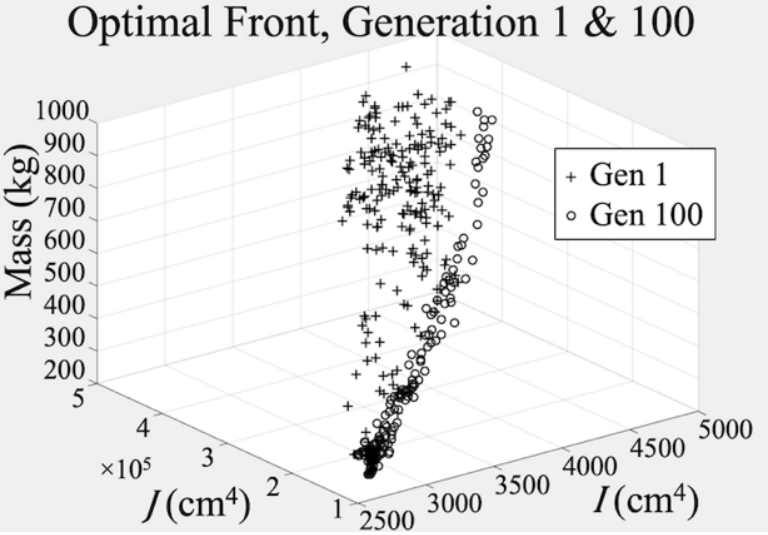

Figure 4.6 Optimal PF compared to first generation

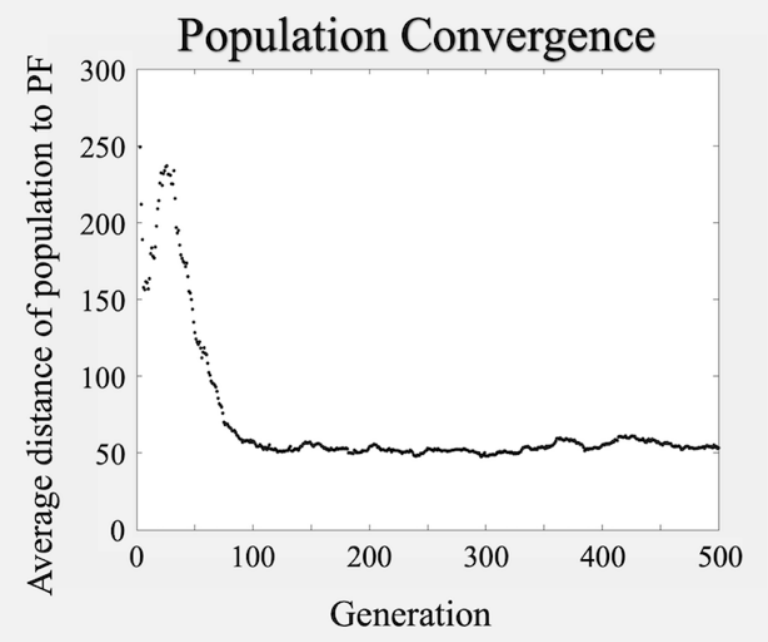

Figure 4.7 Average distance of population to the representative PF

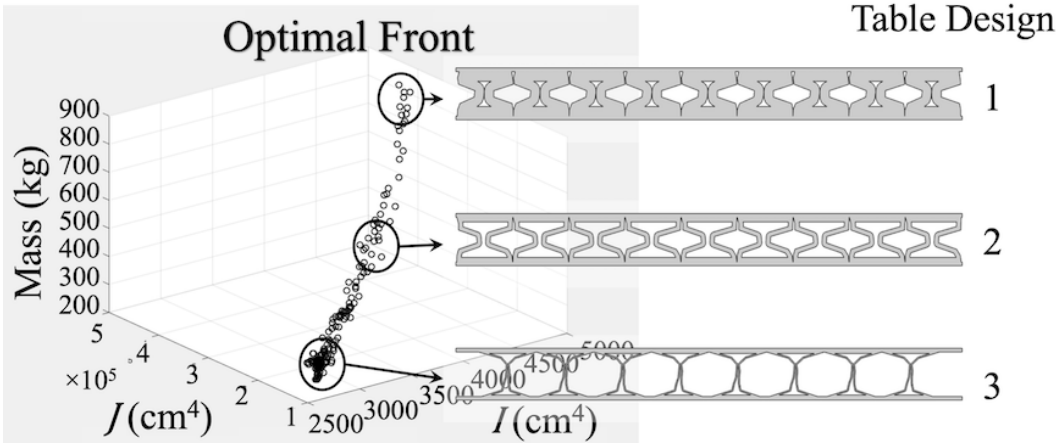

Figure 4.8 Table design examples

Since the shapes generated from the GA may be difficult to manufacture at a low cost, standard shapes were compared to what the GA generated. For example, a table constructed of square tubes and one built from I-beams were considered. It was found that these two designs had slightly smaller *J* values, but comparable mass and *I* values, as shown in Figure 4.9. These standard shapes include rounded corners that avoid stress risers associated with sharp corners. The practical indications of this are that common extrusion and tube shapes, I-beam or square beam, can be used to build the table.

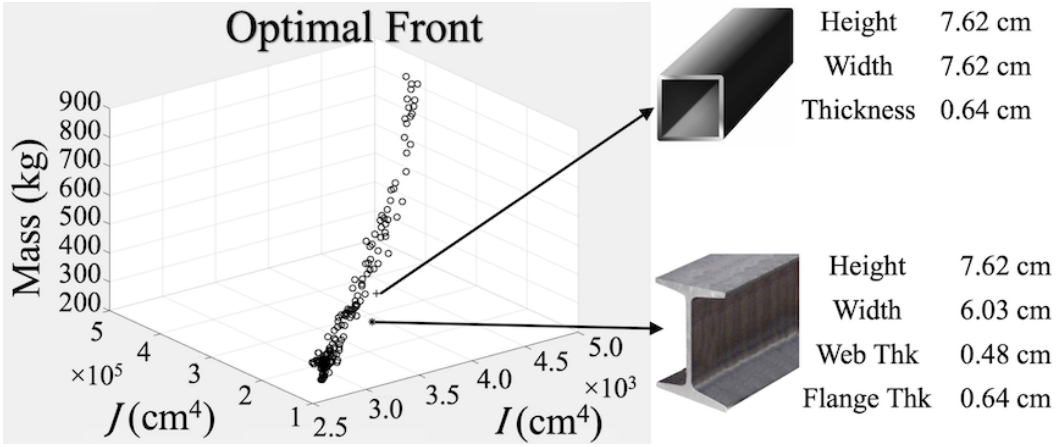

Figure 4.9 Standard shapes comparison

To model the strength of the sandwich structure design, several finite element analyses (FEA) were performed. Three table designs were analyzed (see Figure 4.10). The first design, Figure

4.10(a), had a core constructed of I-beams, same as standard I-beam shown in Figure 4.9, running in the x-direction of the table, the second design, Figure 4.10(b), had a core of I-beams running in the y-direction, and the third design, Figure 4.10(c), had a solid core. All three table designs were modeled with t-slots.

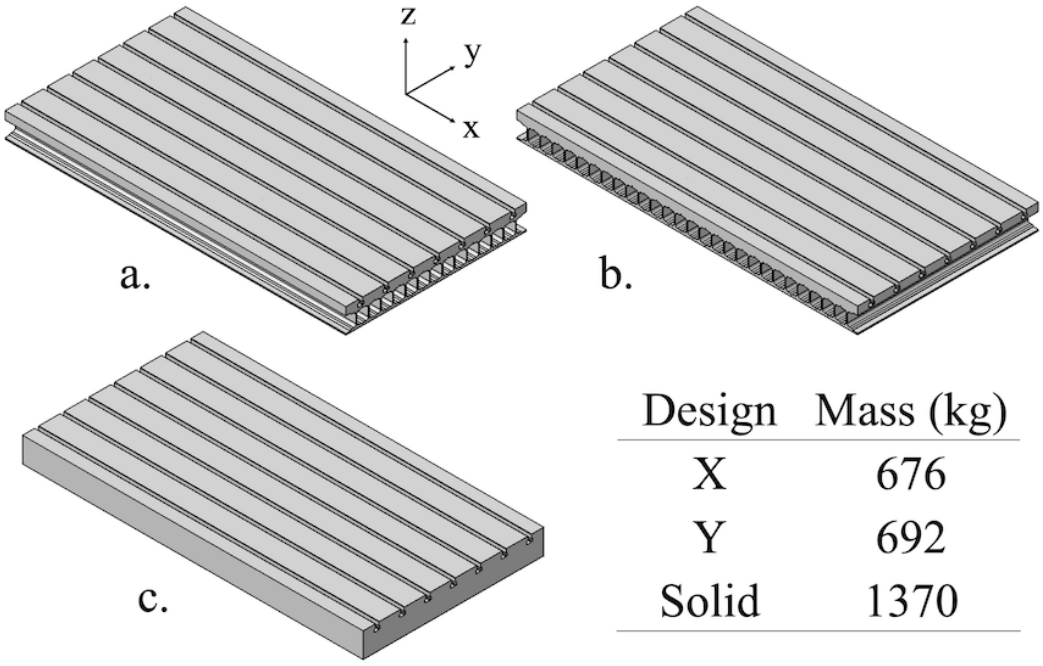

Design	Mass (kg)
X	676
Y	692
Solid	1370

Figure 4.10 Table designs used in FEA: (a) x-axis running beams, (b) y-axis running beams, and (c) solid table

To model the loading conditions, first restraints were placed where the guides would be. Then a force due to table mass was distributed across the whole table, and a force associated with the mass of workpiece (a distributed load of 26700 N) was applied evenly over the top face of the table. Then, a cutting force of 1800 N in the x-direction, 1800 N in the y-direction, and 900 N in the z-direction was applied. The 9 locations to which this set of cutting forces were applied are shown in Figure 4.11, and the FEA was run for each of these 9 applied force locations. The magnitude of the deflections measured in micrometers of these various FEAs can be found in Table 4.1. The I-beam table designs have greater deflections than the solid design, however still very small. These FEAs must be considered in the design of the table, and if the table design does not meet certain requirements, then stiffeners may need to be added or a thicker core used. It is worth noting that these simulations were run at a worst-case scenario due to the max designed load on

the table. Therefore, under normal cutting conditions the tables would have even smaller deflections.

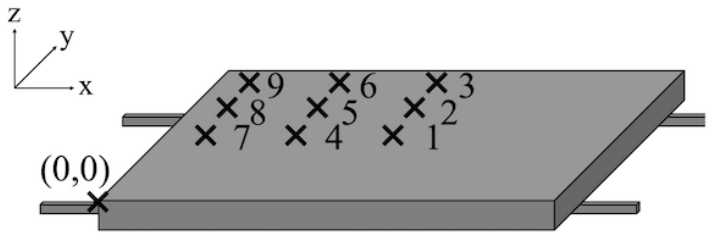

Position	X	Y
1	838.2	469.6
2	838.2	670.56
3	838.2	863.6
4	425.45	469.6
5	425.45	670.56
6	425.45	863.6
7	25.4	469.6
8	25.4	670.56
9	25.4	836.6

Figure 4.11 Loading positions, due to cutting, for the various FEA simulations. Position coordinates in millimeter.

Table 4.1 Magnitude of deflections in μm at each loading position from the FEA simulations

Table design	Position 1	Position 2	Position 3
X	1.136	1.298	4.465
Y	0.977	1.104	2.483
Solid	0.569	0.701	0.894
	Position 4	Position 5	Position 6
X	1.200	1.296	4.660
Y	0.843	1.014	2.591
Solid	0.480	0.780	0.856
	Position 7	Position 8	Position 9
X	1.587	1.948	8.554
Y	1.212	1.842	5.319
Solid	0.706	0.840	1.360

To further explore the design of the table, a sensitivity analysis was performed on the x-axis I-beam table design. The four feature dimensions for the I-beam shown in Figure 4.9 were increased and decreased by 10%. An FEA was performed for each of these scenarios at loading position 1, from Figure 4.11. Loading position 1 was chosen since most cutting will take place near that location. These results can be found in Table 4.2. A positive result indicates an increase of deflection or mass, and a negative result indicates a decrease in deflection or mass. This analysis shows decreasing height and increasing width of the I-beam both decrease deflection and mass.

There are other options to decrease the deflection, but these end up increasing the mass. It should be noted that both the increasing and decreasing the width of the I-beam decreased the deflection. The increasing of the width increases the area of the I-beam that bears the load and therefore produces a stronger I-beam, up to a certain point. The decreasing of the width allows for more I-beams to fit across the core of the table which would understandably increase the stiffness of the table and also the mass. Similarly, the strength of the table would be affected by a change in the overall shape of the table (not just the core), i.e., length, width, and height.

Table 4.2 Sensitivity analyses conducted on the x-axis I-beam table design

		Change in	
Feature		Deflection	Mass
Height	+10%	+0.185	+6.694
	-10%	-0.035	-6.695
Width	+10%	-0.032	-1.897
	-10%	-0.032	+13.889
Web	+10%	-0.035	+13.889
	-10%	+0.050	-5.574
Flange	+10%	-0.043	+10.851
	-10%	+0.078	-10.708

Note: Each feature of the I-beam was modified by +/-10% with the change in deflection (μm) and mass (kg) recorded. The analysis was run at position 1 (see Figure 4.11).

From these two designs, the x-axis and y-axis designs found in Figure 4.10(b) and Figure 4.10(c), about 50% mass savings is accomplished in the table. This is significant since the table will constantly move throughout the cutting of the workpiece. This method of LW meets and exceeds other LW applications reviewed in Section 4.2.2 when comparing mass savings. Other methods had a mass savings from as low as 15% [122] and up to 60% [19]. However, due to their different applications, energy savings will vary significantly. For example, the application of mass savings in the chuck [19] has great potential for energy savings due to the constant movement and high acceleration and deceleration of the spindle. In addition, this method of LW the table has the potential to be of lower cost due to the use of more common materials and manufacturing processes, e.g., rolling of steel I-beams. Other methods require more complex and expensive materials such as CFRP. However, to better compare energy savings due to LW, the link between mass and energy

in the table should be further explored. The next section will discuss the energy reduction potential along with design considerations.

4.5 Discussion

A reduced mass of moving components reduces energy consumption. However, when changing the mass of the MT, additional design changes are necessary, similar to what was shown in Section 4.2.1. These additional design changes include revisiting components that move and support the table, e.g., slides and ball screws. This section will first discuss the energy reduction potential followed by the necessary design changes, specifically, the motors driving the table.

4.5.1 Energy Reduction

In moving a MT table, three stages must be considered: table acceleration, constant velocity, and table deceleration. In all three stages, mass plays a role in the driving force required and thus the energy consumed. Decreasing the mass will decrease the force and therefore the required energy to move the table. The mechanical energy equation and its components can be seen in Table 4.3. η_s is the ball screw efficiency while μ is the coefficient of friction for the ways.

Table 4.3 Mechanical and electrical energy equations

	Mechanical energy $(E = F_x/\eta_s)$	Electrical energy $(E = P_{in} \cdot t)$
$F = F_{acc} + F_v + F_{dec}$	$x = x_{acc} + x_v + x_{dec}$	$P_{in} = V_{out} I$
$F_{acc} = ma_{acc} + \mu mg$	$x_{acc} = {}^1/_2\, a_{acc} t_a^2$	$P_{out} = t \cdot n$
$F_v = \mu mg$	$x_v = v t_v$	$\eta_m = {}^{P_{out}}/_{P_{in}}$
$F_{dec} = \mu mg - ma_{dec}$	$x_{dec} = {}^1/_2\, a_{dec} t_d^2$	$I = {}^T/_{K_T}$
		$T = \dfrac{Fl}{2\pi\eta_s}$

For electrical energy, it can also be seen as to why mass would play a role in reducing energy consumption for a motor. This can be seen in Table 4.3. These equations are for a DC motor, but the role of mass with respect to energy is similar for an AC motor. For a DC motor, much of the time the output voltage, V_{out}, is constant. It is set by the manufacturers of the motor. The current

will change based on the required torque. K_T is the torque constant, l is the ball screw lead, and η_s, as stated before, is the ball screw efficiency. P_{out} is the output power and η_m is the motor efficiency which depends on the ratio of the input power to the output power. This motor efficiency is based on the design load of the motor.

Choosing the right motor for the application is very important. This is because if motors are run below their designed load, or rated power, they will run less efficiently. Motors normally operate more efficiently at 75% of their rated load and above [116]. Motors that run at 50% or less of their rated load operate inefficiently due to the reactive current increase and power factor decrease. An example of this behavior can be seen in Figure 4.12. Saidur [116] found that many motors are not properly sized, in fact Capehart et al. [145] found that 75% of all motors have a load factor of less than 60%. With the reduction of mass in the table, there is a reduction in the required load for the motors to drive the table, which will lower the load factor. With this in mind, there is potential that a design change must be made in regards to the motor size.

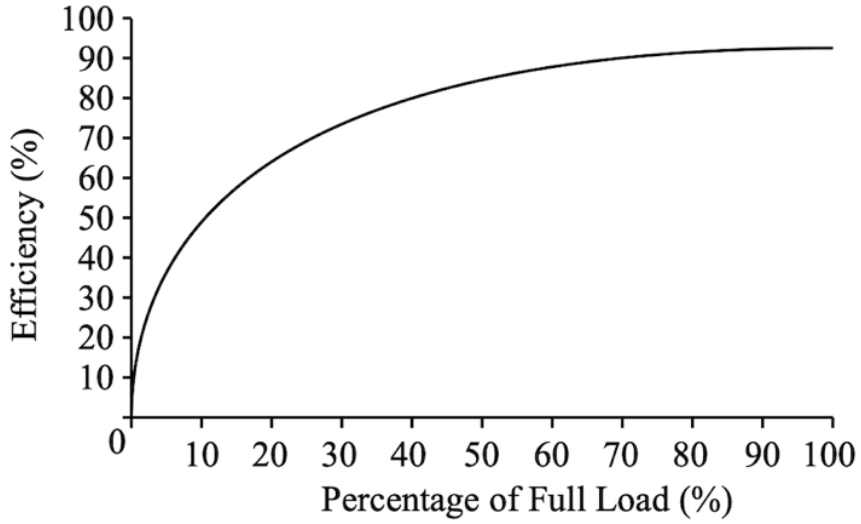

Figure 4.12 An example of a relationship between motor loading and efficiency [116]

To size the motor, a number of characteristics are needed. First the load, or required torque, should be known. Every motor has a continuous torque rating that the motor can run at indefinitely and a peak torque rating that the motor can run at for a short amount of time before overheating. Other specifications that should be known before choosing a motor include inertia/mass of the load, required speed, and required acceleration. Here we will focus on torque and inertia/mass. Standard

running speeds of machine tool tables can be calculated based on recommended cutting conditions from cutting tool manufacturers. Standard accelerations can be found from motor manufactures.

For inertia and mass, more than the mass of the table should be considered, this includes the mass of the workpiece and the inertia of the ball screw. To calculate torque the required force, lead of ball screw, and screw efficiency should be known (see Eq. (4.7)). The force equations can be found in Table 4.3, which was discussed in the previous section. Using a standard running condition along with extreme running conditions, the continuous torque and peak torque, and continuous power and peak power can be found. Then using those values, along with the required speeds of the motor, a motor can be chosen using torque-speed curves. There are other considerations to be made, such as inertia ratio, but the current focus of this chapter will be torque, speed, and power.

$$T = \frac{Fl}{2\pi\eta_s} \tag{4.7}$$

Using the equations in Table 4.3 along with some assumptions as to an "average" velocity profile, an energy savings may be calculated. Using a trapezoidal speed profile as a representative behavior together with rapid traverse during a portion of the movements, along with values for feed, speed, acceleration, and other values from MTs taken from CAM software and MT builders, an energy savings was calculated. For a mass savings of 500 kg, about 1 kWh is saved per day. This means about 2 Wh is saved per 1 kg of mass reduction. However, for this energy savings to be realized, the motor must be properly sized. From the method outlined in this section, looking at required loads and speeds, a continuous torque and peak torque along with continuous power and peak power were found for the new, lighter weight, table configuration. The power rating of the motor must be reduced by 10% to achieve these energy savings otherwise the motor will be oversized and may run inefficiently. Due to the varying types of MTs and parts to cut, e.g., size, material, features, a more detailed analysis would be needed to quantify the energy savings for a particular MT.

4.6 Summary and Conclusions

This chapter proposed a method to assist in the design of lightweight MTs. LW MTs have the potential to reduce the environmental impact of manufacturing by reducing the energy consumed by a MT. This reduction comes from reducing the power required to move a mass and properly sizing the motor for the application. To accomplish this LW, it was proposed to replace the solid table of a MT with a sandwich structure. The core of the structure would be made up of cells running horizontally along the x-axis of the table. The manufacturing of the sandwich structure table would be relatively straight forward.

Optimization of this table was accomplished through a GA. Specifically, the core of the sandwich structure was formed through the use of joined beams, where the cross-sectional shape of each beam (cell shape) was optimized through multi-objective optimization via NSGA-II where mass and strength were the objectives. The strength objectives were represented by I and J of the table since they relate directly to bending and torsion respectively. The fitness of any solution is based on the three objectives: mass, I, and J. The program was run through 100 generations and a PF was generated from the results of the objective functions for each table design. The optimized shapes ended up being similar to I-beams; this is not surprising since I-beams are very resistant to bending.

The optimized table designs provided mass savings that ranged from 216 to 777 kg. Two table designs were modeled using FEA and were shown to have similar stiffnesses to a solid table design. The lighter weight table would save energy since smaller forces would be required to move the table. To achieve the energy savings from LW, the motors that drive the table must be resized too.

This chapter has made a number of key contributions related to lightweight MTs for energy savings:

- For the first time, a LW MT application is considered for energy savings that is accomplished through the replacing of the solid table with a sandwich structure;
- A multi-objective problem is solved through a genetic algorithm that optimizes the core of a sandwich structure table with objectives of minimizing mass and maximizing I and J;

- A novel shape generation method is proposed to find the cross-sectional members of a set of parallel cross sections in a sandwich structure. This method allows for the generation of many different shapes and ease of integration into GA.

Future research directions will include the use of this method in actual design with selection of motors taking into account the inertia and speed/torque requirements of the drive system. A more detailed relationship between mass and energy will then be explored. Dynamics and vibration will be investigated as well due to the potential concerns of the changing natural frequency of the table. Finally, this method will be applied to other moving components within the MT including the spindle.

5. MODELLING THE EFFECT OF SLIDE TABLE MASS ON MACHINE TOOL ENERGY CONSUMPTION: THE ROLE OF LIGHTWEIGHTING

A version of this chapter has been submitted to the Journal of Manufacturing Systems for review

5.1 Introduction

Manufacturing plays an important role in the world's economy through the production of goods needed worldwide by consumers and industries, improvement of the quality of life, and contribution to job and wealth creation. In 2017, industry was attributed with 30% of the global Gross Domestic Product (GDP) [1] with an industrial production rate of 3.2% and accounted for 23.5% of the labor force, while manufacturing is the dominant contributor to industrial activities. In addition to its significant economic role, manufacturing has a large environmental footprint through its energy and resource consumption along with its waste streams [2]. For example, in the US during 2019 26.4% of the energy consumed among all end users was attributed to industry [129]. The utilization of fossil fuels to supply the energy demanded by manufacturing is a significant source of its large environmental footprint [25,26].

Machine tools (MTs) play a significant role in manufacturing. They are used to shape material into the desired part and are heavily used throughout industry. In 2018 their sales were $144.6 billion with a projection of $174 billion in 2023 [6]. With the widespread use of MTs in manufacturing, they contribute considerably to the manufacturing environmental footprint. Diaz et al. [24] found the largest contributor to a MT's carbon footprint is the energy consumed during the use phase, which can account for up to 80% of the energy consumption across a MT's lifecycle.

To reduce the energy consumption of MTs, there have been a number of proposed strategies, e.g., process design [11,12], process parameter selection [13,14], scheduling of machines [15], reduced cutting fluids [108], use of energy efficient components [16], and design optimization [17]. One promising method is lightweighting, i.e., to reduce the mass of moving components within the MT, since greater mass requires more energy to move. This can be seen in the transportation sector with the widespread use of lightweight materials, e.g., composites, aluminum, and magnesium, which serve to reduce component weight and produce greater fuel efficiency [18].

Kroll et al. [120] investigated lightweighting within MTs and found potential for energy reduction along with other benefits that include better process stability and increased acceleration capability. Herrmann et al. [121] examined the lifecycle impact of lightweight components and found energy savings in the use stage can offset additional impacts in the manufacturing stage.

Milling machines are a commonly used MT throughout industry. They come in many sizes and levels of complexity ranging from three to five axes and various levels of automation. A "standard" milling machine, considered in this chapter, is a three-axis mill; a sketch can be seen in Figure 5.1. With a three-axis mill, cutting can be accomplished in three directions: x, y, and z-directions. The workpiece is fixed to the top table and the table moves in the horizontal x and y directions while the cutter rotates and moves vertically in the z direction. The table moves throughout the machining of the part, thus lightweighting the slide table has potential for decreasing energy consumption, as proposed in Triebe et al. [146].

A generic power profile of a three-axis milling machine can be found in Figure 5.2. From the power profile it can be seen that when the machine is turned on there is a spike in power for a brief moment. Shortly after, the power stabilizes at a constant level that includes only the basic power. Basic power consists of power contributions from components that are always running, e.g., control system, computer, and fans. Then, the spindle is turned on and another power spike occurs and the power settles at another level that includes the basic and spindle power. The feed system is engaged and the power increases to include the feed power. Once cutting begins, there is another shift upward due to the cutting power. Once the cutting stops, the power drops back down to the power level that includes the feed, spindle, and basic power regions. When the part is quickly positioned, the feed power jumps up due to the high acceleration and speed from rapid traverse. After cutting is completed, the feed system is turned off and the power drops down to the level including spindle and basic power. The spindle is turned off and the power back drops to only include the basic power. When the machine is turned off the power drops to zero. The mass of the slide table impacts the feed power, shaded in Figure 5.2. The two peaks shaded occur when the table quickly repositions during rapid traverse and is attributed to the feed power. Reducing the mass of the table can reduce the contribution to the cumulative power from the feed power and overall energy consumption.

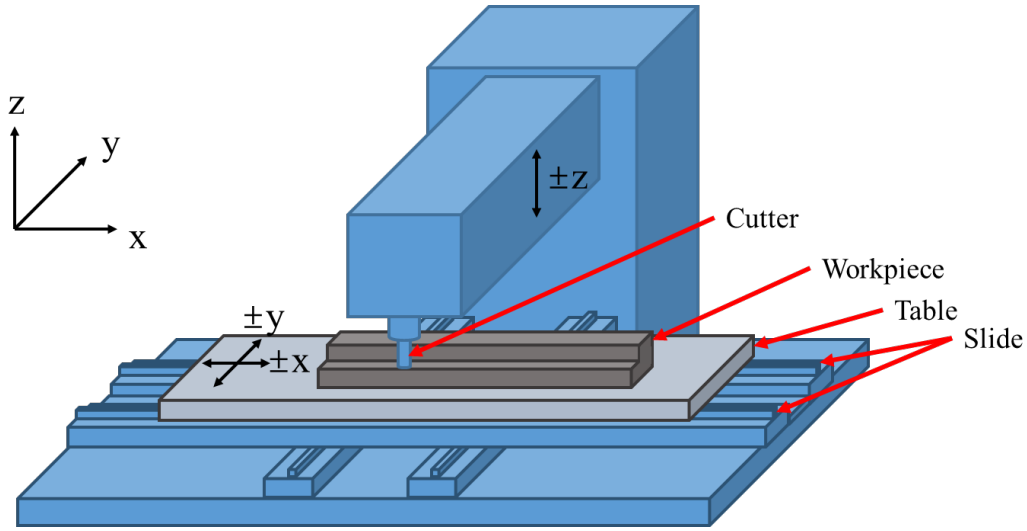

Figure 5.1 Three axis vertical milling MT

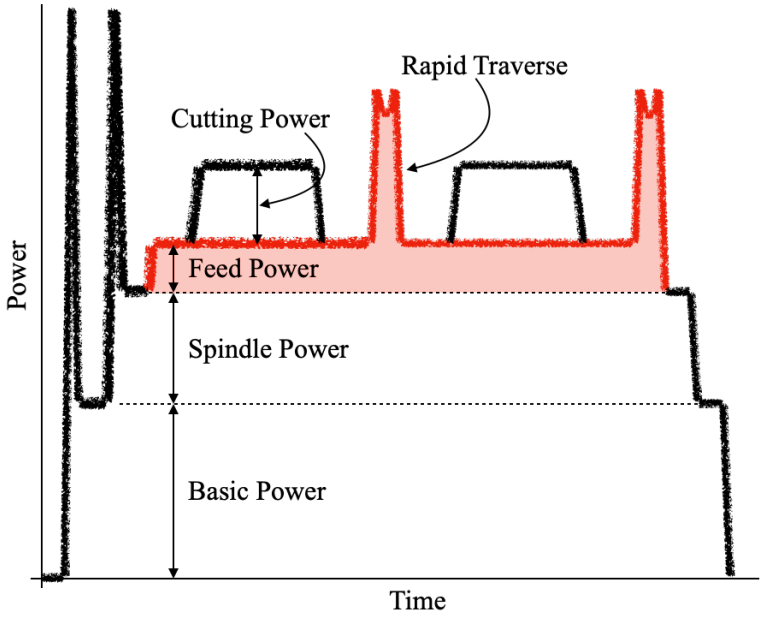

Figure 5.2 Power profile of a vertical milling machine. Mass of the table impacts the shaded portions. Adapted from He et al. [147]

Previous work by the author in Triebe et al. [146] reduced the mass of the table while considering its stiffness, but did not make the link to energy savings. Therefore, the goal of this chapter is to build an energy model to verify the power reduction and energy savings from lightweighting the table with the focus being on the feed power. Understanding how the mass of the table affects the energy consumption of the drive system along with design considerations required to implement these changes is essential to employing lightweighting. In addition, this model will provide insight into potential energy savings from lightweighting other components and systems throughout the MT. This model will consider the power required to move the table during cutting throughout a toolpath; this will include non-cutting moves during rapid traverse. Motor selection will also be covered since a lighter table provides the potential of employing smaller motors to drive the table.

Following this brief introduction, the paper will be structured as follows. First, this chapter will briefly review relevant literature pertaining to lightweighting and energy modeling. Included in this review will be a description of motor energy modeling. Then, an explanation of how the model is constructed will be provided. The paper will then present a case study to demonstrate the model. Results will then be provided followed by some discussion. Finally, the paper will summarize and conclude.

Nomenclature

a	Acceleration of the table
E	Energy
E_{mech}	Mechanical energy
$F_{c,x}$	Cutting force in the x-direction
$F_{c,z}$	Cutting force in the z-direction
$F_{c,o}$	Orthogonal cutting force
$F_{c,t}$	Thrust force
F_d	Drive force, force to move the table
F_T	Force due to the mass of the table
F_W	Force due to the mass of the workpiece
i	Gear ratio
I	Current
J_D	Inertia of ball screw
J_E	Inertia of motor-driven system
J_L	Inertia of external load
K_T	Torque constant of motor
l	Ball screw lead
L	Load fraction of motor
m	Mass of load
m_T	Mass of table
m_W	Mass of workpiece
n	Motor speed
N	Normal force
P_{in}	Power requirement of the motor
P_{out}	Power output of the motor
r	Radius of ball screw
t_f	Final time
t_0	Initial time
T_m	Torque of motor
v	Speed of the table
V	Voltage
η_g	Gear efficiency
η_m	Motor efficiency
η_s	Ball screw efficiency
μ	Coefficient of friction
ϕ	Phase angle
θ	Shear angle

5.2 Literature Review

This chapter explores the energy reduction potential of lightweighting a MT through the construction of an energy model for the slide table of a three-axis milling machine. To provide a background for the present work and understand knowledge gaps, this section briefly reviews past efforts related to i) lightweighting of MTs, ii) MT energy models, and iii) energy modeling of motors.

5.2.1 Lightweighting machine tools

Lightweighting of moving components has the potential to reduce their energy consumption due to the movement of larger mass requiring more energy. Herrmann et al. [121] reviewed the lifecycle impacts of lightweighting through lightweight materials and structures for various products, including MTs. The authors found that the environmental impact during material extraction, manufacturing, and end-of-life generally increases, but is (more than) offset by the reduced energy consumption during the use stage of the product. Kroll et al. [120] investigated the lightweighting of MTs and summarized the benefits as increased process stability, acceleration capability, and responsiveness, and decreased friction forces and reactive energy (related to inertial forces). The authors also found motor energy loss decreases as the mass decreases. From their investigation the authors summarized the lightweighting potential for various MTs: the grinding machine has the least potential and laser cutting equipment has the greatest.

Some applications of lightweighting include structural and non-moving MT components. Li et al. [124] designed a grinding machine column to reduce mass and increase stiffness using the inspiration of the branching pattern of leaf venation. Mass and deformation were decreased by 1.31% and 23.60% respectively. Zhao et al. [125] improved the static and dynamic performance of a tool column through a structural bionic method. Configuration principles from bone and plant stems were used to decrease mass and deflection by 6.13% and 45.9% respectively. These applications improved stiffness and can reduce the amount of material; however, they do not decrease the energy consumed by the MT during use phase.

Applying these methods to moving components has the potential to reduce energy. One such application includes Sulitka et al. [20] who reduced the mass of the crossbeam and columns of a

gantry MT through composites and sandwich structures. The authors were able to reduce the x-axis moving mass by 35% and the crossbeam and columns mass by 52.3%. From this mass reduction the authors were able to drive the gantry with a smaller motor that required 20% less power. Lv et al. [19] explored reducing the inertia of the spindle on a CNC lathe through the use of a lighter weight aluminum chuck. The inertia was reduced from 0.3354 to 0.2380 kg-m^2 which resulted in the reduction of energy consumption and peak power by 20.6% and 21.2% respectively. Zulaika et al. [22] increased the stiffness of the ram of a milling MT while decreasing mass through employing thinner wall thicknesses with additional/redundant guideways of the frame. The authors modeled the representative milling operations and machine dynamics to redesign the ram.

When focusing on the common milling MT, an application that provides great potential for lower energy consumption is lightweighting of the table since it will move throughout the MT's use. One such application includes Zhao et al. [127] who employed hollow stem, sandwich node, and radial root construction methods to design a lighter weight working table. The authors employed fuzzy assessment to assist in the design to determine when each construction method should be used. Suh et al. [21] reduced the mass of the horizontal and vertical slides of a large CNC MT by 26% and 34% respectively. This was accomplished through the bonding of carbon fiber reinforced polymer (CFRP) composite sandwiches to welded steel structures. In addition to the mass reduction, the authors increased the damping without sacrificing stiffness. Through this, the researchers accomplished greater positive and negative accelerations. While performance was improved for these two studies, there was no quantification of reduced energy consumption.

To summarize, the investigation into lightweighting MTs has included both applications to structural/stationary components and moving components with various goals including improved performance, greater stiffness, and reduced energy consumption. The motivation for lightweighting structural/stationary components was to increase stiffness, which will help improve precision but not reduce energy consumption. The goal of lightweighting moving components comprised both of improved performance and decreased energy consumption. These applications include gantry machines, lathes, and milling machines. The research regarding milling machines has focused on the ram, slides, and table. However, there was no quantification of energy savings for either the slides or the table. One method for quantifying energy savings is to build an energy model. The next section will review literature focusing on MT energy models.

5.2.2 Energy modeling

Energy consumption within MTs must be understood and quantified to identify energy saving potentials. Energy modeling and prediction provides this insight of energy flow within MTs. There have been a number of influential papers in the area of MT energy modeling. One of these foundational studies by Gutowski et al. [148] showed how for some MTs the fixed energy consumption is a significant portion of the total energy consumed. The authors showed that the act of cutting can account for but a fraction of the total energy consumed by the MT. Zein [7] further showed the reason for the fixed energy consumption of a MT being so large is due to the effect of automation on power demand. As machines became more automated with more technology included, more systems and components consume energy and the energy consumption due to machining has become a smaller portion of the total energy. Therefore, the overall energy profile has become more complex and modeling the energy consumption of a MT has also become more complicated.

To address this complexity of MT energy consumption there have been a number of energy models built. One form of energy models employed are empirical. These models consist of equations with parameters tuned to power and energy measurements. These include Yoon et al. [36] who built an empirical model to predict the power consumption of a three-axis milling machine. The goal was to relate power to process parameters such as rotational speed, feed, and depth of cut. The authors ran an experiment testing various process parameters while measuring the power and tool wear. Luan et al. [149] built empirical models to predict power consumption of a vertical mill during non-cutting conditions. The authors modeled the basic power, feed power, and spindle idle power. Experiments were run to measure the power of each system and models were fit to the measured data. He et al. [147] built an empirical model for multiple machines. The inputs to this model include the machine choice, type of cut, part design, part material, and cutter selection. The model would then use the CAM file along with an energy-related database to output a power and energy profile. Deng et al. [43] built an empirical model to investigate the specific cutting energy (SCE) and the effects various cutting parameters have on it. Kara and Li [44] and Li and Kara [45] also built empirical models to investigate SCE. Through these two models the authors found a strong relationship between SCE and material removal rate (MRR). As MRR increases SCE decreases. Empirical models may be accurate, but they are built for a single machine;

for each separate machine the model must be recalibrated. These models can advise on how to run the machines, e.g., higher MRR, but would be less helpful in informing design of MTs.

A different modeling approach provided by Balogun and Mativenga [150] was built based on power consumption measurements of various systems. The authors found how much power each system draws when running, then multiplied that power by the time each system is active. The total energy consumption is the sum each individual system's energy. This model has similar limitations to the empirical models discussed earlier in that it must be adapted to each machine through energy/power measurements.

Dietmair and Verl [41] and Verl et al. [40] took a different approach to modeling energy consumption. Similar to Balogun and Mativenga, the authors model energy consumption of systems and components separately but are built from mechanistic calculations of power instead of measurements. Larek et al. [151] simulated power consumption through dividing the total machine power into the individual components powers. The authors used an on/off approach to simulate each component's power and then merged the power together through signal analysis to predict the overall power consumption. This simulation modeled a 2-axis turning machine. Lv et al. [19] built an energy consumption model of the spindle of a CNC lathe based on its acceleration. This model was built from two components: spindle rotation power and spindle acceleration torque multiplied by the spindle motor speed. The model was verified through experiments that included accelerating from various starting speeds to various ending speeds. Time, power, and energy were recorded. These models built off of power relates more directly to the mechanics of the machines and allows for more insight into how to design these machines to consume less energy. While these four models were applied to turning, there is potential in applying these models to systems of a milling machine.

Avram and Xirouchakis [152] modeled energy consumption of a milling machine through power requirements based on the cutter location, spindle speed, and feed rate as specified in the NC code. The authors predicted variable mechanical power and fixed power, and calculated the area under the power curve to find the energy. There is potential to improve this model through the consideration of mass and motor sizing.

Other methods to model energy consumption include Eisele et al. [46] where the authors simulated energy consumption through the modeling of the energetic interactions of the components in a MT. The authors applied this method to the coolant system by modeling the

coolant pump using the electrical equations of the motor. This method could be improved through expanding it to model other systems of the MT. Bi and Wang [50] built an energy model based on the kinematic and dynamic behaviors of a MT. This model helps connect design variables to the energy consumption through the relationship with the manufacturing processes. The authors applied their model to an Exechon machine. There is potential in applying this model to systems of a milling machine.

These models provided different methods to predict energy consumption of MTs. This chapter will now transition from modeling MT energy to modeling motor energy which varies based on load requirements. This next section will explain how drive system requirements relate to a motor's efficiency in order to better understand how to model the table drive system's energy consumption.

5.2.3 Motor energy modeling

Motors are used to transform electricity into mechanical power. In the case of a table feed motor, the motor transforms electricity into mechanical power required to move of the table. This mechanical power overcomes the forces opposing motion including the cutting force and friction forces; these will be discussed later.

Motors are not 100% efficient, which means more electrical power is delivered to the motor than the power the motor produces. These inefficiencies are due to a number of losses that is common to all electrical motors: friction and windage losses, iron losses, stray losses, and wire resistance losses [116]. There has been work to reduce these losses, e.g., kinetic energy recovery [153], larger conductors to reduce resistance [116], and lower friction bearings. However, for this chapter, the focus is not on motor design, but addresses motor selection with an eye towards energy reduction.

Motors are designed for a specific load and speed. Running a motor above these intended loads and speeds for a significant length of time can reduce the life of the motor. In addition, as Figure 5.3 indicates, the efficiencies are poor when a motor operates below the designed load and speed. Therefore, choosing the right motor for the application is very important. Motors running at 75% or greater of their rated load operate more efficiently [116], but when running at 50% or less, motors operate inefficiently due to the increase in reactive current and decrease in power

factor. Saidur [116] and Capehart et al. [145] found many motors have not been properly sized. Capehart et al. found from their energy audit experiences that 75% of all motors run with a load factor that is less than 60%.

Motor selection will be covered later within the energy model section, i.e., Section 5.3.4. However, it is important to understand how to calculate motor efficiency and power. The efficiency of the motor can be calculated from Eq. (5.1). P_{in} is the electrical power input to the motor and P_{out} is the power required from the motor to move the table. P_{out} is calculated using Eq. (5.2). T_m is the torque of the motor and n is the rotational speed. The torque can be related to the force required to move the table through Eq. (5.3) and the rotational speed related to linear velocity through Eq. (5.4) where F_d is the drive force, l is the lead of the ball screw, η_s is the ball screw efficiency, η_g is the gear efficiency, and v is the speed of the table. P_{in}, for alternating current, is defined in Eq. (5.5) as voltage (V) times current (I) times the cosine of the phase angle (ϕ) between voltage and current, known as the power factor. For a direct current motor P_{in} defined as voltage times current (no power factor). Current, defined in Eq. (5.6), is torque (T_m) divided by the torque constant (K_T). The torque constant is determined by the designers of the motor and allows the current to be calculated through the required torque.

Another method to calculate P_{in} is through the efficiency curve of the motor. Every motor has an efficiency curve based off its load fraction defined as required power divided by rated load. An example can be found in Figure 5.3. Knowing the efficiency curve along with the power requirement, P_{out}, the motor efficiency can be found along with the input power to the motor, P_{in}.

$$\eta_m = \frac{P_{out}}{P_{in}} \tag{5.1}$$

$$\mathrm{P_{out}} = T_m \cdot n \tag{5.2}$$

$$T_m = \frac{F_d l}{2\pi \eta_s \eta_g} \tag{5.3}$$

$$n = \frac{2\pi v}{l} \tag{5.4}$$

$$P_{in} = V \cdot I \cdot \cos\phi \tag{5.5}$$

$$I = \frac{T_m}{K_T} \tag{5.6}$$

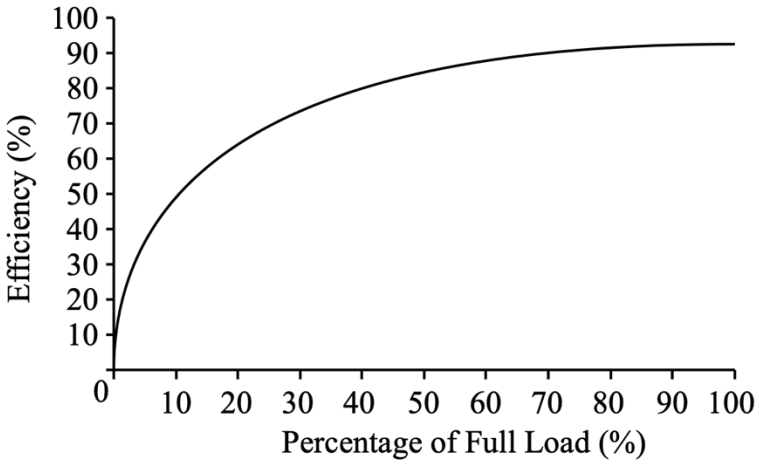

Figure 5.3 An example of a relationship between motor loading and efficiency [116]

5.3 Slide Table Energy Model Formulation

To build an energy model of the table, an understanding of the table drive system, kinematics, and loading must be achieved. This will provide clarity into how the mass of the table affects the drive system energy consumption and any design changes required to implement lightweighting. In addition, this will offer insight into potential savings of applying lightweighting to other components and systems throughout the MT. This section will start off by explaining the configuration of the feed drive components along with the table, then will go into the analysis of forces and movement of the table.

As stated earlier, to cut the workpiece, for a three axis mill the workpiece is clamped to the table and the table moves in the x and y-direction. In some cases, the table will move in the z direction but in many cases the cutting tool will move in the z-direction. For this energy model it is assumed only the tool moves in the z-direction. To allow movement, the table rides on slides in the x-direction and on slides in the y-direction, as shown in Figure 5.1. However, the slides do not move the table; they allow for low friction movement. Instead, a motor attached to a ball screw or lead screw moves the table. For the table to move, the motor must overcome the combination of the cutting force and the table/workpiece friction force. In addition, there are losses in the motor and screw. The forces and motion can be found in the free body diagram in Figure 5.4.

The energy model is built based off these forces, motions, and losses. Each component of the free body diagram will be explained in the following sub sections to show how the model is

built. These sections will consider motion of the table in one direction (X direction), but it is a straightforward matter to extend the model to consider motions in the other directions (Y and Z).

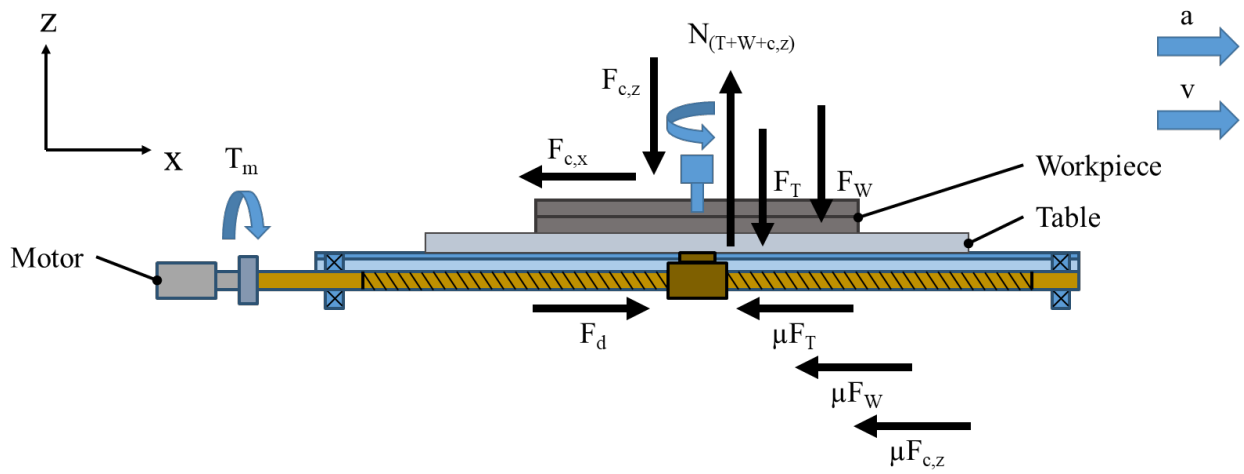

Figure 5.4 Free body diagram of the slide table, x and z directions only

5.3.1 Forces acting on the table

To calculate the energy required to move the table, first we must examine the forces acting on the table (see Figure 5.4). These forces can be separated into two categories: forces associated with the table and workpiece, and forces associated with a machining operation. First, we will examine the forces due the table and workpiece. Gravity acts on the table and workpiece and produces a force due to their mass; these forces act in the downward negative z-direction. Because of friction in the slide the table moves on and in the ball screw, these two forces produce a frictional force that opposes movement. Throughout cutting, the mass of the workpiece changes which results in a changing friction force. Yet, some chips remain on the table during cutting and therefore it is difficult to quantify the friction force due to uncertainty in the mass of the workpiece. With this in mind, the mass of the workpiece was assumed to be constant, and equal to the average of the mass of the uncut and finished workpiece. To move the table the motor must exert a force greater than the frictional forces associated with the mass of the table and the mass of the workpiece. In this chapter the frictional forces are assumed to always be kinetic friction. Static friction was not included since the table is moving during most of the cutting with very few instances of accelerating from a zero velocity.

Forces are associated with a machining operation due to the cutting mechanics of the workpiece. To cut the workpiece, enough force must be exerted to shear the material. This force can be represented by two orthogonal components: the cutting force and the thrust force. Depending on the type of cutting, these two forces can be resolved in all three directions, the x, y, and z components; these can be seen in Figure 5.4. The x and y-components of the cutting force directly oppose, or aid, the motors while the z-component increases the friction force opposing the motor. Therefore, from this free body diagram, it can be seen that the force the motor must overcome, in regards to the cutting force, is the cutting force in the x-direction (or y-direction) plus the coefficient of friction times the cutting force in the z-direction.

Calculation of the cutting forces is less straightforward than the table and workpiece forces. The cutting force constantly changes very quickly and with a periodic shape. Since the table has a large mass, the motor will not see the high frequency variation of the cutting force. This is similar to the case of applying a high frequency force to a spring-mass system with a large inertia. Therefore, the average cutting force is used to calculate power and energy. However, when choosing an axial motor, as described in Section 5.3.4, the maximum force is used. To calculate the average cutting forces in the x, y, and z-directions, first the orthogonal cutting force ($F_{c,o}$) and the thrust force ($F_{c,t}$) must be found. A diagram of orthogonal cutting during milling with the orthogonal cutting force is shown in Figure 5.5 where v_c is the cutting velocity, $F_{c,R}$ is the resultant force, α is the tool rake angle, and β is the friction angle. The orthogonal cutting force depends greatly on the material being cut, the type of cutting, e.g., milling or turning, geometry of the cutting tool, and the MRR. Knowing these, the orthogonal cutting force can be approximated. The orthogonal cutting force can be found using Eq. (5.7) and the thrust force found using Eq. (5.8).

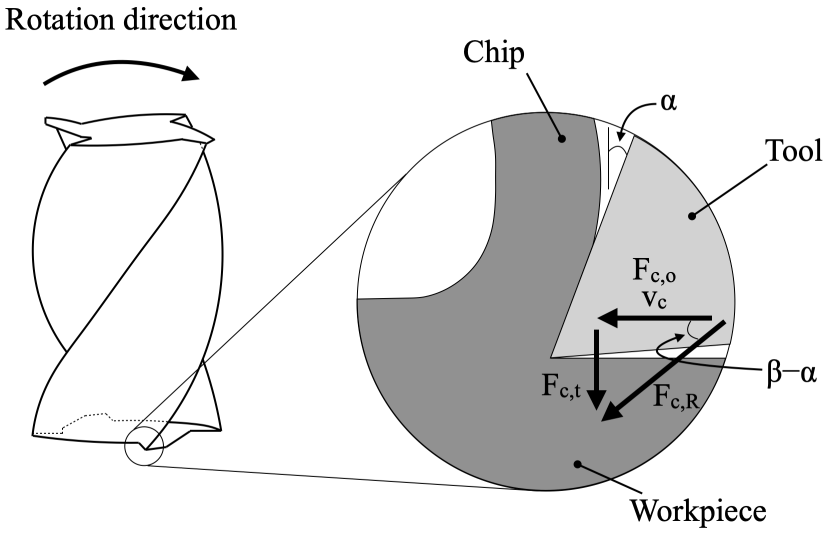

Figure 5.5 Diagram of orthogonal cutting during milling, adapted from Sutherland and DeVor [154]

$$F_{c,o} = \frac{P_u \times MRR}{v_c} \tag{5.7}$$

$$F_{c,t} = \tan(\beta - \alpha) \times F_{c,o} \tag{5.8}$$

where P_u is the specific cutting energy. The specific cutting energy is dependent on the material being cut and can found in the Machining Data Handbook [155]. The thrust force is found through the Merchant circle using the tool rake angle (α) and the friction angle (β). The friction angle (β) can be approximated through simple experimental data such as found in Cook [156]. With the orthogonal cutting force and thrust force, the x, y, and z-components of the cutting force can be found using the method in Pang et al. [157].

5.3.2 Motion of table

Another significant component of building the energy model is understanding the table motion. This is because energy is the integral of power over time and power is defined as force times velocity. The movement of the table can also change the required force since the force depends on whether the table is moving at a constant velocity or is accelerating or decelerating.

Forces vary due to the inertia term, mass times acceleration, which exists when the table has positive or negative acceleration. Friction forces are always present.

As stated earlier, the table will move in the x and y-directions in order to cut the part. This movement will follow a predefined tool path. The velocity is determined by the feed and the acceleration is determined by the motor capability and the velocity profile. For rapid traverse movement of a machine tool in the x-direction, we consider the trapezoidal velocity profile shown in Figure 5.6. To realize this profile the motor will undertake a constant acceleration at the start of the motion and a constant deceleration at the end of the motion. Of course, physically realizing this step change in acceleration may not be possible in reality but it is a reasonable approximation for this work. For other table movements the acceleration may not be constant and will be determined by the toolpath, such as during curved paths. Using the velocity profile along with the desired feed and acceleration, the velocity can be calculated throughout cutting. This can be applied for all three axes.

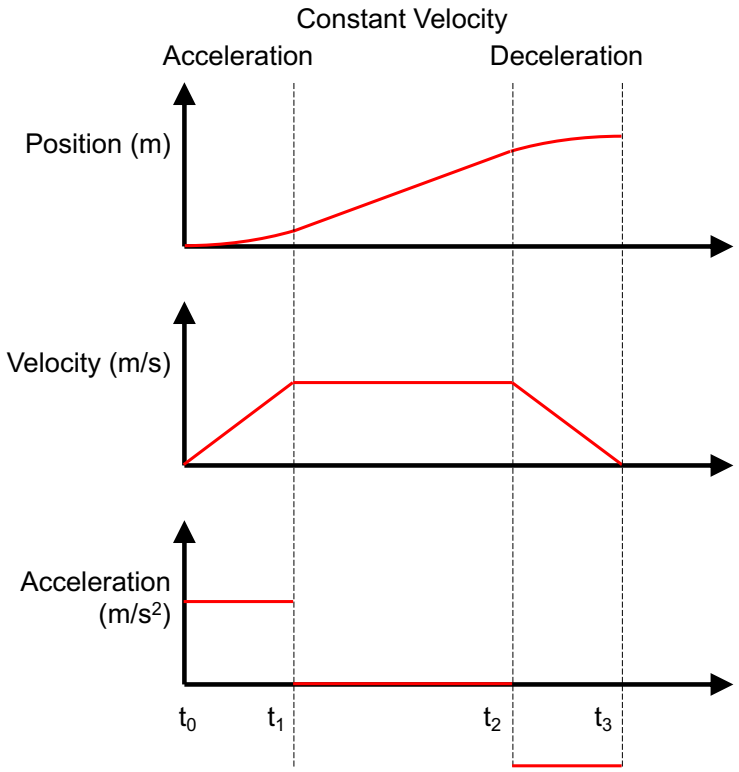

Figure 5.6 Trapezoidal velocity profile of the table

5.3.3 Mechanical energy

Mechanical energy is needed to move a machine tool table. In this case we are interested in the energy required to change its position and velocity. Therefore, mechanical energy is found by calculating the change in kinetic energy, also known as work. Work can be calculated by integrating force times velocity with respect to time. To solve for the work, we can combine the discussion in 5.3.1 with 5.3.2.

Since mechanical energy considers only the position and velocity of the system, the motor losses are not included. For this system the mechanical energy is the energy required to move the workpiece and table while cutting. Mechanical energy can be found using Eq. (5.9) where t_0 and t_f are the starting and ending times, F_d is the drive force, v is the table velocity, η_s is the ball screw efficiency, and η_g is the gear efficiency.

$$E_{mech} = \int_{t_0}^{t_f} \frac{F_d v}{\eta_s \eta_g} dt \tag{5.9}$$

The drive force (F_d) is calculated using Eq. based off of Figure 5.4 where μ is the coefficient of friction, F_T and F_W are the forces due to the mass of table and workpiece, $F_{c,x}$ and $F_{c,z}$ are the cutting forces in the x-direction and negative z-direction, m_T and m_W are the masses of the table and workpiece, and a is the acceleration. The velocity is found from the tool path using the feed, acceleration, and a velocity profile (see Figure 5.6) as discussed in Section 5.3.2. The friction and losses from the ball screw and gear are considered in the energy equation by efficiency constants η_s and η_g respectively. These efficiency constants can be found from the ball screw and gear manufacturers.

$$F_d = \mu\left(F_T + F_W + F_{c,z}\right) + F_{c,x} + (m_T + m_W)a \tag{5.10}$$

Mechanical energy can also be viewed in terms of the required motor torque and speed. The torque is calculated using the drive force, lead of the screw, the screw efficiency, and the gear efficiency (Eq. (5.3)). The motor speed is calculated from the feed or velocity and the lead of the

screw (Eq. (5.4)). The mechanical energy can be found by integrating the product of the torque and speed with respect to time (see Eq. (5.11)).

$$E_{mech} = \int_{t_0}^{t_f} T_m n \, dt \tag{5.11}$$

5.3.4 Power and energy demand of a motor

The mechanical energy is smaller than the actual energy consumed due to losses in the drive system, e.g., motors, table slides, ball screws. These losses can be calculated from efficiencies for each component. The motor efficiency is dependent on its instantaneous running conditions since each motor is designed for a particular load and speed. When the motor is run at a different load and speed, particularly a smaller load, the motor will run less efficiently; higher loads may cause the motor to fail. Due to the wide range of loads and speeds for machining, the motor will rarely run near its targeted efficiency. Therefore, it is important to include motor efficiency in the energy model due to its significant impact on the energy consumed.

To calculate the actual energy requirement, the instantaneous motor efficiency must be known. To find the motor efficiency, first we must know what motor is being used. This section will describe the steps associated with motor selection based on the system requirements and then show how the energy can be calculated.

For this energy model the author selected servo motors from Yaskawa and Siemens. Servo motors are normally utilized in machine tools due to their low inertia and superior dynamic response [158]. Due to the wide range of operating requirements for the axis motors, a variable speed drive has the potential to increase the motor efficiency due to its ability to adjust its supplied power voltage and frequency to meet these operating requirements. However, due to their slower response to speed and load changes servo motors are a better option for axis movement.

When selecting a motor, one has to consider that mechanical energy the motor can deliver relies on the motor efficiency (ηm) (see Eq. (5.1)) and the motor efficiency is dependent on the required load and the motor's rated load. To choose the right motor for the application, the maximum and continuous power, torque, and speed requirements must be found. The inertia of the motor-driven system must be known as well, since system performance (e.g., responsiveness,

avoiding natural frequencies) depends on the ratio of the load inertia to the motor inertia (inertia ratio). A typical inertia ratio is 5:1, for highest performance 2:1 or less is used, and when performance is not critical 10:1 or higher is used. The requirements on power, torque, and speed, can be obtained from Eq. (5.12), Eq. (5.3), and Eq. (5.4), respectively. Inertia of the motor-driven system can be calculated by Eq. (5.13) where JD is the ball screw inertia, JE is the external load inertia, and i is the gear ratio. The ball screw inertia is found using Eq. (5.14) where m is the mass of the ball screw and r is the radius of the ball screw. The external load inertia is found from Eq. (5.15) where m is the mass of the load and l is the lead of the ball screw.

$$P_{out} = \frac{F_d v}{\eta_s} \tag{5.12}$$

$$J_L = \frac{(J_D + J_E)}{i^2} \tag{5.13}$$

$$J_D = \frac{m \cdot r^2}{2} \tag{5.14}$$

$$J_E = m \cdot \left(\frac{l}{2\pi}\right)^2 \tag{5.15}$$

Once these values are found, and an inertia ratio chosen, a motor can be selected. When selecting a motor, it is desired to choose the smallest possible motor to increase efficiency and responsiveness; an oversized motor is inefficient and can be unresponsive. However, the motor rated output must be at least as large as the required continuous power. The maximum power must be below the peak torque-speed curve (torque times speed equals power). The required continuous and maximum torques must be less than or equal to the rated torques of the motor. The maximum and continuous speeds must also not exceed the motor capabilities. The moment of inertia (MoI) of the motor must meet the inertia requirement stated earlier.

With a motor selected, the motor efficiency can be calculated using the current load and the motor efficiency. However, motor manufacturers may not provide efficiency equations. Though manufacturers may provide efficiency, torque, and speed curves that equations can be fit to such as Siemens [159]. To address the lack of efficiency data, Burt et al. [160] created various motor efficiency curves (efficiency as a function of load %) for different motor sizes. Using these efficiency curves, or ones provided by the manufacturer, efficiency equations can be fit to these

curves using software tools, such as the trendline function in Microsoft Excel or the fitobject function in MATLAB. Then, the load fraction (load divided by rated load) can be plugged into the efficiency equation to find the motor efficiency. With the motor efficiency the actual power requirement can be found (see Eq. (5.1)) and the energy consumption can by determined by Eq. (5.16):

$$\mathrm{E} = \int_{t_0}^{t_f} \frac{F_d v}{\eta_s \eta_g \eta_m} dt \tag{5.16}$$

When a motor is decelerating, there is a possibility that the energy consumption can be negative. This happens when the inertia force is negative due to a negative acceleration and is greater than the friction force and the cutting force. When the energy is negative, energy is produced instead of consumed and can be recovered. However, for this chapter it is assumed that when power demand is negative any energy produced is dissipated through a resistor instead of being recovered.

5.4 Case study: Lightweighting of a Machine Tool Table

To demonstrate the effectiveness of lightweighting, a case study was carried out in which two tables were analyzed: a standard table (ST) and a lightweight table (LT). Both are made of steel, AISI 1045, and have the overall dimensions of 134 mm tall by 610 mm wide and 1270 mm long. The LT is constructed of two plates, the upper having t-slots machined into it, and I-shaped cross sections running the length of the table instead of being solid, see Figure 5.7. These I-shaped cross sections have dimensions that match the standard I-beam shape designated by S3 x 5.7 which consists of 76.2 mm (3 in) tall and 59.2 mm (2.33 in) wide with a web thickness of 4.3 mm (0.17 in) and a flange thickness of 6.6 mm (0.26 in). This design was chosen based on previous work of the author where the core was optimized to consider the tradeoffs between stiffness and mass (see Triebe et al. [146]). The mass of the ST is 778.055 kg while the mass of the LT is 457.853 kg. Two workpieces, both made of steel, ASTM-A36, are used to build an energy model based off their associated toolpaths. One measures 457.2x154.2x76.2 mm^3 (W1) while the second is 254x254x76.2 mm^3 (W2). The fixturing used to affix each of the workpieces to each of the tables

was assumed to have a negligible mass. The cuts for both workpieces are carried out via an end milling operation. The intent is to remove a section from W1 measuring 25.4x25.4x457.2 mm^3, along the shoulder, and a section of 127x127x25.4 mm^3 from W2, a pocket. These two workpieces were chosen due to their differing cutting conditions. W1 has a more aggressive cut due to its high feed while W2 requires more change in direction and therefore higher accelerations. These two workpieces are illustrated in Figure 5.8. The average mass of W1, based on its before and after machining state, is 40.573 kg and the average mass of W2 is 37.045 kg.

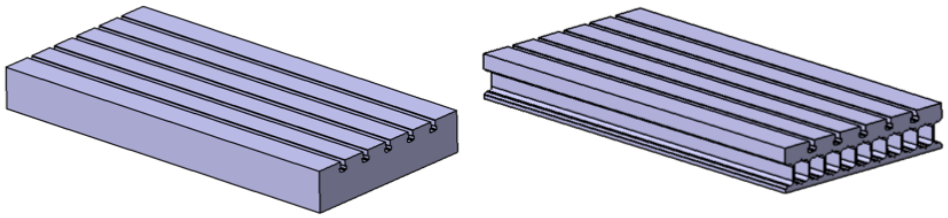

Figure 5.7 Graphical depictions of the Standard Table, ST (left), and Lightweight Table, LT (right)

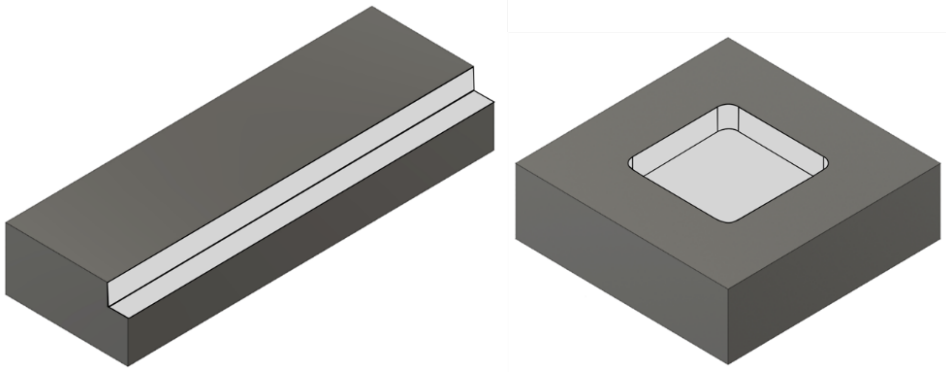

Figure 5.8 Illustration of the two workpieces, W1 on the left and W2 on the right

Autodesk Fusion 360 CAM software was used to create toolpaths for both workpieces which were exported to Microsoft Excel and MATLAB. For W1 a 25.4 mm diameter solid carbide end mill was chosen to cut the shoulder and for W2 a 12.7 mm diameter solid carbide end mill was chosen to cut the pocket. Speeds and feeds were selected by the software and verified against the tool manufacturer's recommendations. For W1, aggressive cutting conditions with high speeds and feeds were employed, and for W2 lower speeds and feeds were utilized. Using these two toolpaths

an energy model was created for both the ST and the LT. The parameters used in this model, including mass and friction, are summarized in Table 5.1 and Table 5.2.

Table 5.1. Table and workpiece force parameters

Mass of ST	$m_{ST} = 778.055$ kg
Mass of LT	$m_{LT} = 457.853$ kg
Average mass of W1	$m_{W1} = 40.573$ kg
Average mass of W2	$m_{W2} = 37.045$ kg
Acceleration	$a_{acc} = a_{dec} = 2460$ mm/s^2
Coefficient of friction	$\mu = 0.15$

Table 5.2. Cutting force parameters

	W1	W2
Material removal rate	$MRR = 502.566$ cm^3/min	$MRR = 122.903$ cm^3/min
Spindle speed	$n_s = 3820$ rpm	$n_s = 3000$ rpm
Cutter radius	$r_c = 12.7$ mm	$r_c = 3.175$ mm
Specific cutting energy	$P_u = 0.050$ kW/cm^3/min [155]	

The next step in building the energy model is to choose motors for both the ST configuration and the LT configuration. As stated in Section 5.3.4 motors are generally selected based on the peak and continuous requirements for power, torque, and speed of the drive system. Of course, for a machine tool there are many operations that can be done which requires a wide range of power, torque, and speed. The motor must be able to operate at these various requirements. The two workpieces W1 and W2 represent this range – W1 uses aggressive cutting conditions while W2 employs lower speeds and feeds. The peak and continuous requirements values can now be calculated based on the two cutting conditions associated with W1 and W2. The peak conditions were calculated considering the largest potential cutting force; as described earlier the cutting force varies periodically. Due to the high torque requirement, two gear ratio settings between the motor and the ball screw were considered: no gear and a gear ratio of 2:1. This will reduce the required torque but increase the speed and decrease the inertia which can allow for use of a smaller motor. In addition to peak and continuous power, torque, and speed requirements the motor must also satisfy the required inertia ratio. For this model the author wanted an inertia ratio near 2:1. The peak and continuous power, torque, and speed requirements, along with the required motor inertia for both the no gear and gear conditions are displayed in Table 5.3, Table 5.4, and Table 5.5. These

values are associated with W1 since its cutting conditions are more aggressive and require a motor that offers high power, torque, and speed. In selecting the motor for these "worst case" cutting conditions, it is to be noted that the peak torque is equal to the continuous torque; this is the case since the largest torque takes place during cutting (when large cutting forces are occurring), which represents a significant portion of the time that the table is moving. The values in Tables 3 and 4 were used to guide motor selection.

Table 5.3. Peak and continuous requirements for no gear configuration

	ST		LT	
	Peak	Cont.	Peak	Cont.
Power (kW)	2.0	0.24	1.2	0.23
Torque (Nm)	12.0	12.0	11.1	11.1
Speed (rpm)	3000	195	3000	195

Table 5.4. Peak and continuous requirements for gear (2:1) configuration

	ST		LT	
	Peak	Cont.	Peak	Cont.
Power (kW)	2.0	0.24	1.2	0.16
Torque (Nm)	6.0	6.0	5.5	5.5
Speed (rpm)	6000	389	6000	389

Table 5.5. Inertia requirements for inertia ratios of 2:1 (kg-m^2)

	No Gear	Gear 2:1
ST	26.2×10^{-4}	6.57×10^{-4}
LT	20.4×10^{-4}	5.1×10^{-4}

For the energy model, all combinations of the following variables were considered: two table conditions (ST and LT) and two gear ratios (no gear and 2:1). It was desired for all four configurations to have an inertia ratio (load to motor inertia) of about 2:1. The smallest possible motor was selected for each configuration. These motors can be found in Table 5.6. The goal is to compare across table designs to see if lightweighting will save energy. Part of the benefit of lightweighting is the potential to use a smaller motor. When not using a gear, it was possible to select a smaller motor for the LT configuration (30D to 20D). However, when using a gear, it was not possible to select a smaller motor for the LT configuration due to limited motor selection. Some parameters of the motors can be found in Table 5.7.

Table 5.6. Motor selection

	No Gear	Gear 2:1
ST	Yaskawa SGM7G-30D	Siemens 1FK7080 CT-5AF71
LT	Yaskawa SGM7G-20D	Siemens 1FK7080 CT-5AF71

Table 5.7. Motor parameters

Motor:	SGM7G-		1FK7080 CT-5AF71
	20D	30D	
Rated Output (kW)	2.0	2.9	2.14
Rate Torque (Nm)	6.36	18.6	6.88
Max Torque (Nm)	19.1	45.1	25
Rated Speed (RPM)	3000	1500	3000
Max Speed (RPM)	6000	3000	6000
MoI ($\times 10^{-4}$ kg·m^2)	2.47	46	15

Having chosen the motors, the instantaneous motor efficiency found in Eq. (5.1) can now be calculated. Using data from Siemens [159] a motor efficiency curve (see Figure 5.9) was constructed for the three motors. In Figure 5.9 the load percentage is the actual power divided by rated power. An efficiency plot was provided in Siemens [159] and a curve was built using the fitobject function in MATLAB to match the plot. Using the motor efficiency curve and Eq. (5.16), energy consumption can be found.

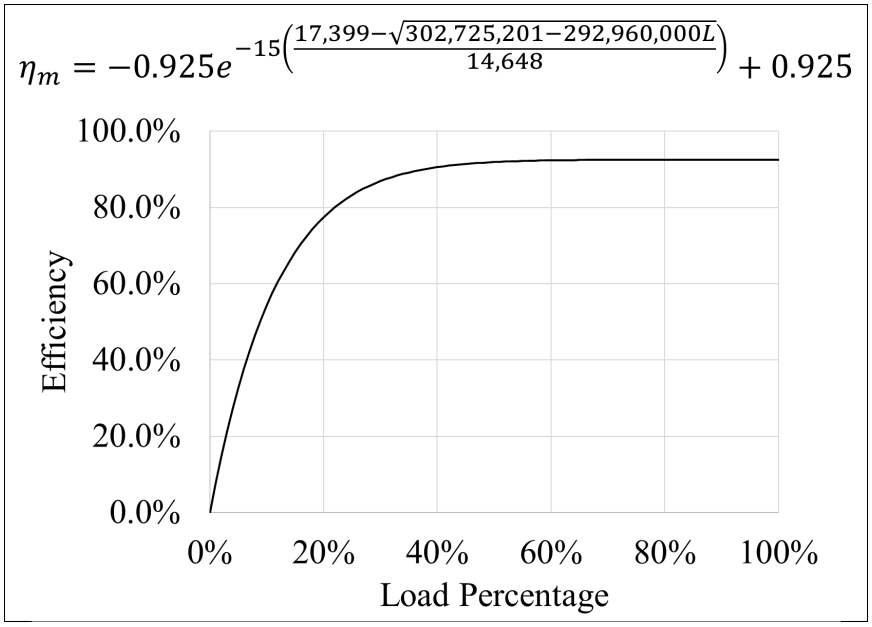

Figure 5.9 Motor efficiency curve and equation

5.5 Results and Discussion

The energy consumption was calculated for each of the four configurations (based on the parameters in Table 5.1 and Table 5.2). These energy values also depend on the motor characteristics in Table 5.7. The results will be presented in this section and a discussion of factors affecting energy consumption will follow. This will provide understanding into how mass affects the drive system energy consumption and the design considerations, i.e., motor sizing, required for lightweighting the table. This will also provide insight into the energy savings that can be achieved by applying lightweighting to other components and systems throughout the MT.

5.5.1 Results

The results for the four configurations can be found in Table 5.8. For the no gear condition changing from a ST to a LT allowed for the use of a smaller motor and therefore a significant energy reduction, 29.37% for the cutting of W1 and 37.81% for the cutting of W2. When a gear was used, a smaller motor could not be selected that met the torque requirement since the difference in torque requirement between ST and LT was much smaller. Motor selection was limited to Yaskawa SGM7 models and Siemens 1FK7 models. This resulted in a much smaller energy reduction, 5.73% for the cutting of W1 and 0.26% for the cutting of W2. The difference in power consumption between the ST and LT for the no gear condition can be seen in Figure 5.10. The portions related to cutting and rapid traverse are labeled (in Figure 5.10(a), the portion of the profile that is indicated with the dashed line is examined in more detail in Figure 5.11). For W2, the portions of the profile where the power drops to zero are associated with table motion that is only occurring in the y-direction.

Table 5.8. Energy results

	No Gear		Gear 2:1	
Workpiece	W1	W2	W1	W2
Time to Cut (s)	39	524	39	524
ST Energy (kJ)	19.7	315.0	240.5	233.1
LT Energy (kJ)	13.9	195.9	15.4	232.5
Savings (kJ)	5.8	223.2	7.4	0.5
Savings (%)	29.37%	37.81%	5.73%	0.26%

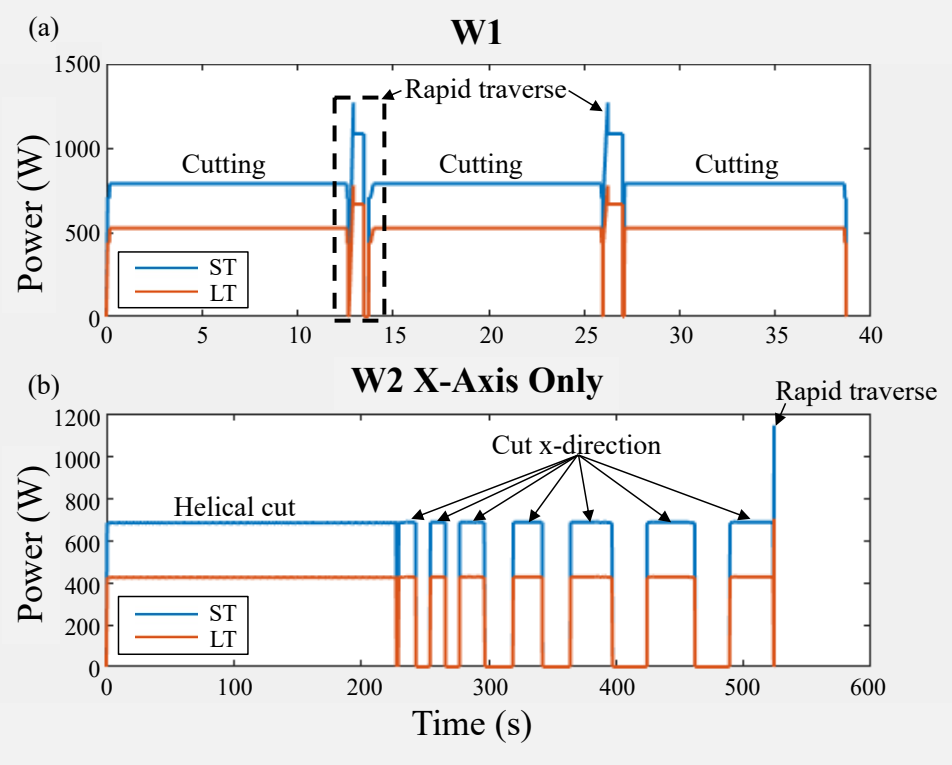

Figure 5.10 LT and ST power for both workpieces (no gear) – a. workpiece W1, b. workpiece W2 x-axis only

These results show that lightweighting can save a significant amount of energy when applied to systems with moving components; a 30% energy savings from lightweighting various systems throughout the MT is not trivial. These results also show motor selection within the drive system is very important. Without a properly sized motor, the savings from lightweighting may not be realized as can be seen in the model with a gear. For this model a smaller motor could not be selected for the LT which resulted in a much lower energy savings (see Table 5.8). Therefore, when applying lightweighting to other systems within the MT, motor sizing must be considered to achieve maximum energy savings. It should be noted that this energy savings will scale based on the size of the table, meaning a smaller table will still save roughly 30% energy consumption. However, due to the need for resizing the motor, there is a greater chance that this energy savings is lost for smaller designs due to the difficulty of choosing a slightly smaller motor as mass savings decreases.

The importance of properly sizing the motor comes from the motor's efficiency. Much of the time the motor is operating at load percentages between 5% and 20% load percentage. A small

increase in the load percentage can greatly increase the motor efficiency, see Figure 5.9. The reason for this small load percentage comes from the large range of operating requirements for the motor. As stated in Section 5.3.4, a variable speed drive has the potential to increase the efficiency due to its ability to adapt to the varying requirements by adjusting its input power voltage and frequency. Though, due to their slower response to speed and load changes, servo motors are a better selection for axis movement. The motor must be able to run at a relatively low speed during cutting but also at a much faster speed during rapid traverse. During cutting the required torque is high while during rapid traverse the torque is much lower. The cutting torque must be less than the rated torque, as opposed to the peak torque, due to the length of time this torque is required. However, during cutting the power is small due to the relatively low required speed. During rapid traverse, the power increases greatly due to the high speeds and high acceleration despite the torque being small. Since rapid traverse occurs for short periods of time, the power requirement during these movements can fall under the peak power of the motor instead of the rated power. Because such a large torque is required during cutting with only a small amount of power, and the largest power requirement only occurring during a short amount of time (rapid traverse), the driving requirement is the torque during cutting. This model shows the energy reduction through lightweighting is possible because the torque during cutting is reduced.

5.5.2 Experimental validation

To validate the results from the case study, the author compared power calculations to experimental findings in the literature. Luan et al. [149] built empirical models for the basic power, feed power, and spindle power of a milling machine during non-cutting conditions. Measured power was provided at various feeds. To measure the feed power, the feed was run at a constant rate until the total machine power reached steady state, then the steady state spindle power and the steady state basic power were subtracted from the total power. The author measured power from a YCM-V116B vertical milling machine in which the axis motor power was 3.8 kW. Table mass was approximated from specifications of a similar machine (YCM-TV116B) since the YCM-V116B is a discontinued model from the manufacturer's website [161]. The coefficient of friction along with the ball screw efficiency were estimated since they were not provided. The machine parameters used in the power calculations can be found in Table 5.9.

Power was calculated for the y-axis motor of the machine since the x-axis motor moved both the table and slides while the y-axis motor moved only the table. Since dimensions of the table were provided on the manufacturer's website, a table mass could be calculated, but details on the slides were not provided. Therefore, a more accurate power calculation could be found for the y-axis motor than for the x-axis motor. The measured power and calculated power for various feeds can be found in Table 5.10. The feed is staggered at uneven intervals since some feeds were used by Luan et al. [149] to build their empirical model and some were chosen at random to test their model. The feed values 500, 1,000, 2,000, 3,000, 4,000, 5,000, and 6,0000 mm/min were used to build their empirical model while the feed values 300, 800, 1,300, 2,800, 4,300 mm/min were used to test their empirical model. From the calculations found in Table 5.10 it can be seen the mechanistic model built in this chapter has lower a prediction capability when the machine is run at a low speed and power demand, but the prediction capability increases greatly as the speed and power demand increase.

Table 5.9. Machine parameters used for power calculation

Mass of table (kg)	720
Coefficient of friction	0.15
Ball screw efficiency	0.97
Axis motor power (W)	3,800

Table 5.10. Measured and calculated y-axis power

Feed (mm/min)	Measured power (W)	Calculated power (W)	Percent error
300	362.08	479.30	32.4%
500	372.01	481.17	29.3%
800	391.59	483.98	23.6%
1,000	410.22	485.86	18.4%
1,300	402.4	488.69	21.4%
2,000	449.65	495.34	10.2%
2,800	475.13	503.02	5.9%
3,000	479.44	504.95	5.3%
4,000	508.41	514.70	1.2%
4,300	515.85	517.65	0.3%
5,000	543.8	524.59	3.5%
6,000	557.35	534.61	4.1%

5.5.3 Other influences on energy consumption

To further study the significance of lightweighting, it is important to look at other factors influencing energy consumption. To do this it is useful to examine the power profile and the factors that contribute to it. For the cutting of W1, the power profile consists of two sections: cutting and rapid traverse (see Figure 5.10(a)). The portion relating to cutting occurs for a majority of the time and the power profile is flat. During this portion the forces consist of the friction and cutting force. There is no inertia force since the table feed is constant and there is no change in direction. For other workpieces and tool paths, such as that associated with W2 where the path is not linear, the inertia force can also occur during cutting. However, the inertia force is relatively small during cutting since the accelerations are low.

A closer view of the power and forces during rapid traverse, as labeled in Figure 5.10(a), for the ST is provided in Figure 5.11. In Figure 5.11 the forces associated with inertia, friction, and cutting are shown in Figure 5.11(a), the power associated with inertia, friction, and cutting are shown in Figure 5.11(b), and the required mechanical power (power demand, P_{out}) and required electrical power to the motor (motor power, P_{in}) are shown in Figure 5.11(c). This figure shows 9

regions, which are separated by vertical dashed lines, which will be used to explain the contributions to the power.

For this portion of the power profile, there is no power contribution from cutting (since no cutting is occurring), as seen by regions 2 through 8. In Figure 5.11, the cutting stops at the end of region 1. During region 2, the table is traveling at the same speed as during cutting but without material removal. Then at the beginning of region 3, the table starts to decelerate and comes to a stop at the end of region 3. At the beginning of region 4 the table begins accelerating to the rapid traverse rate. When the table reaches the rapid traverse speed (see region 5), the acceleration is zero and the table travels at a constant speed. At the beginning of region 6 the table begins decelerating as it approaches the start of the next cutting pass. When the table stops, seen at the beginning of region 7, it accelerates to the speed used during cutting. Then, the table speed reaches the targeted feed for cutting (region 8) and travels at a constant velocity and then cutting starts (region 9).

Building upon the table motion discussion of the previous paragraph, let us turn our attention to the forces. Figure 5.11(a) shows the forces acting on the table and the sum of the forces during the 9 different regions. Within each region the forces acting on the table are constant due to the assumptions of acceleration equaling the maximum motor acceleration, friction always equaling kinetic friction, and the cutting force equaling the average cutting force. During cutting (regions 1 and 9) the cutting force and the friction force act on the table, but there is no inertia force. During regions 2 and 8 the table is moving at constant speed but there is no cutting (no inertia or cutting force). During this time only the friction force acts on the table. Then in regions 3 and 6 while the table decelerates there is a negative inertia force, and of course a friction force, acting on the table. Region 6 lasts for a longer time than region 3 since the table is decelerating from a much higher speed. In regions 4 and 7 the friction force and a positive inertia force act on the table. Region 4 occurs for a longer portion of time due to the final speed being much greater than in region 7. Then, in region 5, while the table travels at the rapid traverse speed only the friction force acts on the table.

Figure 5.11(b) displays the power corresponding to the forces in Figure 5.11(a) (inertia, friction, and cutting forces) and the sum of the power (power demand). Despite forces being assumed to be constant, the powers corresponding to these forces vary due to the changing table speed. The power demand in Figure 5.11 (c) is the sum of the power components, same as in Figure

5.11(b) and the motor power is the required input power to the motor (see Figure 5.9 and discussion in Section 5.2.3). During regions 3 and 6, the power demand (see Figure 5.11(b) & (c)) is negative due to a negative inertia force from deceleration. The motor power is zero due to the assumption made in Section 5.3.4 that there is no regeneration; no energy is recovered.

Knowing the relative contributions of forces (and thus, the powers) associated with such elements as cutting, friction due to table/workpiece, and acceleration allows one to begin to understand the factors that affect energy consumption. These factors include mass (table and workpiece), friction, acceleration, ball screw efficiency, and the cutting force. Examining each may reveal the factors that have the greatest impact on energy consumption.

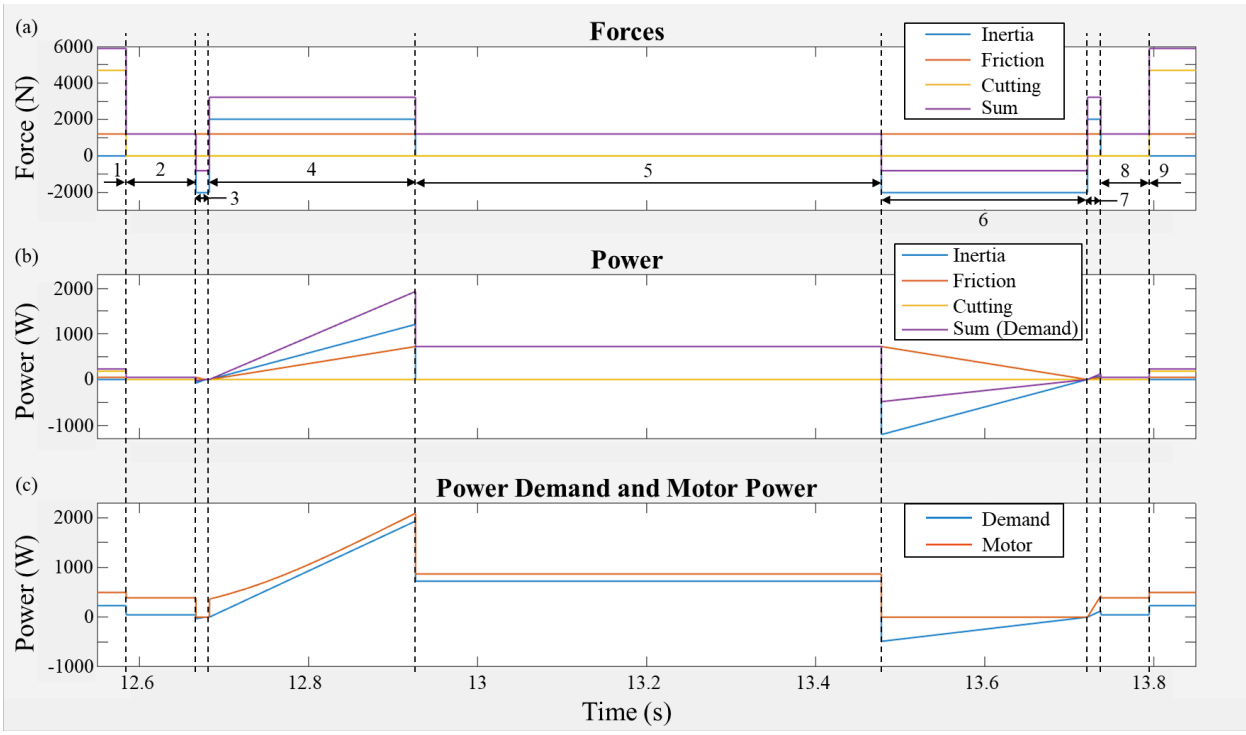

Figure 5.11 Drive system (a) forces, (b) power, and (c) power demand and motor power during rapid traverse associated with W1 employing a ST

Mass impacts the energy through both the inertia force and the friction force. This means that during both cutting and non-cutting table movements, mass plays a role. Reducing the mass of the table will reduce the power throughout the use of the machine as is evident in Figure 5.10. Similarly, friction impacts the energy throughout the use of the machine; when moving the table, the friction term will always be present. Therefore, reducing friction is also an important method

to reduce the energy consumption. However, reduction of friction will not affect the inertia term. This term will only be affected by the mass and the acceleration of the table.

As seen in Figure 5.11(a), the friction force is significantly greater than the inertia force much of the time since the table is not accelerating during the cutting passes of W1. While cutting W2 the inertia force is greater than zero for portions of the toolpath due to a change in direction but is very low due to low acceleration requirements during cutting. However, when the speed is ramping up to the rapid traverse speed (and when the speed is dropping following a rapid traverse motion) the acceleration is non-zero and the inertia force is present. Due to high velocities and acceleration, the power is very large, as seen in Figure 5.11(b) and (c). This large inertia force only occurs for a short amount of time but is significant due to its impact on motor selection.

The acceleration affects the energy consumption through the inertia term, as stated above. Acceleration plays a larger role in more complex toolpaths where changes of direction are more common, e.g., pockets, since a direction change requires acceleration/deceleration. However, acceleration requirements during cutting are low as a result of slow speeds. Therefore, reducing the maximum acceleration value will not significantly reduce energy consumption during cutting. For rapid traverse movements, reducing the maximum acceleration will reduce the maximum power and therefore influence motor selection. The ball screw efficiency also directly relates to energy consumption. However, most ball screw efficiencies are 90% and higher; the ball screw efficiency used here was 97%. A slight improvement in ball screw efficiency will not appreciably affect power demand.

The cutting force greatly impacts the energy consumption since the force is very large compared to the force to move the table and workpiece. However, reducing the cutting force may be challenging due to the required force to remove material. Therefore, reducing the mass and friction may be the most effective methods to reduce energy consumption. This is due to the impact both have on the forces throughout the use of the table.

5.6 Conclusions

This chapter has proposed an energy model of the MT slide table to demonstrate the potential energy savings from lightweighting. This model provides understanding into the effect that mass of the table has on the energy consumption of the drive system along with design considerations

required to implement lightweighting. This will also provide insight into the energy savings that can be achieved by applying lightweighting to other components and systems throughout the MT. The energy savings resulted from the reduced power required to move the LT and the reduced size of the motor. The energy savings was found to heavily rely on the proper sizing of the motor.

To formulate the energy model, three individual models were constructed: a table model, a workpiece model, and a cutting force model. These three models were combined together to form an overall energy model of the slide table. The individual models consisted of the forces attributed to the components of these models, e.g., force due gravity, cutting force, and friction force. These forces were calculated for the various sections of a cutting path, i.e., accelerating, constant velocity, and decelerating portions. Using these forces and speeds, motors were selected for this application and then motor efficiency was calculated. Finally, the energy required to move the table to cut a workpiece was calculated for three models. One model used a gear ratio of 2:1 between the motor and the ball screw while the other two models had no gear but different motors.

It was found that lightweighting of the table reduces the energy required to move the table; a savings of up to 38% in energy is possible for the LT relative to the ST. These results show that lightweighting can save a significant amount of energy when applied to systems with moving components; a 30% or greater energy savings from lightweighting various systems throughout the MT is not trivial. These results also showed the greatest amount of energy is saved when the smallest motor for the application is used. Therefore, when applying lightweighting to other systems within the MT, motor sizing must be considered to achieve maximum energy savings. To employ the smallest possible motor for the drive system it was found that reducing the continuous torque, associated with overcoming the friction and cutting forces, and the inertia of the drive system should be minimized. Both can be reduced through lightweighting of the slide table (while the cutting force cannot be reduced, the friction force can). It should be noted that this energy savings will scale based on the size of the table, meaning a smaller table will still save roughly 30% energy consumption. However, due to the need for resizing the motor, there is a greater chance that this energy savings is lost for smaller designs due to the difficulty of choosing a slightly smaller motor as mass savings decreases.

This chapter has made a number of key contributions and observations related to the modeling and lightweighting of MTs for energy savings:

- This chapter created an energy model of the slide table based on tool path and the components of the table mass, workpiece mass, and cutting force;
- A LT was found to have the potential to reduce the energy consumption of the feed system by up to 38%;
- To fully realize the energy savings from lightweighting, the motor must be properly sized for the application.

In terms of future work, an experimental investigation should be performed to confirm the energy/power benefits of lightweighting. In addition, the effect of table lightweighting on the dynamic response of machine tools must be studied. Cost should also be examined since while a lightweighting design change may reduce the material cost of the machine, it may increase complexity and manufacturing cost.

6. DEVELOPMENT OF A MODEL TO ASSESS THE IMPACT OF LIGHTWEIGHTING ON THE DYNAMIC AND STATIC PERFORMANCE OF A VERTICAL MILLING MACHINE

6.1 Introduction

With manufacturing playing such an important role in the global economy through providing 25% of the global labor force and contributing significantly to the global Gross Domestic Product (GDP) [1], it also has a significant environmental footprint. This footprint is a product of its waste generation and its energy and resource consumption. In 2020, the industrial sector in the US accounted for 36% of end-use energy consumption [4] where a significant portion of the electricity generated comes from fossil fuel sources [5]. Additionally, in 2018, 28% of the electricity generated worldwide by fossil fuels was attributed to industry [162].

Machine tools (MTs) are an important piece of manufacturing equipment that shapes and form material into desired products through processes such as cutting, grinding, forming, and bending. MTs are commonly used worldwide throughout industry. In 2008 MT sales were $119.7 billion and have grown to $144.6 billion in 2018. Demand is expected to continue to grow to $174 billion in 2023 [6]. MTs vary in size, technology, and purpose. Over the years they have increased in technology and complexity while becoming more powerful and automated.

MTs also have a significant environmental footprint through their energy consumption. Reducing the environmental footprint of MTs will help reduce manufacturing's significant footprint. Some methods to reduce MT energy consumption include adjusting process parameters and cutting conditions [11,13], implementing a control system to adjust the machine state [73], designing machines with more efficient components [16,70], and scheduling of machines [15].

One promising method is designing MTs with lighter weight components, i.e., lightweighting. Lightweighting is a design strategy that reduces the mass of a product with a goal of reducing its energy consumption. It has been used with great success in the transportation sector, e.g., automobiles and airplanes. Lightweighting reduces energy consumption due to lower masses requiring less energy to move. Lightweighting of MTs can be effective when applied to moving components. Kroll et al. [120] investigated mass reduction of MTs and found energy consumption can be reduced along with the potential for improving acceleration and enhancing process stability.

Herrmann et al. [121] found the energy savings during the use stage of the MT offsets any potential increase in energy consumption during other lifecycle stages, e.g., increased manufacturing energy requirement due to manufacturing a more complex part.

However, when reducing mass of a MT, there is concern of how it will affect its static and dynamic performance. When changing a design to reduce the mass, there is potential for a reduction in stiffness which will affect the machine's static performance. Greater deflections can occur while the machine is running due to large forces the machine exerts, and depending on what components and systems in the machine were changed, the quality of parts made can be affected. This change in stiffness will also impact the dynamic performance of the MT through a potential change in the natural frequencies. Vibrations naturally occur in a MT due to the running of the different systems, e.g., motors, pumps, and cutting. When these vibrations approach the natural frequencies of the components and systems of the MT, very large vibrations can be produced. The large vibrations can impact the quality of the parts made by the machine and potential harm the machine.

One commonly used MT is the vertical mill. Vertical mills shape material through multi-point cutting and is accomplished by processes such as face milling and peripheral milling. To cut, the material is clamped to the table and the tool spins to cut the workpiece. This form of cutting differs from a lathe where the workpiece spins instead of the tool. An example of a commonly used vertical mill can be seen in Figure 6.1. This milling machine is known as a three-axis machine where the table moves in the x & y-directions while the cutter moves in the z-direction. Some machines have 4 or 5 axes where the table or tool can rotate about one or two additional axes. For the setup shown in Figure 6.1, the table moves throughout cutting and provides a potential application of lightweighting to reduce the energy consumption of the MT. To reduce the mass of the table, sandwich panel designs are employed.

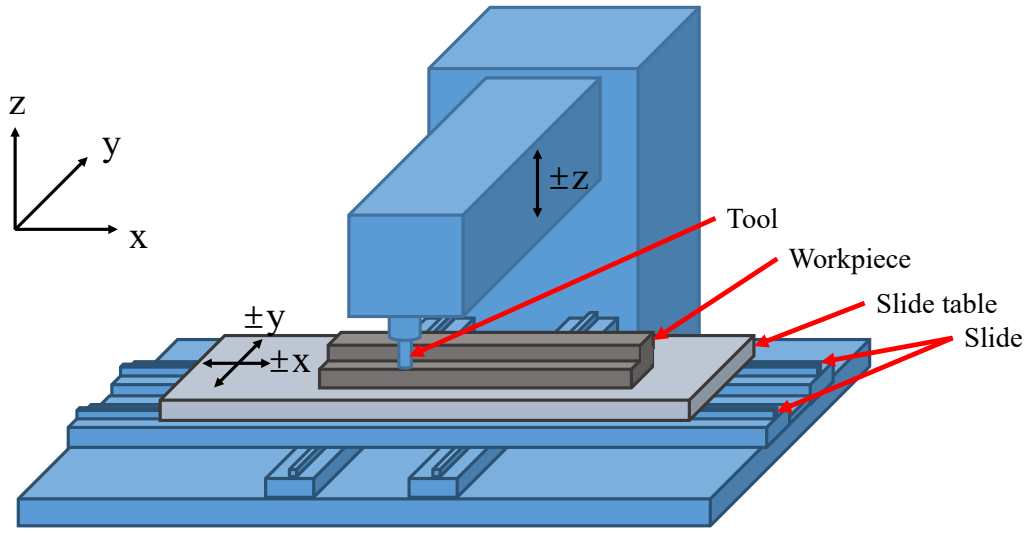

Figure 6.1. Sketch of a vertical milling machine

When reducing the mass of the table in order to reduce the MT energy consumption, static and dynamic performance of the table may be of concern and should be investigated. To address this concern, this chapter built and analyzed a static and dynamic model using finite element analysis (FEA). FEA was chosen due to the complexities of evaluating the static and dynamic performance of a plate, and since the lightweight table designs (sandwich panels) varied greatly from a plate, a different form of analysis was needed. To analyze the static and dynamic performance of the slide table, multiple lightweight table designs were considered and compared to a standard solid table. A finite element model (FEM) is first built for the various lightweight table designs to compare their strength through calculating an approximate stiffness. The FEMs are then used in a frequency analysis to evaluate the dynamic performance of the different table designs. The static results are compared with the dynamic results and help validate frequency analysis due to stiffness being directly related to natural frequency. The paper is be constructed as follows. First, the paper explores where the static and dynamic concerns come from in regards to lightweighting. Then in the same section relevant work of other authors is reviewed. The focus here is of how the authors investigated these concerns and how they were addressed. Following, the construction of the static and dynamic models will be described. Then the results from the static and dynamic analysis will be provided. A discussion of the results will follow and finally the paper will conclude.

6.2 Investigation into static and dynamic concerns

6.2.1 Static and dynamic concerns for lightweighting the table

The table has multiple forces acting on it at once and in different directions. These forces consist of the drive force from the motor, gravity forces from the workpiece and table, and the cutting forces. The forces acting on the table can be seen in the free body diagram found in Figure 6.2. These forces can induce deflection in the table and the periodic nature of the components and systems applying these forces can cause vibration. The table drive motor and the ball screw rotate at varying frequencies, dependent on the required speed of the table. The cutting force is constantly changing due to the shape and rotation of the tool. A sketch of an end mill cutter can be found in Figure 6.3(a). The cutting force is dependent on the shape of the cutting tool, the amount of material being removed, and the rotation of the tool. An example of a milling cutting force profile can be seen Figure 6.3(b). The tool rotates very quickly and produces a rapidly changing periodic force.

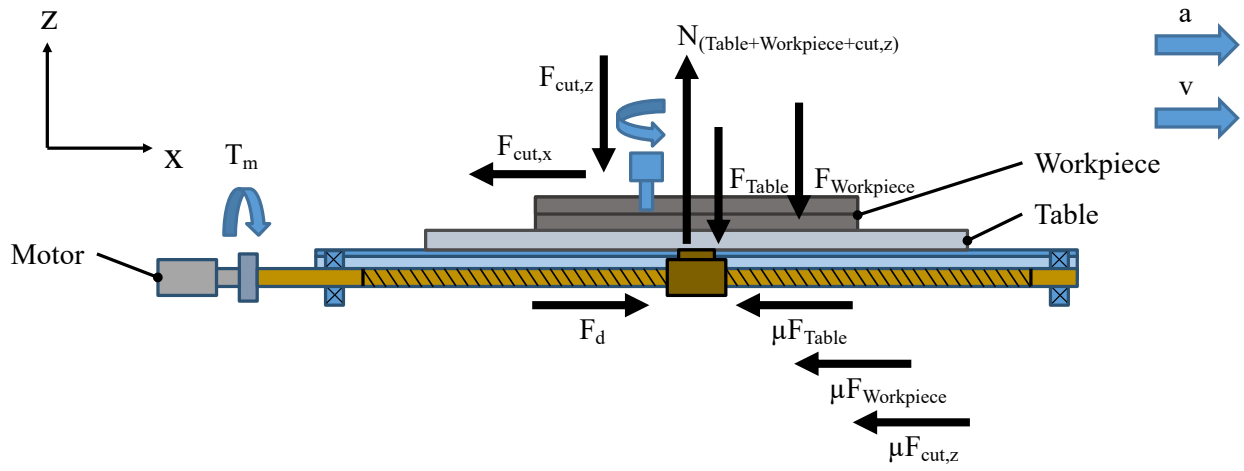

Figure 6.2. Free body diagram of the table

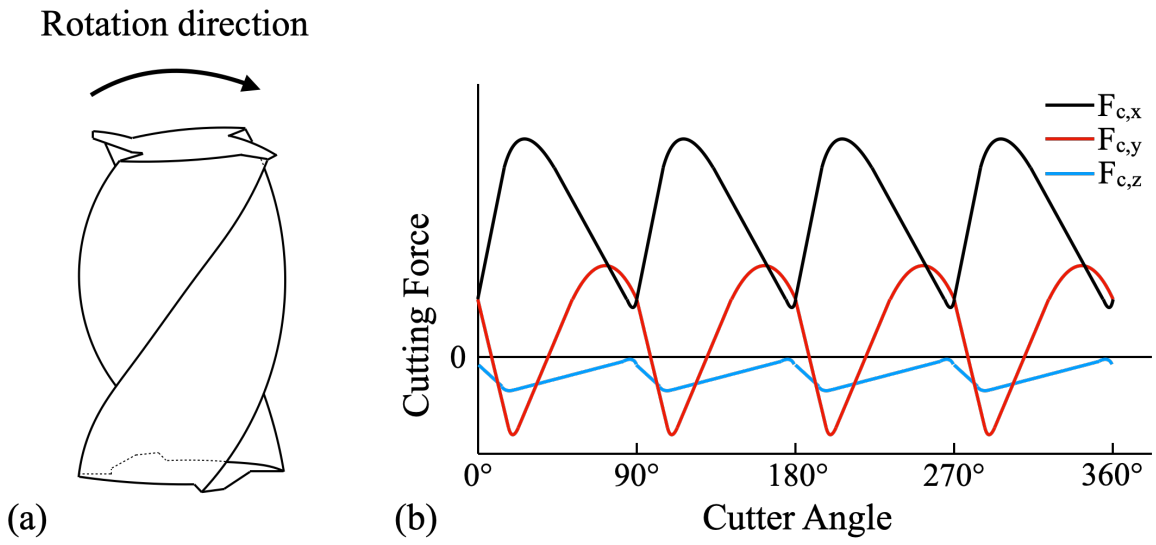

Figure 6.3. (a) End mill sketch, adapted from Sutherland & DeVor [154] (b) Example milling cutting force based on cutter rotation angle, Pang et al. [157]

With these large forces and high frequencies, the MT needs to have a large enough stiffness to reduce deflection as a result of these forces and to have large natural frequencies so as to avoid any vibration near these frequencies. With a goal of lightweighting the table, it must be seen how reducing mass will affect the table's static and dynamic performance. Since static performance has been examined in an earlier paper by the author (Triebe et al. [146]), this chapter will focus on the dynamic performance of the table. A poorer dynamic performance will mean increased vibrations which will result in poorer quality parts produced.

A significant factor in dynamic performance is stiffness since stiffness directly relates to natural frequency as shown by Eq. (6.1)

$$\omega_n \propto \sqrt{k/m} \tag{6.1}$$

where ω_n is the natural frequency, k is the stiffness, and m is the mass. When there is no damping, natural frequency is equal to the right side of Eq. (6.1) but when the system is more complicated calculation of natural frequency becomes more complicated too. As is evident by Eq. (6.1), dynamic performance can be improved (an increase in natural frequency) by an increase in stiffness or a decrease in the mass.

Changing stiffness or mass by itself is not a simple matter since the two are normally linked. This can be seen by taking a closer look at stiffness. Stiffness is defined by Eq. (6.2) where F is the force and δ is the deflection as a result of the applied force. Deflection of a plate (solid table) under three-point bending can be calculated by Eq. (6.3) and deflection of a sandwich panel (lightweight table) under three-point bending is calculated by Eq. (6.4) where l is the distance between the supports, E_p is the elastic modulus of the plate, I_p is the MoI of the plate, E_s is the elastic modulus of the sandwich panel, I_s is the MoI of the sandwich panel, A_s is the area of the cross section of the sandwich panel, and G_s is the shear modulus of the sandwich panel [163]. I_p and I_s relate to mass since moment of inertia (MoI) is defined by the Eq. (6.5) where m_i is the mass of the different point masses and r_i is the distance of each point mass from the axis of rotation.

$$k = F/\delta \tag{6.2}$$

$$\delta_p = \frac{Fl^3}{48E_pI_p} \tag{6.3}$$

$$\delta_s = \frac{Fl^3}{48E_sI_s} + \frac{Fl}{16A_sG_s} \tag{6.4}$$

$$I = \sum_i m_i r_i^2 \tag{6.5}$$

Since mass and stiffness are linked, it is important to consider both while designing MTs in order to improve dynamic performance.

6.2.2 Past efforts to quantify and improve MT dynamics

There has been past investigation into improving the dynamics of MTs. These included lightweighting methods and other design strategies. Abuthakeer et al. [164] investigated various lightweight designs of the bed of a CNC lathe. The authors analyzed the different designs using FEA and validated the results experimentally. The authors found a hollow bed design with vertical ribs decreased mass by 3.29%, decreased deformation by 4.05%, and increased the stiffness by 7.77%. Suh et al. [165] explored improving the vibration characteristics of a lathe spindle steel cover through reinforcing it with carbon fiber epoxy material. The authors determined the stacking sequence of the fibers through FEA while considering the mounting conditions and the vibration

modes. The authors increased the resonant frequencies by 60-80% and were able to increase the dynamic loss factor by about 3-5 times.

Aggogeri et al. [123] explored the effect lightweight materials can have on dynamics by analyzing stiffness of lightweight rams using FEA and then comparing with a modal analysis. The three configurations of the ram studied were aluminum foam sandwich, aluminum corrugated sandwich, and carbon fiber. The authors found on average an increase in stiffness by about 20%. Zulaika et al. [22] explored reducing the mass of the ram on a large milling machine through thinner walls and additional guideways for increased stiffness. To investigate its effect on machine dynamics, the authors built a model using FEA and ran a modal analysis. The redesigned ram reduced the machine mass by 20% and had a lower peak at the resonant frequency. Suh and Lee [21] proposed composite slides for large milling machines to improve acceleration and deceleration. The authors calculated the stiffness of the composite slides through a model of three-point bending and compared with an FEA. The authors used the FEM to estimate deflection under acceleration and compared with an impact hammer response test. The composite designs reduced the mass for the horizontal and vertical slides by 26% and 34%, respectively, while increasing damping by 1.5 to 5.7 times without losing stiffness.

Zhao et al. [125] designed a bionic tool column through configuration principles of plant stems and bone. The authors analyzed the bionic tool column through FEA and physical experiments. The mass and maximum deformation of the column decreased by 6.13% and 45.9% respectively with the first natural frequency increasing by 37%. Li et al. [124] also designed a bionic grinding machine column through a self-optimal growth method with a goal of increasing stiffness and decreasing mass. The authors carried out both FEA and physical experiments to find deformation and natural frequencies. The bionic design decreased mass by 1.31%, decreased maximum deformation by 23.6%, and increased the first natural frequency by 18.55%. Venugopal et al. [166] investigated using epoxy granite to increase the static and dynamic performance and damping of a milling MT column. The authors built an FEM of a traditional cast iron column and compared it to models of 9 different epoxy granite column designs. The design chosen had an equivalent stiffness but improved natural frequencies of 12-20%.

As is evident from past work and earlier discussion in this section, knowing stiffness, mass, and natural frequencies are important to provide insight into the static and dynamic performance of the machine. It is important to understand how changes in design impact the deformation of the

component and its role in vibration (static and dynamic performance). To gain this understanding in regards to the slide table, models will be built and analyzed using FEA. Two separate analyses will be conducted: first to analyze the static performance of the table a static analysis is carried out, and second, to analyze the dynamic performance a frequency analysis is carried out. The static analysis will provide an approximate stiffness that can be compared among the lightweight table designs and the standard solid table design to assess a difference in performance. The frequency analysis will provide the natural frequencies of the table designs along with their mode shapes. Comparisons of the natural frequencies will also provide an assessment in performance. The following section will describe the model creation.

6.3 Model construction

Four table designs are analyzed in this study. One design is a standard solid table while the other three are lightweight designs. The three lightweight designs are sandwich panel structures and are proposed in Triebe et al. [146] and Triebe et al. [126]. Two types of analyses were carried out on the various table designs: a static analysis and a dynamic frequency analysis. Both are conducted using FEA. The static analysis is carried out to provide an approximate stiffness that is compared between the lightweight table designs and the solid table design to evaluate differences in static performance. For the stiffness model, a force is applied in four locations, but each is analyzed individually. The four forces are all applied in the same quadrant with one being applied to the center of the table. The locations of the forces are described in more detail in Section 6.3.2 . The dynamic frequency analysis was conducted to determine how the dynamics of the slide table will change with lightweighting. The mode shapes and natural frequencies are observed and compared between the table designs. The following subsections will describe the table designs and the static and dynamic analyses.

6.3.1 Table designs

Four table designs were analyzed using FEA. These consisted of a solid table and three lightweight sandwich panel designs. The sandwich panel designs consist of two facing plates (top and bottom) with a core in the middle. A generic sketch of a sandwich panel can be found in Figure 6.4. In this figure L is the length of the sandwich panel, W is the width, h is the height of the panel,

h_c is the height of the core, $t_{f,u}$ is the thickness of the upper facing panel, and $t_{f,l}$ is the thickness of the lower facing panel. For each sandwich panel table design the dimensions of the variables in Figure 6.4 can be found in Table 6.1. The thickness of the upper facing plate is larger than the thickness for the lower plate is due to the need for T-slots. For the solid table, the overall height is the same, but there is no core height or facing plates.

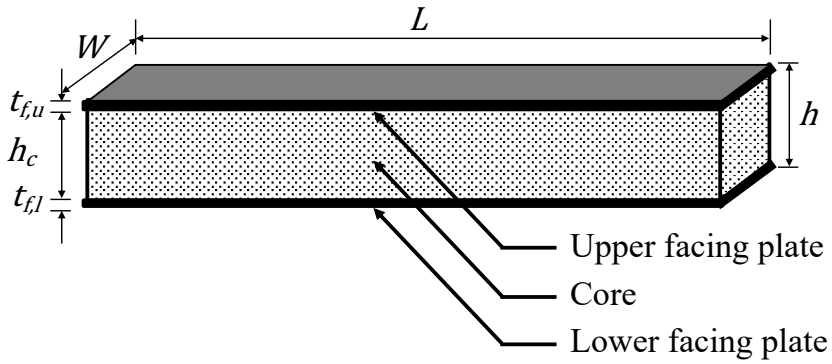

Figure 6.4. Sketch of a sandwich panel

Table 6.1. Standard sandwich panel table design

Parameter	Value (mm)
L	1676.4
W	889
h	122.9
h_c	76.2
$t_{f,u}$	40.35
$t_{f,l}$	6.35

The lightweight table designs consist of three different cores. The first table design (shown in Figure 6.5(a)) has a core constructed of a single row of I-shaped beams running horizontally across the length of the table (x-direction). The second table design (shown in Figure 6.5(b)) also has a core constructed of a single row of I-shaped beams but running horizontally across the width of the table (y-direction). The third table design (shown in Figure 6.5(c)) has a different core design. This core consists of a honeycomb design where the honeycomb runs vertically. This can be seen in Figure 6.6 where the upper facing plate is not shown. The fourth table design (shown in Figure 6.5(d)) is a single plate, no core or facing plates. All four table designs are made of steel, AISI 1045, and their mass can be found in Table 6.2.

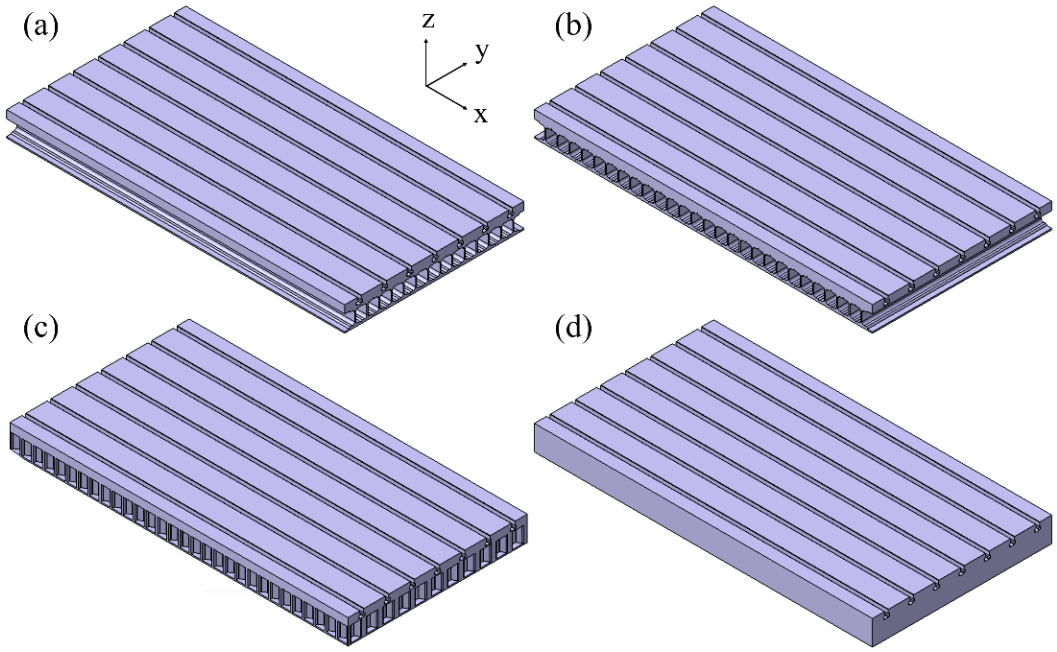

Figure 6.5. Table designs. (a) I-shaped cross sections running the length of the table (x-direction), (b) I-shaped cross sections running the width of the table (y-direction), (c) honeycomb, (d) solid table

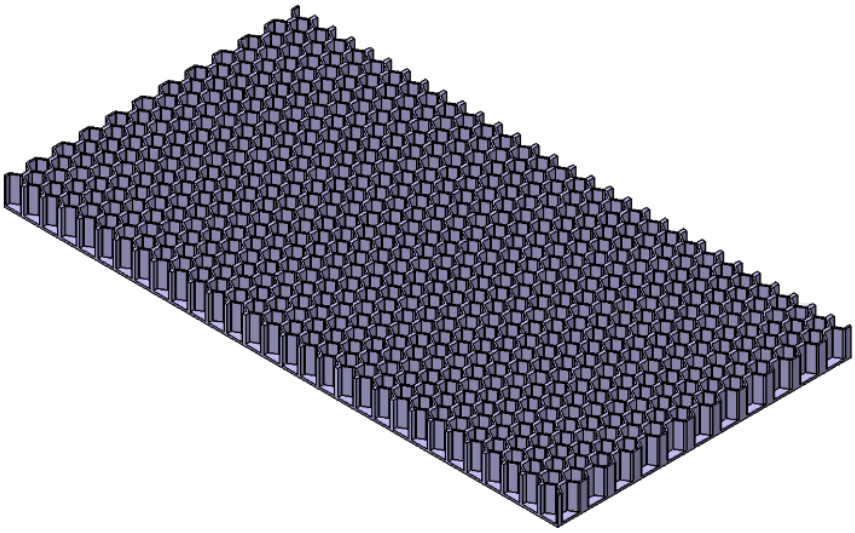

Figure 6.6. Honeycomb core design without the upper facing plate

Table 6.2. Mass of table designs

Table design	Mass (kg)
X	687
Y	692
Honeycomb	677
Solid	1370

The three lightweight tables will require different methods of manufacturing than the traditional solid table. The traditional solid table is cast with extra material to allow for clean-up cuts to produce the final plate. Then the t-slots are cut in the top of the plate. To build the X and Y table designs, first, the I-shaped beams are rolled or extruded and then cut to the desired length. Then, the upper and lower facing plates are both rolled to the required thickness and then cut. The I-shaped beams are arranged horizontally and joined to the upper and lower plates. Finally, the t-slots are machined into the upper plates. For the honeycomb table design, the upper and lower facing plates are produced in similar manners. The core can be made from bending sheet metal and cutting to the proper length and height. One half of the honeycomb can be made from a single sheet bent to look similar to Figure 6.7(a). Then a second sheet can be added to complete a single row of the honeycomb, similar to Figure 6.7(b). More sheets can be added to extend the honeycomb core to the desired width and length. The sheets are joined together, and the upper and lower facing plates are joined to the honeycomb core. Then the t-slots are machined in the top plate.

To evaluate the static and dynamic performance of the four table designs, they were modeled in CATIA V5 and then analyzed using FEA in the same software. A static and frequency analysis were carried out and are described in the following subsections.

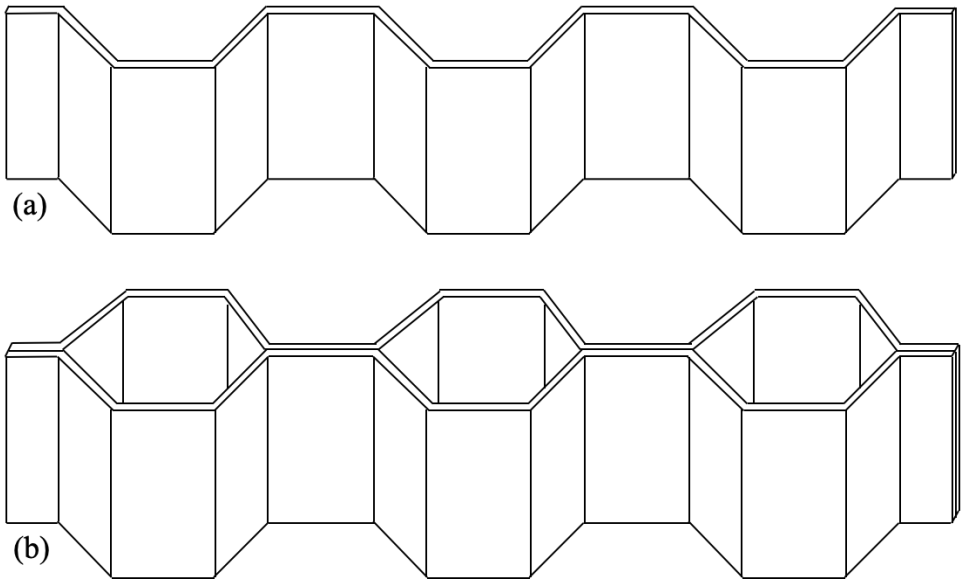

Figure 6.7. (a) Single sheet bent to the shape of half a honeycomb (b) Two sheets combined to produce the honeycomb core shape

6.3.2 Static and dynamic analyses

Having constructed the 3D models of the tables, the static and dynamic analyses can be carried out. The static analysis will provide approximate stiffnesses that can be compared among the lightweight table designs and the solid table design to evaluate a difference in performance. To carry out the static analysis, first, a mesh was generated; the default mesh settings were used. Then constraints for the table were chosen. To constrain the table, a small amount of material was added to bottom of the table where the slides attach. These two strips are 76.2 mm wide and extend the length of the table and can be seen in Figure 6.8. Following, the four forces are applied to the tables, but each force is analyzed individually. The applied force is 2,500 N in the negative z-direction. 2,500 N was chosen since it approximates an extreme cutting condition and is based off analysis from the author's previous work in Triebe et al. [146]. The value of this force is not as important as applying it consistently across the different locations and table designs since the goal of this model is to approximate the stiffness. The locations of the applied forces can be found in Figure 6.9 with the detailed coordinates in Table 6.3. For each force, the maximum deflection is found, and an approximate stiffness is calculated per Eq. (6.2).

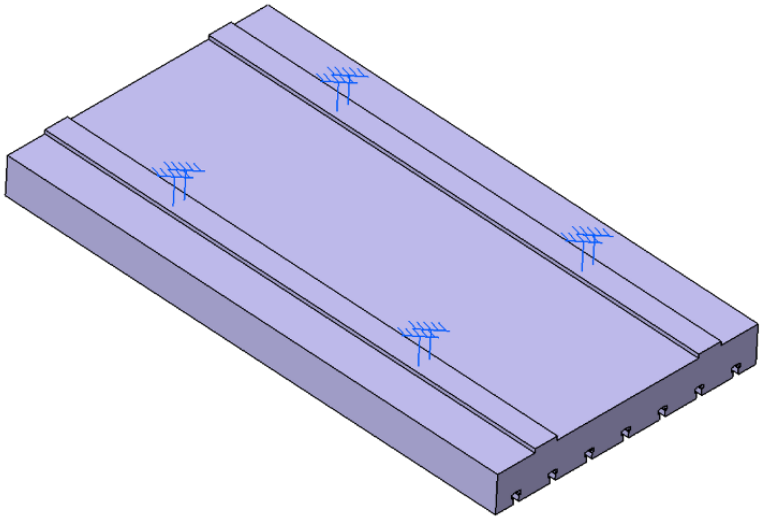

Figure 6.8. Bottom of table showing the restraints used in the FEMs

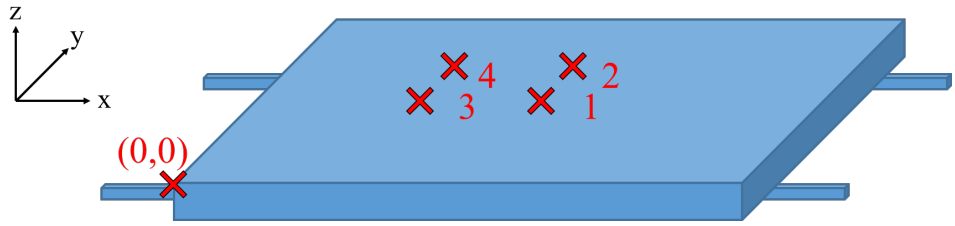

Figure 6.9. Applied force locations for stiffness model. See Table 6.3 for detailed coordinates.

Table 6.3. Position coordinates for force locations of stiffness model (see Figure 6.9)

Position	X (mm)	Y (mm)
1	838.2	469.6
2	838.2	670.56
3	425.45	469.6
4	425.45	670.56

For the frequency analysis, the same constraints were applied (see Figure 6.8) but no forces. The frequency analysis is carried out and the first 4 modes are found. For each mode, the frequency is recorded, and the mode shapes are observed.

6.4 Results

From the static analysis, the deflection of the table under the loads shown in Figure 6.9 and Table 6.3 can be seen in Table 6.4. From those deflections, an average stiffness was calculated and can be found in Table 6.5. Each stiffness is found by dividing the applied force by the maximum deflection found from the static analysis. Each of the lightweight table stiffnesses are compared to the solid table stiffness to find the stiffness reduction as shown in Table 6.5 along with the mass reduction. The results show a significant stiffness reduction in the lightweight table designs but also that the stiffness is not solely dependent on the mass. The X table design has a mass reduction of 50% with a stiffness reduction of 70% while the Y table design and honeycomb table design have a mass reduction of 49% and 51% respectively but a stiffness reduction of 58%.

Table 6.4. Deflection in μm of table under load at each position shown in Figure 6.9 and Table 6.3

Table design	Position 1	Position 2
X	2.490	1.133
Y	1.785	0.835
Honeycomb	1.633	0.833
Solid	0.573	0.398
	Position 3	Position 4
X	2.455	1.105
Y	1.575	0.828
Honeycomb	1.605	0.827
Solid	0.494	0.430

Table 6.5. Stiffness reduction of the four table designs calculated from the static analysis and compared to their mass reduction

Table design	Average stiffness (N/nm)	Stiffness reduction	Mass reduction
X	1.622	70%	50%
Y	2.250	58%	49%
Honeycomb	2.278	58%	51%
Solid	5.381	0%	0%

From the dynamic analysis, the first four modal frequencies for the four table designs can be found in Figure 6.10, frequency reduction comparison found in Table 6.6, and the mode shapes in

Figure 6.11. From Figure 6.10 and Table 6.6 it can be seen there is a significant drop in the natural frequency for the X table design but less of a drop for the Y and honeycomb designs. It can also be seen that, similar to stiffness, the frequency reduction is not solely related to mass reduction since the Y and honeycomb designs have mass reductions similar to the X design but much less of a reduction in natural frequency. From Figure 6.11 it can be seen the first three mode shapes are the same for the four designs but the fourth mode shape for the Y table design differs from the rest. In this regard, performance will be similar.

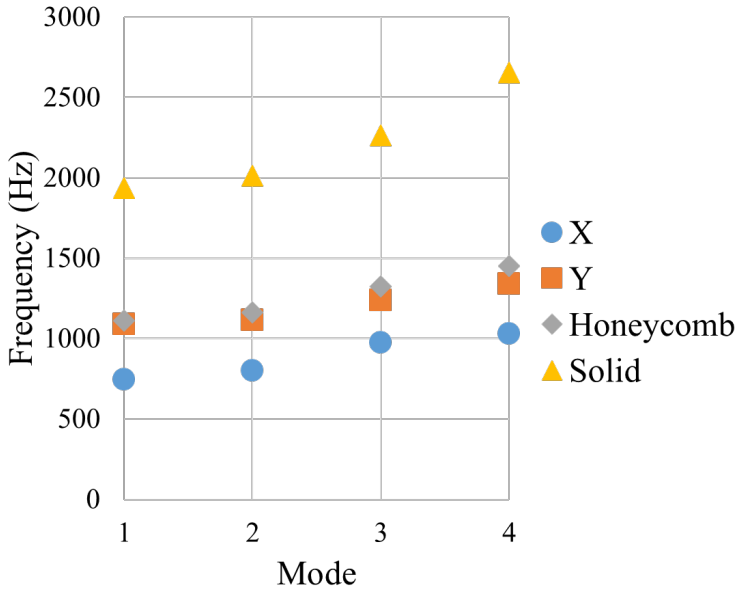

Figure 6.10. First four mode occurrences four the four table designs

Table 6.6. Natural frequency and mass comparisons between the table designs

Table design	Mode 1 (Hz)	Mode 1 reduction	Modes 1-4 average reduction	Mass reduction
X	746	61%	60%	50%
Y	1090	44%	46%	49%
Honeycomb	1111	43%	43%	51%
Solid	1935	0%	0%	0%

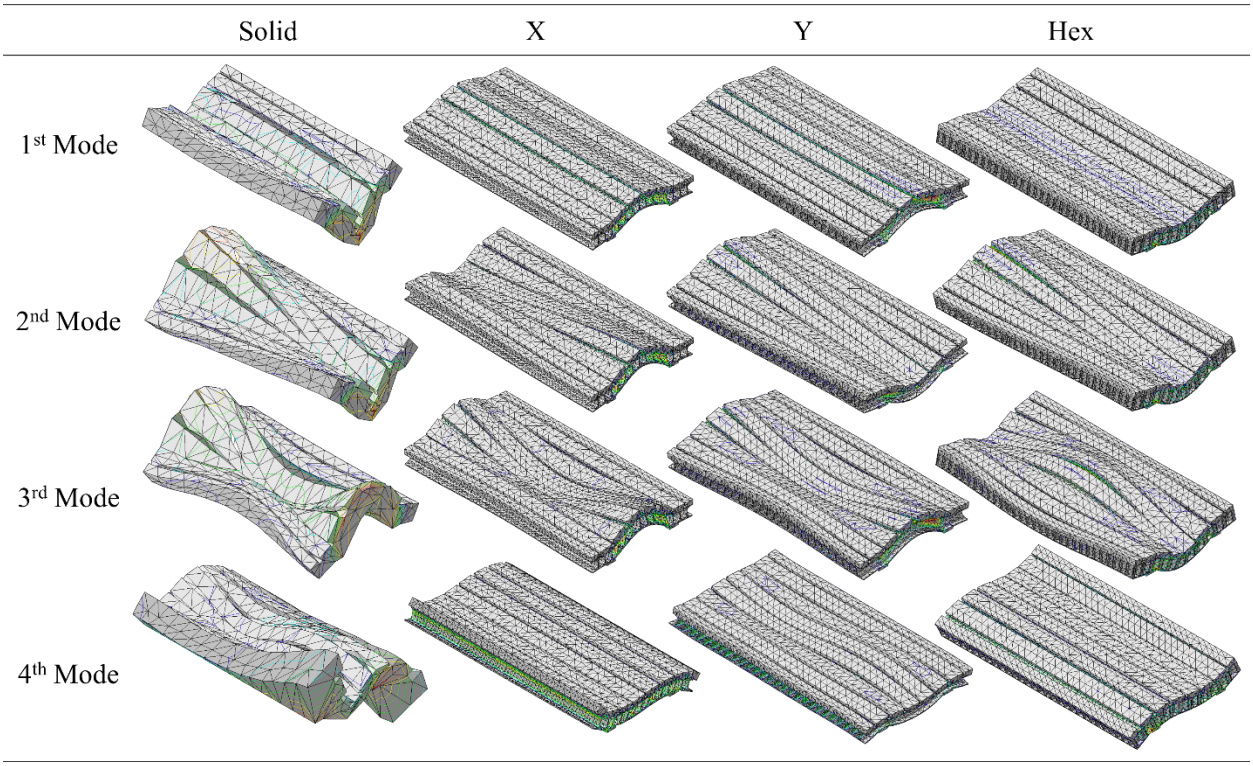

Figure 6.11. Mode shapes 1-4 of the four table designs

The author attempted to analyze a foam core sandwich panel design but due to the complexity of the model, the software could not complete the analysis. To allow for a comparison with a foam design, smaller table designs were built. The table dimensions are the same except for the length and width and can be seen in Table 6.7 and their corresponding mass in Table 6.8. A dynamic analysis was carried using FEA and the results can be found in Figure 6.12 with the average frequency reduction in Table 6.8. These results reinforce the results from the dynamic analysis of the larger tables in that the natural frequency is not solely dependent on mass.

Table 6.7. Small sandwich panel table design

Parameter	Value (mm)
L	457
W	356
h	122.9
h_c	76.2
$t_{f,u}$	39.37
$t_{f,l}$	6.35

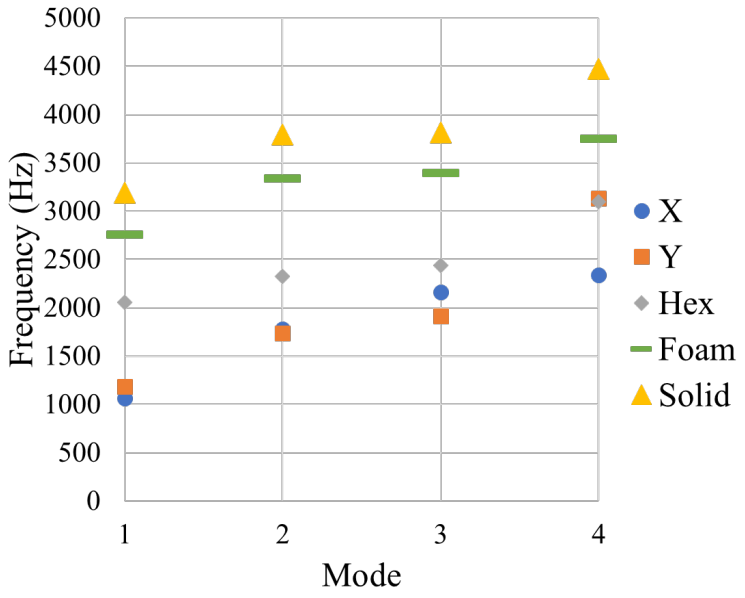

Figure 6.12. Mode occurrences of the smaller table designs

Table 6.8. Mass of small table designs with comparison to the solid table

Table design	Mode 1 (Hz)	Mode 1 reduction	Modes 1-4 average reduction	Mass (kg)	Mass reduction
X	1063	67%	53%	76	51%
Y	1183	63%	49%	74	50%
Honeycomb	2054	36%	35%	73	51%
Foam	2761	13%	13%	83	45%
Solid	3189	0%	0%	149	0%

6.5 Discussion

From the results, a number of observations can be seen. Considering the static performance of the table deigns, Table 6.4 shows the three lightweight designs deflect more under the applied force than the solid table and Table 6.5 shows the stiffness decreases for the lightweight tables. However, it can be seen that the loss of stiffness can be reduced by design. The variation in stiffness loss (stiffness is not linearly proportional to mass) can explain the variation in natural frequency reduction. As seen in Table 6.5 the X-table design has a mass reduction of 50% with a stiffness reduction of 70% while the honeycomb table design has a slightly larger mass reduction but a smaller stiffness reduction.

In regards to the dynamic performance of the different table designs, as can be seen in Figure 6.10, the modes for the lightweight table designs occur at lower frequencies than for the traditional solid table design. This can be problematic depending on if these frequencies approach any frequency of other components in the MT. This can include spindle speed, axis transmissions, and pumps. However, in order for these components to match the natural frequency, the vibrations they produce will have to have very high frequencies. For example, when examining vibration from the cutting spindle, using the first natural frequency of the X design table (~740 Hz) would require a spindle speed to be 44,400 rpm to match the natural frequency. However, if more than one flute is used, for example if a 4-fluted cutter is used, then the spindle speed would need to reach 11100 rpm. This is still very fast and is not a realistic spindle speed. However, since the cutting force is not sinusoidal but is periodic, the cutting force can be described by the sum of sine and cosine functions using Fourier decomposition. These sine and cosine functions may have higher frequencies and should be considered. If looking at the axis drive system, assuming a lead of 12 mm for the ball screw, a feed of 444,000 mm/min would be required to match the natural frequency. If the lead is cut in half the required feed would be half, which is still too large to be a realistic feed. A realistic speed for rapid traverse would be around 40,000 mm/s which would give a 56 Hz vibration; this is much lower than the first natural frequency of any of the four table designs.

In addition to the drop in natural frequency for the lightweight tables, it can be seen in Figure 6.10 that the frequency is not fully dependent on mass, i.e., the honeycomb design has the lowest mass but not the lowest natural frequencies. The honeycomb table design has a 43% drop in the first natural frequency with a 51% reduction in mass while the X table design has a 61% drop in the first natural frequency with a 50% reduction in mass. This is also confirmed in Figure 6.12 with the smaller table designs. The foam design has 45% mass reduction compared to the solid table with only a 13% average decrease in natural frequency. Therefore, mass can be decreased without losing dynamic performance; this depends on the design of the table.

From Figure 6.11 it can be seen that the mode shapes of the lightweight tables are similar to the solid table. The clearest difference is mode 4 of table design Y varies from the solid table. However, since this is the fourth mode, it may not have any consequence since this mode occurs at a much higher frequency, similar to the discussion in the previous paragraph. The similarity in mode shapes means the lightweight tables will have similar dynamic performance.

6.6 Conclusion

This chapter developed a static and dynamic model of the slide table of a vertical milling MT to investigate the impact lightweighting has on the performance of a MT. These models were motivated by the concern that lightweighting the table, in order to reduce the MT energy consumption, will reduce the performance of the machine and impact the quality of parts produced. From this study it was found that the stiffness and natural frequencies of the lightweight table designs decrease when compared to the solid table design. However, for two of the three lightweight table designs, the decrease in stiffness and natural frequency was much less than for the third. Therefore, design of the table can reduce the mass while preserving performance of the MT.

For these static and dynamic models, four table designs were analyzed: a traditional solid table design, two I-beam sandwich panel designs, and one honeycomb sandwich panel design. These table designs were constructed in a 3D CAD software (CATIA V5) and analyzed using FEA in the same software. A static analysis was carried out to find the stiffness of the lightweight tables since stiffness plays a major role in static performance, i.e., greater stiffness means less deformation in the table during cutting. A dynamic analysis was carried out to find the natural frequencies of the tables since cutting and other systems produce vibrations in the table; if these vibrations approach any of the natural frequencies of the table, it can produce much larger vibrations that will impact the quality of the part and potentially harm the machine.

It was found that the lightweight designs modeled in this chapter had a reduced stiffness and natural frequencies when compared to the traditional solid table. However, the reduction in stiffness and natural frequency was much less for two of the three lightweight table designs than for the third. This shows show that design can uncouple stiffness and natural frequency from mass. To further explore the role of design in performance, a foam sandwich panel design was analyzed. Though due to the complexity of the model, the software could not complete the analysis for a larger table of the same dimensions; a smaller table size was analyzed and compared to smaller table designs of the other four designs analyzed earlier. It was found with this analysis that the foam had an even better dynamic performance (higher natural frequencies) than the other three lightweight table designs and approached the performance of the solid table. Similarly, the static and dynamic performance of the table would be affected by a change in the overall shape of the table (not just the core), i.e., length, width, and height.

This chapter made a number of key contributions and observations related to the static and dynamic performance of lightweight table designs:

- Built static and dynamic models of various designs of lightweight slide tables to analyze their performance;
- Found lightweighting can reduce the performance of the slide table but design can remove the link between mass and performance as measured by natural frequencies;
- Examined other systems and their induced vibrations on the table and found the frequencies produced by these systems, i.e., drive system and cutting, are much lower than the lightweight natural frequencies, however, the frequencies from the decomposition of the cutting force should be considered.

Further investigation into static and dynamic performance should be carried out for other systems in the MT in order to provide insight need to lightweight these systems to reduce their energy consumption.

7. DEVELOPMENT OF A COST MODEL FOR VERTICAL MILLING MACHINES TO ASSESS IMPACT OF LIGHTWEIGHTING

Reprinted with permission (portions enhanced/adapted) from Triebe, M. J., Zhao, F., & Sutherland, J. W. (2021). Development of a Cost Model for Vertical Milling Machines to Assess Impact of Lightweighting. *Journal of Manufacturing and Materials Processing*, 5(4), 129

7.1 Introduction

Manufacturing plays an important role in the global economy through its job creation and production of goods. In 2017 industry provided employment for close to 25% of the global labor force of 3.43 billion people and accounted for 30% of the global Gross Domestic Product (manufacturing is the dominant contributor to industrial activities) [1]. Along with its role in the global economy, manufacturing has a significant environmental footprint due to its energy and resource consumption and its waste generation. Considering this, reducing the energy/resource consumption of manufacturing is important. In 2020, 36% of end-use energy consumption in the U.S. was attributed to the industrial sector [4] with a significant portion of the electricity being generated by fossil fuels [5]. Additionally, in 2018, worldwide industry accounted for about 42% of the electricity consumed with 67% of the electricity being generated by fossil fuels [162].

Machine tools (MTs) are essential manufacturing equipment that shape and form raw material into desired products through grinding, cutting, bending, and forming operations. MTs are everywhere; the global demand for MTs for material removal (in terms of sales) grew from $119.7 billion in 2008 to $144.6 billion in 2018 and is projected to grow to $174 billion by 2023 [6]. MTs, such as lathes, mills, drill presses, and grinders can vary greatly in size from fitting on a table-top to filling an entire room. They also vary in complexity and technology and over time, they have become more automated, accurate, and powerful.

MTs have a significant environmental impact and reducing this impact is necessary to reduce manufacturing's large environmental footprint. Across a MT lifecycle, most of the environmental impact associated with a machine is due to its use stage, in particular, the energy consumed during MT use. Assuming a MT has a life of 10 years and based off of global demand data for 2008, 2013, and 2018 from Freedonia Focus Reports [6], it is estimated about 15 million MTs were in service during 2018. This set of MTs consumed approximately 50 TWh of energy per year (calculated

from data of Diaz et al. [24]). This means that just a 10% energy reduction via an improved MT design will reduce energy consumption by 5 TWh. This saved energy can power about 480,000 houses for a month [167].

One potential strategy to reduce MT energy consumption is lightweighting. Lightweighting is a design strategy that lowers energy consumption of a product by reducing its mass since smaller masses require less energy to move. Lightweighting of MTs accomplished by reducing the mass of moving components. Kroll et al. [120] found that lightweighting of MTs has the potential to reduce energy consumption, improve acceleration capability, and enhance process stability. Herrmann et al. [121] also examined lightweighting of MTs, and more broadly lightweighting of components and products, and found the energy savings in the use stage more than offsets any additional impacts occurred during the manufacturing stage, e.g., using a more energy intensive material such as replacing steel with aluminum.

However, reducing the mass of a MT, or any product, generally requires more than a simple material change. Design changes may be required, such as dimensional changes, due to differences in material stiffness, hardness, etc. A result of these design changes may be that the material cost for a MT is less, but the design changes may also have unintended or undesired consequences. One major concern from lightweighting is the potential increase in the cost to manufacture the machine. While lightweighting may reduce a user's operation cost during the MT use stage through energy reduction, design changes could increase the complexity of the machine and the manufacturing processes needed to fabricate components to build the machine. As a result, the cost to build a lightweight MT may be larger than a standard MT. If cost significantly increases, MT builders may be hesitant to implement lightweighting – especially if the overall lifecycle cost to a customer will be higher. Therefore, it is important to understand the cost drivers of MTs including how much of the cost is driven by the mass of the MT or materials in the MT and how much of the cost is due to the complexity of design, i.e., will additional complexity outweigh the reduction in mass in terms of cost.

Currently, there has been no investigation into how lightweighting with the intent to reduce energy consumption affects the MT cost. Therefore, this chapter will explore the cost drivers associated with building a MT. This will be accomplished by collecting data on the features associated with a wide variety of MTs and the associated cost/price of the machines. Ideally the cost to manufacture the MT would be used in place of the price but since MT builders are hesitant

to provide that data, the price of the machine is used instead. Per personal communications [10], MT builders price their machines close to the manufacturing cost since the MT industry is extremely competitive. Therefore, in this chapter it is assumed the price of the machine is proportional to the cost to manufacture the machine; there is a consistent markup among the machines. This markup is assumed to be equal to the S&P 500 Operating Profit Margins for Industrial Machinery which is 12.9% for 2021 [11]. Then, empirical models will be fit to this MT data. First, simple linear regression models are fit to individually assess the relative importance of each feature to describing the variation in price data. Then, using stepwise regression, empirical models are fit for the price based on the features since the features are not independent of each other. The resulting cost/price models will be examined to reveal insights into how design changes (i.e., differences among the MTs) affect the overall cost/price of the MT. While these models may not consider aspects such as some of the technology in the MT, they will allow us to link environmentally minded design changes (lightweighting) to the cost of MTs. The remainder of this chapter is organized as follows. Section 7.2 reviews the environmental impact of MTs, the potential impact reduction through lightweighting, lightweighting cost implications, and cost models related to MTs and manufacturing. Data collection and model formulation are described in Section 7.3 along with the results. Section 7.4 discusses the MT cost drivers, the implications of the results, and how this model can be used in the design of lower energy consuming MTs. Finally, Section 7.5 concludes the paper and provides insights for future directions.

7.2 Literature review – environmental impact reduction, lightweighting, & costs

Due to the importance of MTs and their impact on the environment, this section reviews methods to reduce their carbon footprint, methods for lightweighting MTs, cost implications of lightweighting, and cost models related to manufacturing and MTs.

7.2.1 Machine tool environmental impact reduction

MTs contribute significantly to manufacturing's environmental impact through their considerable carbon footprint and widespread use. Much of a MT's carbon footprint is due to its energy consumption during use. Because of the significant energy consumption and carbon

footprint of MTs, much work has been done to reduce their environmental impact. This sub-section will review reported efforts for reducing MT energy consumption and environmental impact.

A foundational study by Dahmus and Gutowksi [8] showed how cutting can account for only a portion of the total energy consumed by MTs. Dahmus and Gutowski studied multiple MTs and found that the supporting systems, those not directly related to cutting, can account for a large portion of the MT energy consumption. Zein [7] showed that the power demand of a MT, including the demand of the support systems, has become more complex due to the implementation of automation. Therefore, it is important to look at a variety of strategies to reduce MT energy consumption.

According to Flum et al. [51], methods for reducing MT energy consumption include energy recovery (e.g., thermo-electric devices to recover waste heat), energy demand reduction, and energy reuse (e.g., kinetic energy associated with spindle braking/deceleration is converted to electrical energy). Much work has focused on energy demand reduction and is covered here as well. Energy demand reduction research can be conducted by process-related and machine-related efforts [51] that will be expanded upon in the following sub-sections.

Process-related improvements for energy reduction

Toolpath selection is an important part of process design, and the proper choice of a toolpath may lead to reduced energy consumption. Li et al. [72] presented a methodology to optimize toolpaths for lower energy consumption and carbon footprint in the milling process. The authors used their method to find toolpaths and then compared these with conventional milling toolpaths; the proposed method reduced the toolpath length and resulted in an energy savings of up to 21%. Hu et al. [168] explored the relationship between processing sequence of features of a part (PSFP) and the energy consumption during the transition between features. The authors applied depth-first search and genetic algorithm (GA) to find the optimal PSFP and achieved a 28.6% energy reduction during feature transition.

Cutting conditions can also be modified to reduce energy consumption. Jdidia et al. [169] used Particle Swarm Operation (PSO) to optimize the cutting parameters to lead to a lower energy consumption during milling operations. The authors optimized the parameters of rotational speed, feed per tooth, and axial depth of cut. Mori et al. [13] measured power consumption of machining

centers under various conditions with a goal of choosing better process parameters. The authors found for drilling and face/end milling, energy consumption can be reduced by setting cutting conditions to a high feed/speed condition but within a range that does not compromise tool life or surface finish. Beyond the issue of energy consumed during cutting, Diaz et al. [14] noted that many elements within a MT consume energy (e.g., controller, cutting fluid pump, chip conveyor), and that the energy consumption of these elements allocated to a single component can be lowered by reducing the cycle time per component (the non-cutting energy is allocated to more components). It should be noted that these works related to cutting parameters and conditions considered conventional cutting as opposed to high-speed machining (HSM) where cutting conditions differ greatly. During HSM it has been found forces can decrease with an increased cutting speed, and a higher dimensional accuracy and surface quality can be achieved for certain materials of workpieces [170]. It is also important to note that if a machine sits idle between jobs, even if the cutting time has been reduced based on Mori et al. [13] and Diaz et al. [14], any energy savings is lost due to the machines running but not cutting parts.

Modifying machine and component states can also reduce energy consumption. Schlechtendahl et al. [73] designed a control system to change the state of systems and components in the MT for energy consumption reduction. The control system would change the state to a lower energy consumption state if possible. Can et al. [171] proposed a method to shut down components and subsystems of MTs during non-productive periods while allowing them the ability to produce components on demand. The authors were able to shut down two components during an idle state while not compromising the readiness of the machine and reduced energy consumption by 25% when compared to a machine with all components running while idle.

Machine-related improvements for reducing environmental impact

A strategy of machine-related improvements for energy reduction is designing machines with more energy efficient components and systems. Albertelli [16] investigated the energy saving potential of spindle direct drive. The author analyzed two spindle units, one traditional gear-based spindle and one direct-drive spindle. It was found that up to 7% of the overall MT energy consumption can be saved by replacing a traditional gear-based spindle with a direct-drive spindle system. Mori et al. [172] investigated the energy consumption of a hot-gas-bypass spindle cooling

system. The authors proposed an on-off cooling method that could reduce the power consumption of the cooling unit by up to 75% with minimal thermal displacement. Zhao et al. [173] explored the relationship between tool geometry, i.e., geometric angles, and energy consumption. The authors employed a multi-objective optimization model to optimize tool geometry, e.g., cutting edge diameter, helix angle, rake angle, along with cutting parameters. From the results the authors found an average energy savings of 16.6%.

Another machine-related improvement strategy is component structure and arrangement. One example of this strategy is demonstrated by Gao et al. [17] where energy consumption of a hydraulic press was reduced by optimizing the size of the clearances. Clearance size affects the amount of oil leakage and friction but can also impact forming accuracy. The authors optimized the clearance size to minimize energy loss while not impacting forming accuracy. Lightweighting is another example of this strategy. Since lightweighting is the focus of this chapter, it will be discussed in its own section.

7.2.2 Lightweighting design to reduce environmental impact

Lightweighting strategies usually fall into one of three categories: change in material type, manufacturing enabled design improvements, and product structure change. Lightweighting via a material change involves replacing a high-density material with a lower density material, e.g., replacing steel with aluminum or titanium. Implementing manufacturing enabled design improvements for lightweighting involves the use of "new" manufacturing methods that allow for the reduction of parts or amount of material. Examples include semisolid thixo-forming, tailor-rolled blanks, and additive manufacturing (to enable product changes not achievable with conventional manufacturing methods). Product structure changes involve the design/redesign to optimize the product structure. This includes topology analysis, shell design instead of frame construction, and the use of fewer sub-assemblies and fasteners. It should be noted that there is overlap in these three categories and that all require design changes, e.g., a change of materials requires dimensional changes due to different material properties.

Lightweighting has been used to reduce energy consumption and environmental impact (through CO2 linked to energy consumption) of products, especially in the transportation sector. Lightweighting can also reduce a MT's energy consumption (and CO2 linked to energy) when it

is applied to moving components. This is due to a smaller mass needing less energy to move. Some applications of lightweighting MTs include the mass reduction of a gantry machine. Sulitka et al. [20] explored lightweighting the crossbeam and columns by applying composites and sandwich structures. The x-axis moving mass was reduced by 35% and the crossbeam and columns mass was reduced by 52.3%. This mass reduction allowed for the employment of a smaller motor with a 20% power reduction. Another lightweighting MT application includes lathes. Lv et al. [19] explored reducing the inertia of the spindle by using an aluminum chuck. The authors decreased the mass of the chuck by 60% and the reduced spindle inertia from 0.3354 to 0.2380 kg-m2. This decrease in inertia reduced the energy consumption and peak power by 20.6% and 21.2%, respectively.

Other applications include milling machines. Zulaika et al. [22] explored lightweighting through thinner wall thicknesses in the ram. The authors decreased the mass while increasing stiffness with additional/redundant guideways of the frame. When redesigning the ram, the authors modeled machine dynamics and representative milling operations. Suh et al. [21] lightweighted a large computer numerical control (CNC) MT by reducing the mass of the horizontal and vertical slides by 26% and 34% respectively. Carbon fiber reinforced polymer (CFRP) composite sandwiches were bonded to welded steel structures to reduce the mass. This also increased damping without reducing stiffness and allowed for greater acceleration and deceleration. Zhao et al. [127] designed a lightweight working table through different construction methods: hollow stem, sandwich node, and radial root. To determine which construction method should be applied, the authors used a fuzzy assessment to assist in the design. Another application of lightweighting milling machines proposed by Triebe et al. [126,146] lightweighted the MT slide table. Since the table moves throughout the use of the machine, for many types of mills, there is potential to reduce energy consumption within the feed system. In Triebe et al. [126,146] the authors proposed a GA to optimize the core of a sandwich structure table. Various types of sandwich structures were proposed including metal foam core, honeycomb core (cells running vertically), and a single row of cells running horizontally. The proposed method allowed for a mass savings by up to 50%. This application will be discussed in more depth in Section 7.4.

7.2.3 Embodied monetary and environmental costs of materials

Cost of materials is very important within manufacturing. According to Kalpakjian and Schmid [174], the approximate breakdown of costs in manufacturing is as follows:

- Design 5%
- Material 50%
- Direct Labor 15%
- Overhead 30%

While this is true in general, researchers may wish to develop cost breakdowns more appropriate to specific applications, e.g., MTs. However, since in general materials make up approximately 50% of manufacturing cost, it is important to consider both the type and amount of each material being used. This breakdown also helps to explain the economic motivation for lightweighting: reduce the amount of materials so as to decrease the product cost. Though the method of lightweighting must be considered. For example, if lightweighting is accomplished by a material change, then the new material cost must be considered. Ashby [175] provided approximate ranges of material prices; the price range of metals from Ashby can be found in Figure 7.1(a).

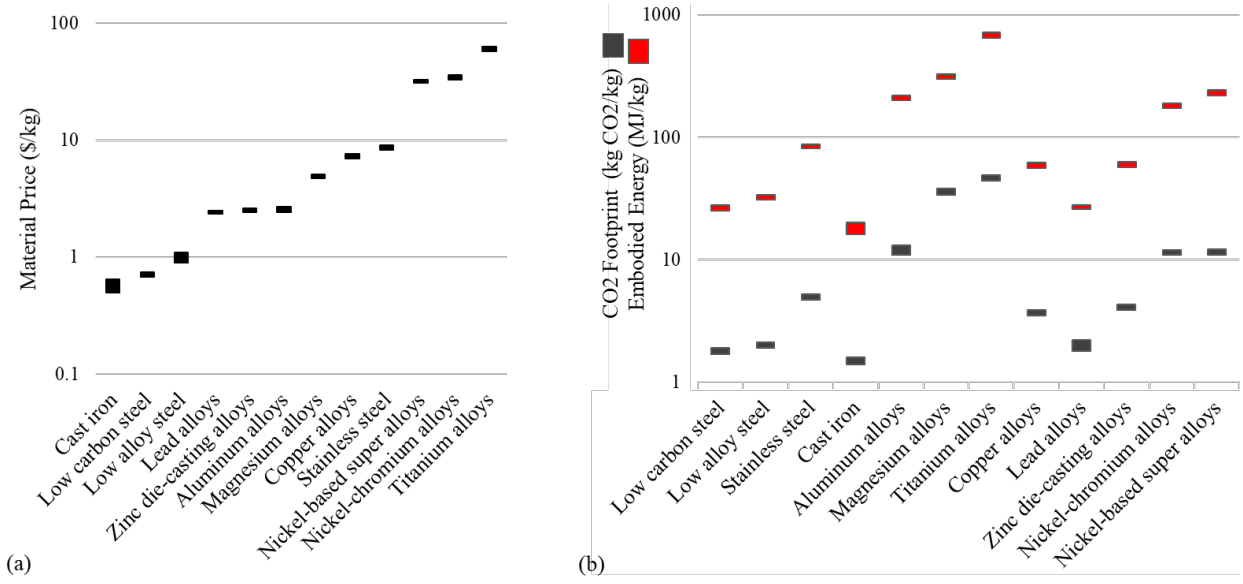

Figure 7.1 (a) Cost of materials based on mass (data taken from Ashby [175]); (b) Embodied energy and carbon footprint of various metals (data taken from Ashby [175])

If lightweighting is accomplished through a product structure change or manufacturing improvement, e.g., reducing the number of sub-assemblies and fasteners through bonded structures or switching from high-pressure die-casting to super vacuum die-casting, then the new method of manufacturing must be considered. Allen and Swift [176] calculated the cost of various manufacturing methods and showed cost depends on both the type of process being used and on how many parts are being made. This occurs for a number of reasons including the cost of the machinery and how long it takes to pay off the machine or machines.

Besides material and manufacturing cost, lightweighting can reduce energy costs and CO2 emissions. Reduction of energy and CO2 emissions during the use stage has already been described in Section 7.2.2. However, there is potential for reducing energy and CO2 further upstream in the lifecycle. This potential comes from the extraction and processing of the materials. Reducing the amount of material, or substituting the material with a lower embodied energy and carbon footprint, can reduce the upstream energy and CO2 emissions. From Figure 7.1(b) it can be seen as to which materials have lower energy and carbon footprints and which materials have the largest potential for reducing upstream impacts. In 2018, approximately 18.6 GJ of energy was consumed per metric ton of iron and steel produced [177]. The iron and steel industry produced 2.1 Gt of CO2 [178] while 1.82 Gt of crude steel were produced worldwide [179]. This means for every kilogram of steel reduced in a MT, 5.167 kWh of energy and 1.15 kg CO2 are saved during the extraction and processing of the ore to produce the steel.

7.2.4 Manufacturing and MT cost models

Manufacturing and MT related cost models typically consist of lifecycle cost (LCC) models, total cost of ownership (TCO) models, and machining cost models. There are a few cost models associated with the acquisition of large pieces of manufacturing equipment. All these different types of cost models will be reviewed here.

LCC consists of all costs related to a product from conception to end-of-life [180]. LCC models of MTs include Enparantza et al. [27] who built an LCC calculation and management program that had a goal of providing LCC data to customers when purchasing a machine and to assist in the design of MTs. The program allowed for the calculation of LCC costs and performance data. Bengtsson and Kurdve [181] performed an LCC analysis on turning equipment at an

automotive driveline manufacturing company to see if the machines, which are past their life length, should be replaced, reconditioned, or run with increased cost and risk. Using project costs, acquisition costs, operation costs, and maintenance costs, the authors found purchasing a new machine would have the lowest LCC due to lower life support costs and life operations cost.

Total cost of ownership (TCO) is similar to LCC but instead of adopting the product perspective (costs related to the product from conception to end-of-life) as LCC does, TCO adopts the purchaser's perspective (costs incurred by the purchaser from purchase to disposal) [182]. Roda et al. [183] proposed a methodology to build a TCO aimed at supporting decision-making for manufacturing asset lifecycle management. The requirements to address were uncertainty in asset operations, systemic performance losses, and quantifying costs. Heilala et al. [184] developed a TCO through component-based simulation, overall equipment efficiency (OEE), and cost of ownership to assist in the design of modular assembly systems. The authors broke down costs into fixed and recurring or variable and used a simulation of a semi-automated assembly line as a case study.

Other authors explored the costs of machining. Anderberg et al. [185] connected productivity and cost efficiency improvements with energy savings by building a machining cost model that included energy and carbon costs. The machining costs comprised MT costs, labor costs, and tool change costs while energy costs included energy directly and indirectly related to machining, e.g., costs associated with unloaded motors, fans, and running of computers. Wang and Liang [186] proposed a method to ensure quality and reduce production costs through addressing tolerance, process selection, and machining parameter optimization. To calculate production cost, the authors considered machining cost, quality cost, and expected cost to machine a feature.

Work related to acquisition cost models for MTs and other large equipment include that of Ciurana et al. [128] who built two cost models for vertical high-speed machining centers based on machine characteristics. These models included a buyer's cost model and a manufacturer's cost model. These were built through multiple regression analysis (MRA) and artificial neural networks (ANN), and ANN was found to create more accurate cost models. Chen and Keys [187] presented a method to model the total cost of heavy equipment including their use. The authors' model included the delivered costs (cost of the machine plus its delivery), installation costs, cost of securing capital, miscellaneous ownership costs (e.g., taxes), and operating costs (maintenance, energy, and operators' costs). Thokala et al. [188] examined the lifecycle costs of an unmanned

aircraft vehicle (UAV). The authors defined acquisition cost as the sum of each individual component and defining characteristics such as material, type of component, and manufacturing method. The authors then approximated repair costs through a simulation that calculated how often an UAV would require repairs. Roth et al. [189] examined the costs of automobile bodies to determine if aluminum could be a cost-effective alternative to steel. The motivation for this switch comes from the regulatory pressures to meet fuel efficiency and recycling standards. From the study, the authors found that for small and midsize automobiles, material cost was the second largest contributor, with tooling cost being the first.

7.3 Cost model development

The cost to manufacture a MT depends on many factors, such as the size, number of axes, and capability of the MT. Understanding how these characteristics and specifications affect cost is important to both customers and manufacturers. For customers, being able to choose a machine that will satisfy their requirements and be within budget is very important. For MT builders, knowing how design changes will affect the final cost is also important. It can allow for design improvements that reduce a MT's energy consumption without significantly increasing the price of the machine. With this knowledge, manufacturers may be better equipped to reduce environmental impact through lightweighting without increasing manufacturing cost. To investigate the relationship between costs and various MT features, data on the features associated with a wide variety of MTs and the associated prices of the machines were collected. Since MT builders are hesitant to supply the cost to manufacture their machines, price of the machine was used in place of cost to manufacture the machine. Per personal communications [10], MT builders price their machines close to the manufacturing cost since the MT industry is extremely competitive. Therefore, it is assumed the price of the machine is proportional to the cost to manufacture the machine; there is a consistent markup among the machines. This markup is assumed to be equal to the S&P 500 Operating Profit Margins for Industrial Machinery which is 12.9% for 2021 [11]. Two sets of empirical models were then fit to this MT data: simple linear regression models and stepwise regression models; stepwise regression was employed since the features are not independent of each other. The resulting cost/price models, though built from price data instead of manufacturing cost data, reveals insights into how differences among the MTs

affect the overall cost/price of the MT. This section will describe the data collection, formulation of the model, and demonstrate the results.

7.3.1 Data collection and model formulation

The data collected includes various MT features and specifications in terms of capabilities, sizes, and complexities. This data will be used to build a model that considers a wide range of machines. This section will describe data collection and construction of model.

Data acquisition

Data was acquired from three MT builders who were willing to provide price data: Hurco, Mazak, and Haas. All the machines were CNC vertical milling machines. These included a range of sizes and capabilities of MTs across the three different companies. Information from Hurco, Mazak, and Haas was retrieved by various means, e.g., literature from distributors and company websites. Hurco provided basic specifications of MTs on their website but had no pricing information. However, a distributor provided price information and a catalog of three machines with detailed specifications. Similarly, Mazak only provided basic specifications on their website. A distributor provided more in-depth catalogs as well as price ranges from the least to the most expensive. It was assumed that the extremes of the price range accurately reflected the extremes of the machines. A total of four Mazak machines were analyzed. The Haas website provided the specifications of each machine as well as their pricing. A total of 72 machines were considered.

A single data set was created using only the data provided by the Haas website. This data set included 72 MTs and considered a range of machine types. A second data set was constructed from the data provided by the three companies. However, due to having far more data from Haas, not all the Haas machines were included in the multi-company data set to avoid skewing the results (a comparable number of each company's machines were included in the data set). The multi-company data set had 3 Hurco MTs, 4 Mazak MTs, and 13 Haas MTs. Of these machines, both 3 and 5 axis machines were included from different series.

When building the Haas data set, 16 variables were used. For the multi-company data set, not all features could be found for all three companies and therefore less features were included than for the Haas only data set. The multi-company data set included 12 variables. The MT price

was used as the dependent variable (response). The 16 features for the Haas data set (e.g., working volume, travel in the x, y, and z axes, maximum speed, number of axes, and mass) and the 12 features for the multi-company data set served as the independent variables. The Haas data set can be found in Table 7.1. However, due to confidentiality concerns, the data provided by Hurco and Mazak are not provided in this chapter. Though, a total list of features can be found in Table 7.2. For both data sets, the features were standardized using Eq. (7.1):

$$Q_C = \left(Q_U - \frac{Q_{max} + Q_{min}}{2}\right)\frac{2}{Q_{max} - Q_{min}} \tag{7.1}$$

where QC is the coded (standardized) value, Qmax is the maximum value of the features, Qmin is the minimum value of the features, and QU is the uncoded feature value. Standardization provides for similar scaling among all the features.

Model formulation

There are many features of a MT, and the price is not impacted equally by each feature. With the goal of finding the major price drivers (assuming cost to manufacture is correlated to the price of the machine) it is important to find which features have the largest impact on the price of the MT. Specifically, given our interest in lightweighting, it is important to find out if the mass of a MT significantly impacts its price. Working with the two data sets (Haas and multi-company), two types of models are built: simple linear regression models and stepwise regression models. We first explored simple linear regression to individually assess the relative importance of each feature to describing the variation in price data. Then, using stepwise regression, we developed empirical models for the price based on the features since the features are not independent of each other.

Simple linear regression was used to build models relating each feature individually to price. The linear regression models provide an initial view as to which features are most influential to the price of the machine through an R^2 value. The R^2 value describes how much of the variation in the price data is described by the feature (independent variable). These models were built for both the Haas data set (16 features) and the multi-company data set (12 features). These results can be found in Table 7.2. As is evident from the table, the features whose models have the highest

R^2, larger than 50%, are identified (shaded). For the Haas data set these high impact variables are mass, volume, z-axis travel, and x-axis travel. For the multi-company data set these high impact variables include mass, x-axis travel, spindle torque, y-axis travel, and z-axis travel. The significance of mass comes from the cost of materials. Volume is tied closely to mass and would therefore be significant in determining price. This is similar for x, y, and z-axis travel. The reason for torque being important in the multi-company data set but not in the Haas data set could be due to that the Haas data set represents a wider range of sizes and types of vertical milling machines.

Table 7.1. Haas data (Data set #1)

MTs	Volume mm^3	Spindle Speed (RPM)	X-Axis (mm)	Y-Axis (mm)	Z-Axis (mm)	Axes	Max Rating (kW)	Max Torque (Nm)	Max Cutting (m/min)	Rapids on X (m/min)	Rapids on Y (m/min)	Rapids on Z (m/min)	Max Thrust X (N)	Max Thrust Y (N)	Max Thrust Z (N)	Mass (kg)	Price ($)
VF-1	104,773,984	8,100	508	406	508	3	22.4	122	16.5	25.4	25.4	25.4	11,343	11,343	18,683	3,539	49,995.00
VF-2	157,160,976	8,100	762	406	508	3	22.4	122	16.5	25.4	25.4	25.4	11,343	11,343	18,683	3,539	52,995.00
VF-2TR	157,160,976	8,100	762	406	508	5	22.4	122	16.5	25.4	25.4	25.4	11,343	11,343	18,683	3,765	123,995.00
VF-2SS	157,160,976	12,000	762	406	508	3	22.4	122	21.2	35.6	35.6	35.6	8,874	8,874	13,723	3,539	64,995.00
VF-2YT	196,644,768	8,100	762	508	508	3	22.4	122	16.5	25.4	25.4	25.4	11,343	11,343	18,683	3,539	60,995.00
VF-2SSYT	196,644,768	12,000	762	508	508	3	22.4	122	21.2	35.6	35.6	35.6	8,874	8,874	13,723	3,539	71,995.00
VF-3	327,741,280	8,100	1,016	508	635	3	22.4	122	16.5	25.4	25.4	25.4	11,343	11,343	18,683	6,124	67,995.00
VF-3SS	327,741,280	12,000	1,016	508	635	3	22.4	122	21.2	35.6	35.6	35.6	13,723	13,723	17,450	6,124	79,995.00
VF-3YT	425,805,600	8,100	1,016	660	635	3	22.4	122	12.7	18	18	18	11,343	18,238	18,238	6,804	77,995.00
VF-3SSYT	425,805,600	12,000	1,016	660	635	3	22.4	122	21.2	35.6	35.6	35.6	13,723	13,723	17,450	6,804	89,995.00
VF-3YT/50	425,805,600	7,500	1,016	660	635	3	22.4	460	12.7	18	18	18	15,124	18,238	24,910	7,485	99,995.00
VF-4	409,676,600	8,100	1,270	508	635	3	22.4	122	16.5	25.4	25.4	25.4	11,343	11,343	18,683	6,124	70,995.00
VF-4SS	409,676,600	12,000	1,270	508	635	3	22.4	122	21.2	35.6	35.6	35.6	13,723	13,723	17,459	6,124	82,995.00
VF-5SS	532,257,000	12,000	1,270	660	635	3	22.4	122	21.2	30.5	30.5	30.5	14,902	14,902	14,902	5,761	99,995.00
VF-5/40	532,257,000	8,100	1,270	660	635	3	22.4	122	12.7	18	18	18	11,343	18,238	18,238	5,761	85,995.00
VF-5/40TR	532,257,000	8,100	1,270	660	635	5	22.4	122	12.7	18	18	18	11,343	18,238	18,238	5,761	163,995.00
VF-5/40XT	638,708,400	8,100	1,524	660	635	3	22.4	122	12.7	18	18	18	15,124	18,238	18,238	7,100	96,995.00
VF-5/50	532,257,000	7,500	1,270	660	635	3	22.4	460	12.7	18	18	18	15,124	18,238	24,910	7,371	114,995.00
VF-5/50TR	532,257,000	7,500	1,270	660	635	5	22.4	460	12.7	18	18	18	15,124	18,238	24,910	7,371	177,995.00
VF-5/50XT	638,708,400	7,500	1,524	660	635	3	22.4	460	12.7	18	18	18	15,124	18,238	24,910	7,371	128,995.00
VF-6/40	1,007,316,756	8,100	1,626	813	762	3	22.4	122	12.7	15.2	15.2	15.2	15,124	15,124	24,910	10,116	123,995.00
VF-6SS	1,007,316,756	12,000	1,626	813	762	3	22.4	122	21.2	30.5	30.5	30.5	15,124	15,124	15,124	10,116	133,995.00
VF-6/40TR	1,007,316,756	8,100	1,626	813	762	5	22.4	122	12.7	15.2	15.2	15.2	15,124	15,124	24,910	11,839	194,995.00

VF-6/50	1,007,316,756	7,500	1,626	813	762	3	22.4	460	12.7	15.2	15.2	15.2	15,124	18,238	24,910	11,567	150,995.00
VF-6/50TR	1,007,316,756	7,500	1,626	813	762	5	22.4	460	12.7	15.2	15.2	15.2	15,124	18,238	24,910	12,003	212,995.00
VF-7/40	1,322,025,804	8,100	2,134	813	762	3	22.4	122	12.7	15.2	15.2	15.2	15,124	15,124	24,910	11,612	143,995.00
VF-7/50	1,322,025,804	7,500	2,134	813	762	3	22.4	460	12.7	15.2	15.2	15.2	15,124	18,238	24,910	12,021	170,995.00
VF-8/40	1,258,836,192	8,100	1,626	1,016	762	3	22.4	122	12.7	15.2	15.2	15.2	15,124	15,124	24,910	11,250	154,995.00
VF-8/50	1,258,836,192	7,500	1,626	1,016	762	3	22.4	460	12.7	15.2	15.2	15.2	15,124	18,238	24,910	13,155	182,995.00
VF-9/40	1,652,125,728	8,100	2,134	1,016	762	3	22.4	122	12.7	15.2	15.2	15.2	15,124	15,124	24,910	12,837	175,995.00
VF-9/50	1,652,125,728	7,500	2,134	1,016	762	3	22.4	460	12.7	15.2	15.2	15.2	15,124	18,238	24,910	13,109	203,995.00
VF-10/40	1,888,254,288	8,100	3,048	813	762	3	22.4	122	9.1	9.1	15.2	15.2	15,124	15,124	24,910	13,654	203,995.00
VF-10/50	1,888,254,288	7,500	3,048	813	762	3	22.4	460	9.1	9.1	15.2	15.2	15,124	18,238	24,910	14,334	230,995.00
VF-11/40	2,359,737,216	8,100	3,048	1,016	762	3	22.4	122	9.1	9.1	15.2	15.2	15,124	15,124	24,910	15,150	225,995.00
VF-12/40	2,360,317,860	8,100	3,810	813	762	3	22.4	122	9.1	9.1	15.2	15.2	15,124	15,124	24,910	16,466	255,995.00
VF-12/50	2,360,317,860	7,500	3,810	813	762	3	22.4	460	9.1	9.1	15.2	15.2	15,124	18,238	24,910	16,874	279,995.00
VF-14/40	2,949,671,520	8,100	3,810	1,016	762	3	22.4	122	9.1	9.1	15.2	15.2	15,124	15,124	24,910	16,466	299,995.00
VF-14/50	2,949,671,520	7,500	3,810	1,016	762	3	22.4	460	9.1	9.1	15.2	15.2	15,124	18,238	24,910	16,874	319,995.00
UMC-500	100,549,960	8,100	610	406	406	5	22.4	122	16.5	22.9	22.9	22.9	14,680	14,680	18,015	5,400	124,995.00
UMC-750	196,644,768	8,100	762	508	508	5	22.4	122	16.5	22.9	22.9	22.9	12,233	12,233	15,124	6,464	154,995.00
UMC-750SS	196,644,768	12,000	762	508	508	5	22.4	122	16.5	30.5	30.5	30.5	12,233	12,233	15,124	6,464	194,995.00
UMC-1000	409,676,600	8,100	1,016	635	635	5	22.4	122	16.5	22.9	22.9	22.9	14,680	14,680	18,015	7,077	199,995.00
UMC-1000-P	409,676,600	8,100	1,016	635	635	5	22.4	122	16.5	22.9	22.9	22.9	14,680	14,680	18,015	7,077	224,995.00
UMC-1000SS	409,676,600	12,000	1,016	635	635	5	22.4	122	16.5	30.5	30.5	30.5	14,680	14,680	18,015	7,711	229,995.00
UMC-1000SS-P	409,676,600	12,000	1,016	635	635	5	22.4	122	16.5	30.5	30.5	30.5	14,680	14,680	18,015	7,711	259,995.00
UMC-1500-DUO	393,289,536	8,100	1,524	508	508	5	22.4	122	16.5	22.9	22.9	22.9	12,233	12,233	15,124	9,120	219,995.00
VR-8	1,784,177,280	20,000	1,626	1,016	1,080	5	18	21	12.7	15.2	15.2	15.2	15,124	15,124	24,910	11,410	299,995.00
VR-9	2,341,595,520	20,000	2,134	1,016	1,080	5	18	21	12.7	15.2	15.2	15.2	15,124	15,124	24,910	11,410	329,995.00

VR-11	3,344,509,440	20,000	3,048	1,016	1,080	5	18	21	9.1	9.1	15.2	15.2	15,124	15,124	24,910	15,320	369,995.00
VR-14	4,180,636,800	20,000	3,810	1,016	1,080	5	18	21	9.1	9.1	15.2	15.2	15,124	15,124	24,910	15,320	419,995.00
VC-400	115,292,632	8,100	559	406	508	3	22.4	122	12.7	20.3	20.3	20.3	15,035	15,035	15,035	7,947	119,995.00
Mini Mill	31,452,820	6,000	406	305	254	3	5.6	45	12.7	15.2	15.2	15.2	8,896	8,896	8,896	1,815	32,995.00
Super Mini Mill	31,452,820	10,000	406	305	254	3	11.2	23	21.2	30.5	30.5	30.5	8,896	8,896	8,896	1,815	43,995.00
Mini Mill 2	73,424,288	6,000	508	406	356	3	5.6	45	12.7	15.2	15.2	15.2	8,896	8,896	8,896	2,314	39,995.00
Super Mini Mill2	73,424,288	10,000	508	406	356	3	11.2	23	21.2	30.5	30.5	30.5	8,896	8,896	8,896	2,314	49,995.00
VM-2	196,644,768	12,000	762	508	508	3	22.4	122	12.7	18	18	18	15,124	15,124	24,910	4,264	86,995.00
VM-3	425,805,600	12,000	1,016	660	635	3	22.4	122	12.7	18	18	18	18,238	18,238	18,238	6,940	99,995.00
VM-6	1,007,316,756	12,000	1,626	813	762	3	22.4	122	12.7	15.2	15.2	15.2	15,124	18,238	24,910	10,887	139,995.00
DT-1	81,261,712	10,000	508	406	394	3	11.2	62	30.5	61	61	61	11,343	11,343	18,683	2,336	49,995.00
DT-2	113,734,404	10,000	700	406	394	3	11.2	62	30.5	61	61	61	11,343	11,343	18,683	2,427	51,995.00
DM-1	81,261,712	10,000	508	406	394	3	11.2	62	30.5	61	61	61	11,343	11,343	18,683	2,336	59,995.00
DM-2	113,734,404	10,000	711	406	394	3	11.2	62	30.5	61	61	61	11,343	11,343	18,683	2,427	61,995.00
TM-1	94,358,460	4,000	762	305	406	3	5.6	45	5.1	5.1	5.1	5.1	8,896	8,896	8,896	2,042	30,995.00
TM-1P	94,358,460	6,000	762	305	406	3	5.6	45	10.2	10.2	10.2	10.2	8,896	8,896	8,896	2,042	34,995.00
TM-2	167,473,376	4,000	1,016	406	406	3	5.6	45	5.1	5.1	5.1	5.1	8,896	8,896	8,896	2,359	34,995.00
TM-2P	167,473,376	6,000	1,016	406	406	3	5.6	45	10.2	10.2	10.2	10.2	8,896	8,896	8,896	2,359	37,995.00
TM-3	209,547,968	4,000	1,016	508	406	3	5.6	45	5.1	5.1	5.1	5.1	8,896	8,896	8,896	2,813	40,995.00
TM-3P	209,547,968	6,000	1,016	508	406	3	5.6	45	10.2	10.2	10.2	10.2	8,896	8,896	8,896	2,813	43,995.00
CM-1	23,628,350	30,000	305	254	305	3	3.7	11	12.7	19.2	19.2	19.2	5,111	5,111	5,111	917	59,995.00
GR-510	1,328,061,483	8,100	3,073	1,549	279	3	11.2	65	20.3	20.3	53.3	27.9	11,210	4,537	9,119	8,800	125,995.00
GR-712	2,218,495,563	8,100	3,683	2,159	279	3	11.2	65	20.3	20.3	53.3	27.9	11,210	4,537	9,119	10,887	169,995.00
GM-2-5AX	8,191,809,626	24,000	3,683	2,223	1,000	5	12	15	20.3	20.3	53.3	27.9	20,017	7,340	8,896	10,000	369,995.00

With some understanding of the relative importance of each variable on price for the different data sets, attention now shifts to developing a single empirical model for MT price for each data set. We might initially consider employing a standard multiple linear regression model. Such a model envisions that the predicted price is the sum of terms (one for each independent variable), with each term (or predictor) being the product of the independent variable and a coefficient. If desired, terms (predictors) may also be added to consider interactions among features (for an interaction term, the independent variable is the product of the feature values, e.g., Volume x Mass). Conventionally, we can then drop terms from the model that are not important. However, for our data sets, the variables are not independent of one another. For example, if the x-axis travel distance increases, this would most likely increase the volume of the machine as well as the mass. This can be seen in that a more productive machine, greater power and cutting speeds, will require greater stiffness and moment of inertia. This would potentially mean larger mass in the structural components. This relationship can be seen in Table 7.3 (a) & (b) (Table 7.3 is split due to size) and Table 7.4 where Table 7.3 (a) & (b) shows the variance-covariance matrix for the Haas data set and Table 7.4 shows the variance-covariance matrix for the multi-company data set. The variance is shown in bold across the diagonal and significant covariances (those greater than the respective variance) are shaded. It can be seen there are a number of interactions between the variables. Therefore, if building a model through multiple linear regression, dropping a term (or adding one) may have a dramatic effect on the other terms. To understand which features are important to determining the price of the machine when the explanatory variables are not independent, stepwise regression is often employed, and this was the method we utilized in this case.

The goal of stepwise regression is to iteratively develop a multi-term (multi-predictor) regression model for the response. The procedure to accomplish this goal includes three steps and can be seen in Figure 7.2. The process starts by fitting a simple linear regression model for each variable (i.e., find a coefficient for each variable). A t-test is performed to judge the significance of each model coefficient (a p-value is determined). Each p-value (significance value) is then compared to the significance-to-enter value, α_E. If any of the significance values are smaller than α_E, then the coefficient with the smallest significance value is chosen. Now that a starting single-variable model is available, the process moves on to the second step of testing terms not in the model. Similar to the first step, regression models are fit for each variable not in the model. These

regression models include the variable(s) already in the model plus an additional variable to be tested. A significance test is then performed for each of the models and the corresponding p-value determined. Each p-value (significance value) is compared to the α_E. If any of the p-values is smaller than α_E then the term with the smallest significance value is added to the model. This second step is repeated until no more terms can be added to the model. The process then moves on to the third and final step. In this step the features in the model are tested to see if their significance has changed due to the addition of other terms. The significance of the terms in the most up-to-date regression model are evaluated (corresponding p-values calculated), and each p-value (significance value) is compared to the significance-to-remove value, α_R. If any terms have a significance greater than α_R then the term with the largest p-value is removed. The model is then refit and the step is repeated until no more terms can be removed. Then the process stops.

From the stepwise regression it was found the top three influencers of price for the multi-company data set are mass, volume, and spindle power; for the Haas data set the top three influencers of price are number of axes, mass, and spindle speed.

Table 7.2. Simple linear regression models including R^2 values for each feature where the values greater than 0.5 are shaded (nomenclature shown in the Features column is used in Table 7.3 (a) & (b) and Table 7.4)

Features	Haas Data Set			Multi-Company Data Set		
	Intercept	Coefficient	R^2	Intercept	Coefficient	R^2
Mass	1.639×10^5	1.380×10^5	0.6823	2.188×10^5	1.530×10^5	0.7237
Max Cutting Speed	1.300×10^5	-6.085×10^4	0.0823			
Spindle Power	1.119×10^5	5.324×10^4	0.1441	1.129×10^5	7.218×10^4	0.2751
Max Thrust X	1.326×10^5	1.702×10^5	0.4497			
Max Thrust Y	1.219×10^5	6.808×10^4	0.1627			
Max Thrust Z	1.155×10^5	8.013×10^4	0.2726			
Spindle Torque	1.545×10^5	2.954×10^4	0.0402	2.151×10^5	1.607×10^5	0.6098
Number of Axes	1.750×10^5	6.247×10^4	0.3371	1.603×10^5	2.844×10^4	0.0532
Rapid Travel X	1.137×10^5	-7.184×10^4	0.1184	1.388×10^5	2.604×10^4	0.0201
Rapid Travel Y	1.341×10^5	-2.821×10^4	0.0211	1.430×10^5	3.243×10^4	0.0407
Rapid Travel Z	1.240×10^5	-5.191×10^4	0.0565	1.436×10^5	3.604×10^4	0.0472
Spindle Speed	2.058×10^5	1.111×10^5	0.1638	1.383×10^5	-2.936×10^4	0.0307
Volume	3.288×10^5	2.380×10^5	0.6129	2.098×10^5	1.062×10^5	0.4063
X Axis Travel	1.830×10^5	1.250×10^5	0.5798	2.336×10^5	1.508×10^5	0.6439
Y Axis Travel	2.350×10^5	1.648×10^5	0.4002	1.965×10^5	1.397×10^5	0.5589
Z Axis Travel	1.649×10^5	1.546×10^5	0.6218	1.396×10^5	1.232×10^5	0.5322

Table 7.3. (a) Variance-Covariance matrix for the Haas data with the variances (across the diagonal) in bold and the significant covariances shaded (see Table 7.2 for nomenclature)

	Vol	SS	XAT	YAT	ZAT	NA	SP	ST
Vol	**1.59×10^{18}**	2.40×10^{12}	1.05×10^{12}	3.63×10^{11}	1.67×10^{11}	2.48×10^{8}	7.42×10^{8}	1.10×10^{10}
SS	2.40×10^{12}	**1.98×10^{7}**	5.77×10^{5}	3.92×10^{5}	3.32×10^{5}	1.26×10^{3}	-1.23×10^{3}	-1.99×10^{5}
XAT	1.05×10^{12}	5.77×10^{5}	**1.00×10^{6}**	2.76×10^{5}	1.18×10^{5}	4.07×10^{1}	1.34×10^{3}	3.35×10^{4}
YAT	3.63×10^{11}	3.92×10^{5}	2.76×10^{5}	**1.26×10^{5}**	3.43×10^{4}	4.59×10^{1}	3.01×10^{2}	6.02×10^{3}
ZAT	1.67×10^{11}	3.32×10^{5}	1.18×10^{5}	3.43×10^{4}	**3.91×10^{4}**	5.93×10^{1}	6.79×10^{2}	7.57×10^{3}
NA	2.48×10^{8}	1.26×10^{3}	4.07×10^{1}	4.59×10^{1}	5.93×10^{1}	**7.61×10^{-1}**	1.12×10^{0}	-1.13×10^{1}
SP	7.42×10^{8}	-1.23×10^{3}	1.34×10^{3}	3.01×10^{2}	6.79×10^{2}	1.12×10^{0}	**3.91×10^{1}**	4.23×10^{2}
ST	1.10×10^{10}	-1.99×10^{5}	3.35×10^{4}	6.02×10^{3}	7.57×10^{3}	-1.13×10^{1}	4.23×10^{2}	**2.05×10^{4}**
MCS	-1.47×10^{9}	4.68×10^{3}	-1.95×10^{3}	-1.68×10^{2}	-3.70×10^{2}	-1.59×10^{-1}	-1.28×10^{0}	-1.87×10^{2}
RTZ	-5.36×10^{9}	8.21×10^{3}	-5.79×10^{3}	-1.26×10^{3}	-8.73×10^{2}	-5.06×10^{-1}	-2.14×10^{0}	-3.84×10^{2}
RTY	1.64×10^{8}	1.40×10^{4}	-1.52×10^{3}	7.12×10^{2}	-8.28×10^{2}	-3.16×10^{-1}	-9.99×10^{0}	-4.85×10^{2}
RTZ	-3.03×10^{9}	1.00×10^{4}	-3.64×10^{3}	-6.65×10^{2}	-7.31×10^{2}	-4.95×10^{-1}	-2.29×10^{0}	-3.72×10^{2}
MTX	1.97×10^{12}	1.73×10^{6}	1.45×10^{6}	5.25×10^{5}	4.14×10^{5}	6.68×10^{2}	1.14×10^{4}	1.65×10^{5}
MTY	5.73×10^{11}	-2.13×10^{6}	9.23×10^{5}	9.11×10^{4}	4.79×10^{5}	4.12×10^{2}	1.74×10^{4}	3.56×10^{5}
MTZ	2.08×10^{12}	-6.75×10^{5}	2.53×10^{6}	4.67×10^{5}	8.60×10^{5}	6.37×10^{2}	2.74×10^{4}	4.90×10^{5}
Mass	3.86×10^{12}	1.85×10^{6}	3.88×10^{6}	1.03×10^{6}	6.90×10^{5}	6.24×10^{2}	1.48×10^{4}	2.75×10^{5}

Table 7.3. (b) Variance-Covariance matrix for the Haas data with the variances (across the diagonal) in bold and the significant covariances shaded (see Table 7.2 for nomenclature)

	MCS	RTX	RTY	RTZ	MTX	MTY	MTZ	Mass
Vol	-1.47×10^{9}	-5.36×10^{9}	1.64×10^{8}	-3.03×10^{9}	1.97×10^{12}	5.73×10^{11}	2.08×10^{12}	3.86×10^{12}
SS	4.68×10^{3}	8.21×10^{3}	1.40×10^{4}	1.00×10^{4}	1.73×10^{6}	-2.13×10^{6}	-6.75×10^{5}	1.85×10^{6}
XAT	-1.95×10^{3}	-5.79×10^{3}	-1.52×10^{3}	-3.64×10^{3}	1.45×10^{6}	9.23×10^{5}	2.53×10^{6}	3.88×10^{6}
YAT	-1.68×10^{2}	-1.26×10^{3}	7.12×10^{2}	-6.65×10^{2}	5.25×10^{5}	9.11×10^{4}	4.67×10^{5}	1.03×10^{6}
ZAT	-3.70×10^{2}	-8.73×10^{2}	-8.28×10^{2}	-7.31×10^{2}	4.14×10^{5}	4.79×10^{5}	8.60×10^{5}	6.90×10^{5}
NA	-1.59×10^{-1}	-5.06×10^{-1}	-3.16×10^{-1}	-4.95×10^{-1}	6.68×10^{2}	4.12×10^{2}	6.37×10^{2}	6.24×10^{2}
SP	-1.28×10^{0}	-2.14×10^{0}	-9.99×10^{0}	-2.29×10^{0}	1.14×10^{4}	1.74×10^{4}	2.74×10^{4}	1.48×10^{4}
ST	-1.87×10^{2}	-3.84×10^{2}	-4.85×10^{2}	-3.72×10^{2}	1.65×10^{5}	3.56×10^{5}	4.90×10^{5}	2.75×10^{5}
MCS	**3.16×10^{1}**	6.75×10^{1}	7.04×10^{1}	6.47×10^{1}	-2.06×10^{3}	-6.53×10^{3}	-6.95×10^{3}	-1.01×10^{4}
RTZ	6.75×10^{1}	**1.58×10^{2}**	1.47×10^{2}	1.48×10^{2}	-6.30×10^{3}	-1.09×10^{4}	-1.12×10^{4}	-2.63×10^{4}
RTY	7.04×10^{1}	1.47×10^{2}	**1.82×10^{2}**	1.50×10^{2}	-3.18×10^{3}	-2.02×10^{4}	-1.94×10^{4}	-1.71×10^{4}
RTZ	6.47×10^{1}	1.48×10^{2}	1.50×10^{2}	**1.44×10^{2}**	-4.35×10^{3}	-1.15×10^{4}	-9.23×10^{3}	-1.95×10^{4}
MTX	-2.06×10^{3}	-6.30×10^{3}	-3.18×10^{3}	-4.35×10^{3}	**7.60×10^{6}**	7.47×10^{6}	1.20×10^{7}	8.98×10^{6}
MTY	-6.53×10^{3}	-1.09×10^{4}	-2.02×10^{4}	-1.15×10^{4}	7.47×10^{6}	**1.45×10^{7}**	1.90×10^{7}	9.87×10^{6}
MTZ	-6.95×10^{3}	-1.12×10^{4}	-1.94×10^{4}	-9.23×10^{3}	1.20×10^{7}	1.90×10^{7}	**3.66×10^{7}**	1.91×10^{7}
Mass	-1.01×10^{4}	-2.63×10^{4}	-1.71×10^{4}	-1.95×10^{4}	8.98×10^{6}	9.87×10^{6}	1.91×10^{7}	**2.01×10^{7}**

Table 7.4. Variance-Covariance matrix for the multi-company data with the variances (across the diagonal) in bold and the significant covariances shaded (see Table 7.2 for nomenclature)

	Vol	SS	XAT	YAT	ZAT	SP	ST	NA	RAT	RAY	RAZ	Mass
Vol	**3.90×10^{20}**	-6.35×10^{12}	7.80×10^{12}	1.51×10^{12}	1.49×10^{12}	6.17×10^{9}	1.07×10^{12}	-2.38×10^{9}	8.46×10^{10}	8.15×10^{10}	7.14×10^{10}	4.42×10^{13}
SS	-6.35×10^{12}	**7.39×10^{6}**	-9.23×10^{5}	-1.17×10^{5}	-3.63×10^{4}	-1.27×10^{2}	-6.75×10^{4}	5.39×10^{2}	1.55×10^{4}	1.48×10^{4}	1.40×10^{4}	-2.55×10^{6}
XAT	7.80×10^{12}	-9.23×10^{5}	**8.40×10^{5}**	1.33×10^{5}	1.06×10^{5}	2.49×10^{3}	8.35×10^{4}	-1.39×10^{2}	-1.82×10^{3}	-9.58×10^{2}	-8.85×10^{2}	3.92×10^{6}
YAT	1.51×10^{12}	-1.17×10^{5}	1.33×10^{5}	**3.71×10^{4}**	2.54×10^{4}	5.89×10^{2}	1.39×10^{4}	5.07×10^{0}	-2.46×10^{2}	-1.55×10^{2}	-1.56×10^{2}	7.99×10^{5}
ZAT	1.49×10^{12}	-3.63×10^{4}	1.06×10^{5}	2.54×10^{4}	**2.32×10^{4}**	5.75×10^{2}	1.24×10^{4}	-1.12×10^{1}	2.59×10^{1}	1.04×10^{2}	7.35×10^{1}	5.37×10^{5}
SP	6.17×10^{9}	-1.27×10^{2}	2.49×10^{3}	5.89×10^{2}	5.75×10^{2}	**3.82×10^{1}**	3.32×10^{2}	1.59×10^{0}	5.32×10^{0}	6.85×10^{0}	8.54×10^{0}	1.45×10^{4}
ST	1.07×10^{12}	-6.75×10^{4}	8.35×10^{4}	1.39×10^{4}	1.24×10^{4}	3.32×10^{2}	**1.15×10^{4}**	2.96×10^{0}	-6.12×10^{1}	3.87×10^{1}	1.53×10^{1}	4.19×10^{5}
NA	-2.38×10^{9}	5.39×10^{2}	-1.39×10^{2}	5.07×10^{0}	-1.12×10^{1}	1.59×10^{0}	2.96×10^{0}	**6.74×10^{-1}**	7.16×10^{-1}	5.89×10^{-1}	6.95×10^{-1}	5.73×10^{2}
RTX	8.46×10^{10}	1.55×10^{4}	-1.82×10^{3}	-2.46×10^{2}	2.59×10^{1}	5.32×10^{0}	-6.12×10^{1}	7.16×10^{-1}	**8.26×10^{1}**	7.65×10^{1}	7.33×10^{1}	-1.71×10^{3}
RTY	8.15×10^{10}	1.48×10^{4}	-9.58×10^{2}	-1.55×10^{2}	1.04×10^{2}	6.85×10^{0}	3.87×10^{1}	5.89×10^{-1}	7.65×10^{1}	**7.23×10^{1}**	6.91×10^{1}	1.60×10^{3}
RTZ	7.14×10^{10}	1.40×10^{4}	-8.85×10^{2}	-1.56×10^{2}	7.35×10^{1}	8.54×10^{0}	1.53×10^{1}	6.95×10^{-1}	7.33×10^{1}	6.91×10^{1}	**6.78×10^{1}**	1.94×10^{3}
Mass	4.42×10^{13}	-2.55×10^{6}	3.92×10^{6}	7.99×10^{5}	5.37×10^{5}	1.45×10^{4}	4.19×10^{5}	5.73×10^{2}	-1.71×10^{3}	1.60×10^{3}	1.94×10^{3}	**2.59×10^{7}**

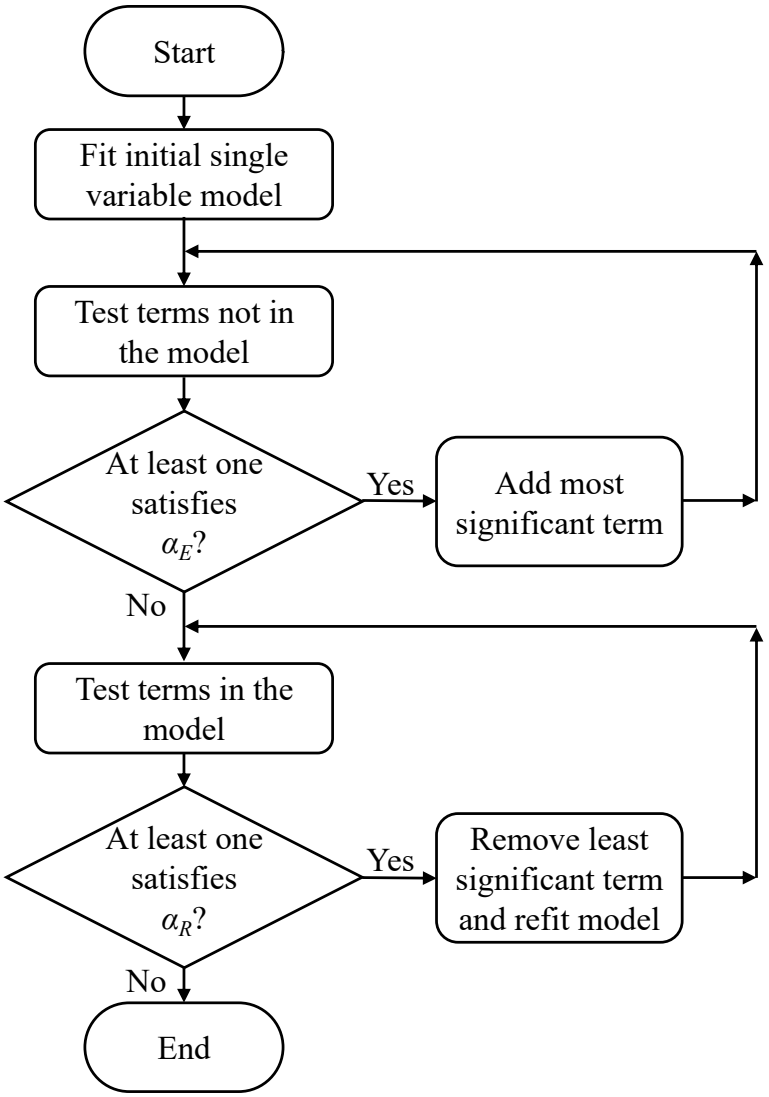

Figure 7.2 Flow chart of the procedure for stepwise regression

7.3.2 Cost model results

From the data provided by the MT builders, multiple empirical cost (price) models were created: simple linear regressions for each feature of both data sets, a stepwise regression for the multi-company data set, and a stepwise regression for the Haas data set. The simple linear regression model results can be found in Table 7.2. The coded (standardized) stepwise regression model for the Haas data set can be found in Eq. (7.2) and the uncoded model can be found in Eq. (7.3). The coded (standardized) stepwise regression model for the multi-company can be found in Eq. (7.4) and the uncoded model can be found in Eq. (7.5). The nomenclature and data ranges for the

stepwise models can be found in Table 7.5. In the models a subscript of "C" represents a coded value (standardized), and a subscript of "U" represents an uncoded value (not standardized). The standard error and p-values for the Haas model can be found in Table 7.6 and the standard error and p-values for the multi-company model can be found in Table 7.7.

$$C = 2.434 \times 10^5 + 6.776 \times 10^4 V_C + 3.648 \times 10^4 S_C + 3.477 \times 10^4 X_C - 3.430 \times 10^4 Y_C + 4.492 \times 10^4 A_C + 8.309 \times 10^4 m_C \quad (7.2)$$

$$C = -1.4245 \times 10^5 + 1.659 \times 10^{-5} V_U + 2.806 S_U + 19.840 X_U - 34.8400 Y_U + 4.49 \times 10^4 A_U + 10.414 m_U \quad (7.3)$$

$$C = 2.194 \times 10^5 + 6.190 \times 10^4 V_C + 3.294 \times 10^4 P_C + 1.037 \times 10^5 m_C \quad (7.4)$$

$$C = -2.197 \times 10^4 + 1.904 \times 10^{-4} V_U + 3.921 \times 10^3 P_U + 11.468 m_U \quad (7.5)$$

Table 7.5. Significant MT Features from Stepwise Regression

Nomenclature		Acquired Data Range	
		Haas	Multi-Company
A	Number of axes	3, 5	
m	Mass (kg)	917-16874	1815-19900
P	Spindle power (kW)		5.6-22.4
S	Spindle speed (rpm)	4000-30000	
V	Volume (m^3)	0.024-8.19	0.031-65
X	X-axis travel	305-3810	
Y	Y-axis travel	254-2223	

Table 7.6. Standard error and p-values for Haas cost (price) model (found in Eq. (7.2))

Coefficient	Feature	Standard Error	p-value
6.776×10^4	Volume (mm^3)	1.919×10^4	7.666×10^{-4}
3.648×10^4	Spindle speed (RPM)	8.639×10^3	7.663×10^{-5}
3.477×10^4	X-axis travel (mm)	1.256×10^4	7.324×10^{-3}
-3.430×10^4	Y-axis travel (mm)	1.181×10^4	5.009×10^{-3}
4.492×10^4	Number of axes	3.038×10^3	1.794×10^{-22}
8.309×10^4	Mass (kg)	8.794×10^3	8.075×10^{-14}

Table 7.7. Standard errors and p-values for multi-company cost (price) model (found in Eq. (7.4))

Feature	Standard Error	p-value
Volume (V, mm^3)	1.814×10^{4}	3.570×10^{-3}
Spindle Power (P, kW)	1.516×10^{4}	4.518×10^{-2}
Mass (m, kg)	2.205×10^{4}	2.389×10^{-4}

7.4 Discussion

From the results presented above, a number of conclusions may be drawn as to the main cost drivers of a MT (price was used to build the models but it was assumed price is proportional to cost to manufacture the MT). This section will discuss these results and implications along with methods to design MTs considering both energy and cost.

7.4.1 Cost drivers

From the results in Table 7.6 and Table 7.7, and Eqs. (7.2) – (7.5), several observations about cost drivers can be made. The first model, Haas only (results in Table 7.6), shows that the complexity of the MT (as represented by the number of axes), machine size (shown by mass, volume, and X and Y-axis travel), and MT capability (represented by spindle speed and spindle power), have the most significant impact on the price of the machine. The number of axes has the largest impact on price followed by mass, then spindle speed, volume, and finally X and Y-axis travel. The second model, multi-company (results in

Table 7.7), shows similar results in that size (represented by mass and volume) and machine capability (represented by spindle power) significantly affect machine price. The model shows mass has the largest impact, followed by volume, with spindle power having the smallest impact of the three.

These results show that mass is very important in determining the price of the machine; this is undoubtedly due to the fact that greater mass means larger material costs. Volume, and X and Y-axis travel, are also shown to be important. However, these variables also relate to the mass of the MT and the associated material costs. This is consistent with the discussion in Section 7.2.3 that reported on how material cost plays a significant role in the cost of the product (in this case, the cost of a MT). With both models showing mass to be a significant cost driver, it can be

concluded that lightweighting a MT should reduce the overall machine price. However, since mass and size of the MT are not the only price drivers, other design elements should still be considered. These include the complexity of the MT (seen by the number of axes) and the capability of the MT (spindle power, spindle speed, and X & Y-axis travel). The three price driver categories are summarized below:

- Size (mass, volume, X & Y-axis travel)
- Complexity (number of axes)
- Capability (spindle power spindle speed, X & Y-axis travel)

What is not described though in the model is the design of the technology, e.g., material choice, control, drive selection, that is required for HSM. These may have a significant impact on cost beyond some of the features described in the model. Further investigation into the technology and design of the machines may be required. In addition, these machines may not necessarily be optimized in their design due to many being modular in order to meet many different requirements. This will also impact the cost model.

7.4.2 Case study: design of MTs with consideration of energy and cost

With an understanding of how the mass of the MT, more specifically the materials, affects the price of a MT, strategies may be implemented to consider both energy and cost while designing a machine. This section will explore design methods that consider both energy and cost based on prior work of the author.

Lightweighting design method

Previous work of the author [126,146] explored lightweighting the table of a milling machine to reduce its energy consumption. The table was chosen since it moves throughout cutting and provides a potential for energy reduction during the use of the machine. Other components within the MT will provide a greater opportunity for mass reduction and therefore price reduction, e.g., the housing and columns, but do not move and will not provide the energy savings during use. Since the goal of this chapter is to examine how lightweighting with the intent of reducing energy consumption will impact the cost of the machine, the table was chosen.

Both papers proposed GAs to design the table with reduced mass. Triebe et al. [126] examined and compared two lightweight sandwich panel designs, i.e., a honeycomb core and a metal foam core, to a solid table. The GA varied parameters such as honeycomb core thickness and height to search for designs that minimized mass while minimizing bending. Triebe et al. [146] also searched for lightweight sandwich panel table designs. These designs consisted of a single row of cross-sectional beams that run along the length of the table. An example with square cross-sections (or cells) is shown in Figure 7.3. The GA searches for shapes of cells that minimize the mass of the table while maximizing its resistance to bending (stiffness); stiffness was assumed to be proportional to the inverse of the moment of inertia (MoI) and polar moment of inertia (PMoI). The GA found that cells with an I-shaped cross section were best suited to reduce mass while retaining strength. The final design was compared to a solid table design using finite element analysis (FEA) and found the I-shaped cross section design did deflect more under a load than the solid table, but the deflection was small.

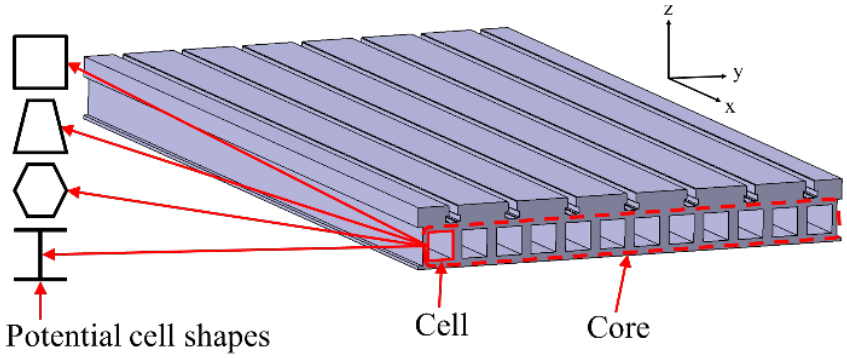

Figure 7.3 Sandwich panel table with a core of square cells, adapted from Triebe et al. [146]

GA was chosen to search for table designs due to its ability to find multiple solutions, allow for multiple objectives, and for its ability to demonstrate tradeoffs between the objectives. This allowed for the comparison between mass and stiffness. GA also reduces the chance of convergence at a local optimum through the introduction of mutations and broad consideration/searching of the entire solution space. The final population of solutions provides various design options that allow for a choice with an acceptable stiffness and a small mass.

When lightweighting the table it is important to consider vibrations since vibrations contribute to the precision of the machine and quality of the finished part. A lighter weight table

can increase vibrations due to a potential decrease in the natural frequencies as a result of the lower mass. Future work will explore the dynamic performance of the lightweight table. However, for this chapter, the reduction in mass with its impact on cost will be the focus in the following subsections.

Including cost/price and energy in the design

With the cost model built in Section 7.3 (price was used to build the model but it was assumed price is proportional to cost to manufacture the MT), MT cost can now be considered during design. Due to the link found in this chapter between the mass of the MT and its cost, instead of adding MT cost as an objective, mass and cost can be considered simultaneously as a single objective. This allows for cost to be considered during design while attempting to reduce energy consumption. To consider MT cost simultaneously, the mass savings, calculated from comparing the lightweight table design to the original table design, is plugged into the equation and all other terms are deleted since they are not considered in the optimization. This will provide a cost (price) savings. For an estimation of total cost (price), the rest of the machine tool specifications should be included in the calculation.

Since lightweighting reduces the amount of materials in the MT, as is in the case of Triebe et al. [126,146], upstream energy consumption and CO_2 can also be considered in the design of the MT. This is similarly accomplished by including the relationship between materials and energy consumption/CO_2 within the GA. However, if switching between materials, energy and CO_2 will change. These relationships between material and energy/CO_2 can be found in Figure 7.1(b).

Example: lightweighting table

Using the lightweighting method outlined in Triebe et al. [146], the cost (price) savings along with upstream CO_2 and energy savings can be calculated. The standard table (shown in Figure 7.4(a)) will be considered as a baseline for comparison purposes. This table is assumed to be made from steel and has dimensions of 889×1676×122.9 mm with a mass of 1370 kg. A lightweight table design is shown in Figure 7.4(b) and has the same dimensions as the solid table but has a mass of 687 kg. With a mass savings of 683 kg, the manufacturing cost savings and the savings from reduced mass in terms of embodied energy and CO_2 can be calculated. This is dependent on

how the table is manufactured, e.g., if the table is machined from the same amount of material as the first table then there will be no embodied energy savings. Embodied energy and CO_2 savings are calculated using the values in Figure 7.1(b) (N.B., there will also be energy and CO_2 savings during use of the reduced mass table, but this issue is not considered here). Changes to the machine tool that might be possible owing to a table with reduced mass are also not considered here; for example, a smaller motor may be possible when the table has reduced mass. However, these other design changes will most likely not increase the overall mass (in fact, more likely that they will reduce the mass even further). Therefore, assuming strictly a reduction in table mass can provide a lower bound to any savings resulting from the mass reduction. The cost/price, embodied energy, and embodied CO_2 savings can be found in Table 7.8. The cost/price savings is about half, but some savings is lost to a greater complexity of design.

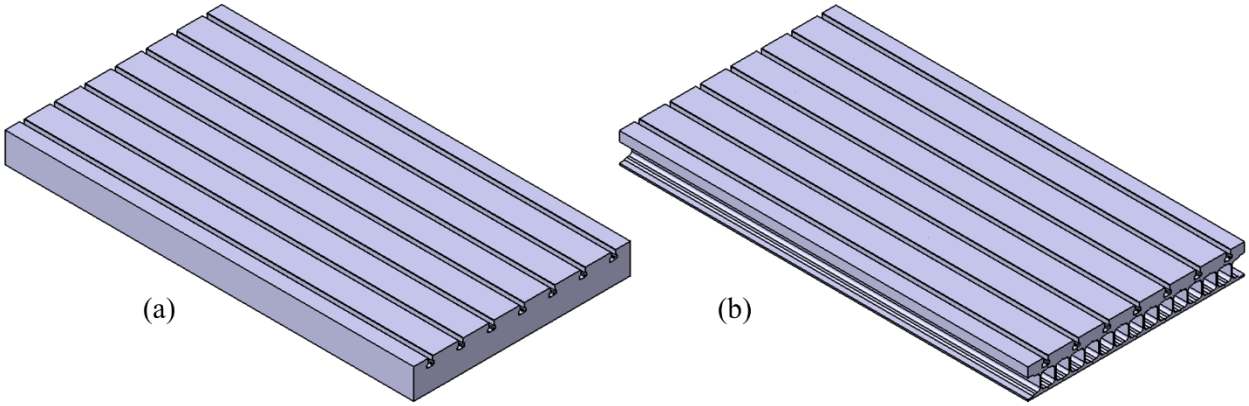

Figure 7.4 (a) Standard solid table design having a mass of 1370 kg. (b) Lightweight table design having a mass of 687 kg.

Table 7.8. Cost/price, embodied energy, and embodied CO2, savings from lightweighting the table

Savings	
Cost	$7,112
Embodied Energy	22,200 (MJ)
Embodied CO_2	485 (kg CO_2)

Complexity of the MT is considered in the cost/price model through the number of axes. However, this would be difficult to apply to a change in complexity of other components and

systems of the MT. To further explore the issue of MT complexity, estimations of cost for the solid table design and the lightweight X-table design will be compared from Figure 7.4.

To manufacture the solid table from Figure 7.4(a), first the table would be cast. Then the sides and top and bottom would be machined to the required dimensions. Finally, the t-slots would be machined. To manufacture the lightweight table from Figure 7.4(b), more processes will be needed. To build the core of the sandwich panel design, the I-shaped beams are rolled and then cut to length. Then the beams are arranged horizontally as shown in Figure 7.4(b) and joined to the top and bottom facing plates. Both the bottom and top facing plates are made from rolled steel. The top plate includes machined t-slots.

The cost of the two tables can be calculated from the cost of each manufacturing step plus the material cost. It was assumed that the material cost for the solid table is about $4.50/kg. The mass of the cast plate was assumed to be 1620 kg, which is about 18% more massive than the finished plate; this extra material allowed for cleanup cuts to produce the final plate. The material cost of the 1620 kg cast plate is $7,300. The casting and machining processes add a relatively small amount compared to the material cost. For the lightweight table, the cost of the I-beams, lower facing plate, and upper facing plate are about $1,200, $800, and $2,700 respectively. The cost to purchase the I-beams and plates is about $4,700 (this includes the material and manufacturing costs) [190]. The joining and machining would add a relatively small amount compared to the material price. The cost to join and machine the lightweight table should be similar to the cost to cast and machine the solid table. As a result, there would be a cost savings of about $2,600. While the savings is not as high as predicted (see Table 7.8), there is still a cost reduction due to lightweighting. Part of this difference may also be due to that the models built in this chapter were built from price data instead of cost data. This savings though is calculated from manufacturing cost data.

7.5 Conclusion

This chapter has developed an empirical cost model for (or cost of an individual/company to purchase) a MT that may be used to estimate the economic benefits of lightweighting (reducing MT mass). Price data was used to build the model since MT builders are hesitant to provide cost data. Per personal communications [10], MT builders price their machines close to the

manufacturing cost since the MT industry is extremely competitive. Therefore, it was assumed that price is proportionally related to cost; there is a consistent markup among the machines. This development effort was motivated by the concern that lightweighting to reduce energy consumption may increase the cost of the machine due to a more complex design. This model, though it was built from price data, provides the desired insight into how lightweighting affects MT cost. From building the cost model, it was found that the mass of the MT is a cost driver. This means reducing the mass through lightweighting will reduce MT cost due to less materials being used. However, the method of lightweighting must still be considered due to the potential for increasing the design complexity and therefore cost.

This cost model was built considering various features of the MT including mass, spindle power, and number of axes. Two data sets were developed from which empirical models for MT purchase price were created. The first data set reflected information obtained from a single company (Haas), and the second data set contained data from multiple companies (Haas, Hurco, and Mazak). Simple linear regression models were made for each feature considered from both data sets, and a stepwise regression model was built for both data sets. The simple linear regression models provided some understanding of the relative importance of each variable on price but due to the variables not being independent of each other, the simple linear regression models may not be completely accurate. Therefore, stepwise regression models were built.

From the stepwise regression model built from the Haas only data it was found that the number of axes was the most significant cost driver followed by mass. The following were also important, but the results show they were not as significant: spindle speed, volume, and X and Y-axis travel. Results from the multi-company data set showed that mass was the most significant followed by volume and spindle power. From these results it is seen that lightweighting of a MT will not increase the cost of a machine; rather, it will decrease it. What is not described though in the model is the fine-tuning of the design or the modularity of the machines to meet various requirements. Further investigation may be required to describe these.

Using the slide table of a milling machine as an example it was shown how cost, energy, and CO2 can be considered during the design of the MT. The table was chosen since it moves throughout cutting and provides a potential for energy reduction during the use of the machine. Other components within the MT will provide a greater opportunity for mass reduction and therefore price reduction, e.g., the housing and columns, but do not move and will not provide the

energy savings during use. Since the goal of this chapter is to examine how lightweighting with the intent of reducing energy consumption will impact the cost of the machine, the table was chosen. Previous work by the author, Triebe et al. [126,146], showed how to reduce the mass of the table through a sandwich panel design. In these papers the table design was optimized by a multi-objective GA. Using this approach, it was found that cost, energy, and CO2 could be included in the GA as an objective. In this manner the MT slide table could be designed to reduce its mass and the MT cost, energy, and CO2 emissions while preserving the strength of the table.

This chapter has made a number of key contributions and observations related to the cost modeling and the design of MTs for energy savings:

- This chapter created a cost model of CNC vertical milling machines, assuming price of the machines is proportional to the cost to manufacture, based on various features of the MTs to find the cost drivers;
- Mass was found to be a significant driver for MT cost and therefore lightweighting has the potential to decrease the cost of a MT, but complexity of design can reduce or even eliminate the cost savings depending on the manufacturing processes and cost of material (if material is changed);
- This chapter provided an example illustrating the potential cost, embodied energy, and embodied CO2 savings through the design of a vertical milling machine slide table.

It is suggested that future work should explore the application of lightweighting to other components and systems to further improve the energy efficiency of MTs.

8. SUMMARY AND CONCLUSIONS

In this dissertation, lightweighting was considered to reduce the energy consumption of a vertical milling machine. First, the slide table of the machine tool was chosen for the application of lightweighting. A sandwich panel design was selected to replace the solid table design due to its lightweight but stiff characteristics. Following the development of the application, an energy model of the slide table drive system was constructed to provide insight into how the mass of the table affects the drive system energy consumption. This model also provided insight into design considerations required to implement lightweighting. Then static and dynamic models were built to understand how lightweighting affects the performance of the machine tool. When reducing the mass of components, there is concern that the stiffness and performance of the machine will be reduced and affect the quality of parts produced. Finally, a cost model was built to explore how lightweighting impacts the cost of machine tools. Lightweighting design changes have potential for increasing the cost of the machine due to an increase in complexity. If the cost increases greatly, then machine tool builders may be hesitant to incorporate energy saving changes, i.e., lightweighting. The four tasks are concluded below.

First, the lightweighting application was proposed. The slide table of a vertical milling machine was chosen for the application of lightweighting due it moving throughout cutting. A sandwich panel design was selected as the design to reduce the mass of the table since sandwich panels allow for mass reduction while providing increased stiffness and resistance to bending. This is helpful since the table will be subjected to large forces. The sandwich structure consisted of two plates, one on the bottom and one on the top, with a core in the middle. The upper plate was thicker to include the t-slots. The sandwich panel core consisted of a single row of horizontally running beams so as to reduce the complexity of the design and therefore provide an easier table to manufacture. To reduce bending and deflection in the table, the core of the sandwich structure was optimized with a genetic algorithm to find the optimal shape of the cross-sections of the beams. The results of the optimization were I-shaped cross-sections. Two lightweight table designs were constructed with standard I-shaped beams and were analyzed using finite element analysis and compared to a solid table design. The lightweight tables were shown to have a similar stiffness while reducing the mass of the table.

Second, a mechanistic energy model was presented to provide insight into how the mass of the table affects the machine tool energy consumption and provides understanding into the design consideration required to implement lightweighting of the table. This model described the energy required by the drive system motors to move the table during cutting and non-cutting moves. The energy model was built considering the forces to drive the table. These include the force due to gravity for the table and the workpiece, and the forces from cutting. The energy model was built for two drive systems: one consisting of a standard table and one consisting of a lightweight table. For both drive systems, motors were sized based on the requirements of each system. It was found from constructing the energy model for both drive systems that the sizing of the motor is very important since much of the time the motor is running inefficiently, that is, running at a load much lower than what it was designed for. Therefore, a small improvement in sizing can have a large impact on efficiency. Without resizing the motor when replacing the solid table drive system with the lightweight table drive system, the energy savings would be much lower. From resizing the motor for the lightweight table drive system, a drive system energy savings of over 30% was achieved. It should be noted that this energy savings will scale based on the size of the table, meaning a smaller table will still save roughly 30% energy consumption. However, due to the need for resizing the motor, there is a greater chance that this energy savings is lost for smaller designs due to the difficulty of choosing a slightly smaller motor as mass savings decreases.

Third, static and dynamic models were constructed to evaluate how lightweighting affects the performance of the machine tool. If the static and dynamic performance of the machine tool drops significantly, it can affect the quality of the parts manufactured. To address the static performance of the machine tool, multiple static models were built. During the first task of optimizing the sandwich panel core structure, the stiffness was modeled using the moment of inertia (MoI) and polar moment of inertia (PMoI). MoI relates directly to bending and PMoI relates directly to torsion. A large MoI means less bending and a large PMoI means less torsion. Then when the final core design was chosen, a finite element model was built to analyze the lightweight table stiffness as compared to the solid table. As described earlier, it was found the lightweight table design had a similar stiffness to the solid table design. Then to analyze the dynamics of the table, a second static model was built along with a dynamic model. Both the static and dynamic models were built using finite element software. Approximate stiffnesses were found for the lightweight and standard table designs. The lightweight stiffnesses were compared to the solid

table and a reduction in stiffness was observed but it was found that stiffness can be decoupled from mass through design. Then with the dynamic models, the natural frequencies and mode shapes were found. Similar to the stiffness analysis, a reduction in natural frequencies were found but the design of the table was found to play a major role in natural frequency in addition to mass. The natural frequencies were still found to be very high compared to the frequencies caused by the systems interacting with the table, i.e., cutting and feed systems. However, since the cutting force is not sinusoidal but is periodic, the cutting force can be described by the sum of sine and cosine functions using Fourier decomposition. These sine and cosine functions may have higher frequencies and should be considered.

Lastly, data from a wide variety of machine tool features was gathered and then empirical cost models were fit to the data to provide insight into the cost drives of the machine tools. The data came from three different machine tool builders and covered a wide variety of vertical milling machines. Simple linear regression models were built for each feature to assess the relative importance of each feature in determining the cost of the machine. Then, since the variables are not independent of each other, stepwise regression was used to construct a cost model considering all the features. From this it was found that mass plays a significant role in determining the cost of a machine tool. Since manufacturing cost data was not available it was assumed the cost to manufacture a machine tool is linearly related to the purchase price. Following, the role of complexity of design in the cost of the machine was explored. Using the slide table as a case study, the cost to manufacture the solid table was compared to three lightweight table designs. First, using the developed cost model, the cost savings was calculated for each of the table designs based on the difference in mass. The cost to manufacture each table was then calculated and compared to the savings found from the cost model. It was found that much of the cost was attributed to the materials, but some cost savings was lost due to the lightweight tables being more complex to manufacture.

From completing these four tasks it is shown that lightweighting can be an important tool to reducing machine tool energy consumption. The slide table provided a proof of concept for a lightweighting application, and the energy model provided a link between the mass and energy consumption in the machine tool. It was shown that more than 30% of the drive system energy could be saved by lightweighting the table. A 30% savings is substantial, especially if applied to multiple systems throughout the machine tool. The static and dynamic models showed that

designing lightweight components can be accomplished without sacrificing performance. Various design tools, e.g., finite element analysis, can be used to address static and dynamic concerns. The cost model showed how lightweighting will not increase the cost of the machine tool and therefore will not discourage machine builders from implementing lightweighting to reduce energy consumption.

Limitations of this research are included in the following discussion. There was a lack of comparison to other lightweight table designs including designs built from topology optimization and other evolutionary algorithms. However, designs from other evolutionary algorithms could produce more expensive tables. The x-direction I-beam design used throughout the research could also allow for increased bending due to the I-beams running along the length of the table, the same direction as the slides. This would allow for bending between the beams. The y-direction table design does not have this limitation. Limitations can also be found in the redesign of the drive table system since motor selection plays such a large role in the energy consumption. If a larger factor of safety is required due to any uncertainty, the energy savings could be easily lost. In addition, design of the table was found to reduce the loss in stiffness but damping due to structure of the table was not investigated. An experiment would have been helpful in determining if design could increase damping within the structure. Finally, the manufacturing cost could not be separated out from the purchase cost. It was assumed that the two were related linearly but that may not be the case. Future work should include the application of lightweighting to other components and systems throughout the machine tool.

The contributions of this research are summarized as follows:

1. A shape optimization method to design the sandwich panel table, accomplished through a genetic algorithm. This provides a lower cost lightweighting application.
2. A mechanistic model linking mass to energy consumption. This provides insight into design considerations required to implement lightweighting
3. Static and dynamic models of the milling machine slide table. These provide understanding of how lightweighting affects the performance machine tools
4. A cost model of milling machines. This provides insight into how lightweighting affects the machine tool cost.

REFERENCES

[1] Central Intelligence Agency. (2017). *The World Factbook: Economy---Overview*. https://www.cia.gov/library/publications/resources/the-world-factbook/geos/print_xx.html

[2] Sutherland, J., Skerlos, S. J., Haapala, K. R., Cooper, D., Zhao, F., & Huang, A. (2020). Industrial sustainability: Reviewing the Past and Envisioning the Future. *Journal of Manufacturing Science and Engineering*, 1–33. https://doi.org/10.1115/1.4047620

[3] Ritchie, H. (2020). *Sector by sector: where do global greenhouse gas emissions come from?* https://ourworldindata.org/ghg-emissions-by-sector

[4] EIA. (2021). *Use of energy explained Energy use in industry*. https://www.eia.gov/energyexplained/use-of-energy/industry.php

[5] U.S. Energy Information Administration. (2021). *Annual Energy Outlook 2021 with projections to 2050*. https://www.eia.gov/outlooks/aeo/

[6] Freedonia Focus Reports. (2019). *Global Machine Tools* (Issue November).

[7] Zein, A. (2012). *Transition Towards Energy Efficient Machine Tools*. https://doi.org/10.1007/978-3-642-32247-1

[8] Dahmus, J. B., & Gutowski, T. G. (2004). An Environmental Analysis of Machining. *Manufacturing Engineering and Materials Handling Engineering*, *2004*(47136), 643–652. https://doi.org/10.1115/IMECE2004-62600

[9] He, K., Tang, R., & Jin, M. (2017). Pareto fronts of machining parameters for trade-off among energy consumption, cutting force and processing time. *International Journal of Production Economics*, *185*(December 2016), 113–127. https://doi.org/10.1016/j.ijpe.2016.12.012

[10] Li, W., Zein, A., Kara, S., & Herrmann, C. (2011). An Investigation into Fixed Energy Consumption of Machine Tools. In *Glocalized Solutions for Sustainability in Manufacturing* (Vol. 82, Issue 3, pp. 268–273). Springer Berlin Heidelberg. https://doi.org/10.1007/978-3-642-19692-8_47

[11] Zhao, F., Murray, V. R., Ramani, K., & Sutherland, J. W. (2012). Toward the development of process plans with reduced environmental impacts. *Frontiers of Mechanical Engineering*, *7*(3), 231–246. https://doi.org/10.1007/s11465-012-0334-3

[12] Jiang, Z., Zhang, H., & Sutherland, J. W. (2012). Development of an environmental performance assessment method for manufacturing process plans. *International Journal of Advanced Manufacturing Technology*, *58*(5–8), 783–790. https://doi.org/10.1007/s00170-011-3410-7

[13] Mori, M., Fujishima, M., Inamasu, Y., & Oda, Y. (2011). A study on energy efficiency improvement for machine tools. *CIRP Annals - Manufacturing Technology*, *60*(1), 145–148. https://doi.org/10.1016/j.cirp.2011.03.099

[14] Diaz, N., Redelsheimer, E., Dornfeld, D., & Houlton, S. (2011). Energy Consumption Characterization and Reduction Strategies for Milling Machine Tool Use. *Manufacturing Chemist*, *82*(3), 22–24. https://doi.org/10.1007/978-3-642-19692-8

[15] Fang, K., Uhan, N., Zhao, F., & Sutherland, J. W. (2011). A new approach to scheduling in manufacturing for power consumption and carbon footprint reduction. *Journal of Manufacturing Systems*, *30*(4), 234–240. https://doi.org/10.1016/j.jmsy.2011.08.004

[16] Albertelli, P. (2017). Energy saving opportunities in direct drive machine tool spindles. *Journal of Cleaner Production*, *165*, 855–873. https://doi.org/10.1016/j.jclepro.2017.07.175

[17] Gao, M., Huang, H., Liu, Z., Li, X., & Sutherland, J. (2016). Design and Optimization of the Slide Guide System of Hydraulic Press Based on Energy Loss Analysis. *Energies*, *9*(6), 434. https://doi.org/10.3390/en9060434

[18] Helms, H., & Lambrecht, U. L. (2007). The potential contribution of light-weighting to reduce transport energy consumption. *The International Journal of Life Cycle Assessment*, *12*(1), 58–64. https://doi.org/DOI 10.1065/lca2006.07.258

[19] Lv, J., Tang, R., Tang, W., Liu, Y., Zhang, Y., & Jia, S. (2017). An investigation into reducing the spindle acceleration energy consumption of machine tools. *Journal of Cleaner Production*, *143*, 794–803. https://doi.org/10.1016/j.jclepro.2016.12.045

[20] Sulitka, M., Novotny, L., Sveda, J., Strakos, P., Hudec, J., Smolik, J., & Vlach, P. (2008). MACHINE TOOL LIGHTWEIGHT DESIGN AND ADVANCED CONTROL TECHNIQUES. *MM Science Journal*, *2008*(03), 30–34. https://doi.org/10.17973/MMSJ.2008_10_20081002

[21] Suh, J. D., Lee, D. G., & Kegg, R. (2002). Composite machine tool structures for high speed milling machines. *CIRP Annals - Manufacturing Technology*, *51*(1), 285–288. https://doi.org/10.1016/S0007-8506(07)61518-2

[22] Zulaika, J. J., Campa, F. J., & Lopez De Lacalle, L. N. (2011). An integrated process–machine approach for designing productive and lightweight milling machines. *International Journal of Machine Tools and Manufacture*, *51*(7–8), 591–604. https://doi.org/10.1016/j.ijmachtools.2011.04.003

[23] Duflou, J. R., Sutherland, J. W., Dornfeld, D., Herrmann, C., Jeswiet, J., Kara, S., Hauschild, M., & Kellens, K. (2012). Towards energy and resource efficient manufacturing: A processes and systems approach. *CIRP Annals - Manufacturing Technology*, *61*(2), 587–609. https://doi.org/10.1016/j.cirp.2012.05.002

[24] Diaz, N., Helu, M., Jayanathan, S., Chen, Y., Horvath, A., & Dornfeld, D. (2010). Environmental analysis of milling machine tool use in various manufacturing environments. *Proceedings of the 2010 IEEE International Symposium on Sustainable Systems and Technology, ISSST 2010*, 1–6. https://doi.org/10.1109/ISSST.2010.5507763

[25] IEA. (2019). *Total primary energy supply by fuel, 1971 and 2017*. https://www.iea.org/data-and-statistics/charts/total-primary-energy-supply-by-fuel-1971-and-2017

[26] US EIA. (2019). *December 2019 Monthly Energy Review*. https://doi.org/10.1044/leader.ppl.24062019.28

[27] Enparantza, R., Revilla, O., Azkarate, A., & Zendoia, J. (2006). A Life Cycle Cost Calculation and Management System for Machine Tools. *13th CIRP International Conference on Life Cycle Engineering*, *2*, 717–722.

[28] Kordonowy, D. N. (2002). A Power Assessment of Machining Tools [Massachusetts Institute of Technology]. In *Massachusetts Institute of Technology*. http://hdl.handle.net/1721.1/31108

[29] Zhou, L., Li, J. J., Li, F., Meng, Q., Li, J. J., & Xu, X. (2016). Energy consumption model and energy efficiency of machine tools: A comprehensive literature review. *Journal of Cleaner Production*, *112*, 3721–3734. https://doi.org/10.1016/j.jclepro.2015.05.093

[30] Beck, M., Helfert, M., Burkhardt, M., & Abele, E. (2016). Rapid Assessment: Method to Configure Energy Performant Machine Tools in Linked Energy Systems. *Procedia CIRP*, *48*, 514–519. https://doi.org/10.1016/j.procir.2016.03.012

[31] Behrendt, T., Zein, A., & Min, S. (2012). Development of an energy consumption monitoring procedure for machine tools. *CIRP Annals - Manufacturing Technology*, *61*(1), 43–46. https://doi.org/10.1016/j.cirp.2012.03.103

[32] Denkena, B., Flöter, F., & Hülsemeyer, L. (2012). Energy-efficient machine tools and technologies. *The 15th International Machine Tool Engineers' Conference (IMEC)*, 174–187.

[33] Moradnazhad, M., & Unver, H. O. (2017). Energy consumption characteristics of turn-mill machining. *International Journal of Advanced Manufacturing Technology*, *91*(5–8), 1991–2016. https://doi.org/10.1007/s00170-016-9868-6

[34] Warsi, S. S., Jaffery, S. H. I., Ahmad, R., Khan, M., Ali, L., Agha, M. H., & Akram, S. (2018). Development of energy consumption map for orthogonal machining of Al 6061-T6 alloy. *Proceedings of the Institution of Mechanical Engineers, Part B: Journal of Engineering Manufacture*, *232*(14), 2510–2522. https://doi.org/10.1177/0954405417703424

[35] Peng, T., & Xu, X. (2014). Energy-efficient machining systems: a critical review. *The International Journal of Advanced Manufacturing Technology*, *72*(9–12), 1389–1406. https://doi.org/10.1007/s00170-014-5756-0

[36] Yoon, H.-S., Lee, J.-Y., Kim, M.-S., & Ahn, S.-H. (2014). Empirical power-consumption model for material removal in three-axis milling. *Journal of Cleaner Production*, *78*, 54–62. https://doi.org/10.1016/j.jclepro.2014.03.061

[37] Zein, A. (2012). Energy Demand of Machine Tools and Performance Management. In Intergovernmental Panel on Climate Change (Ed.), *Climate Change 2013 - The Physical Science Basis* (Vol. 53, Issue 9, pp. 5–36). Cambridge University Press. https://doi.org/10.1007/978-3-642-32247-1_2

[38] Jedrzejewski, J., & Kwasny, W. (2017). Development of machine tools design and operational properties. *The International Journal of Advanced Manufacturing Technology*, 1051–1068. https://doi.org/10.1007/s00170-017-0560-2

[39] Sutherland, J. W., Rivera, J. L., Brown, K. L., Law, M., Hutchins, M. J., Jenkins, T. L., & Haapala, K. R. (2008). Challenges for the Manufacturing Enterprise to Achieve Sustainable Development. *Manufacturing Systems and Technologies for the New Frontier*, 15–18. https://doi.org/10.1007/978-1-84800-267-8_4

[40] Verl, A., Abele, E., Heisel, U., Dietmair, A., Eberspächer, P., Rahäuser, R., Schrems, S., & Braun, S. (2011). Modular Modeling of Energy Consumption for Monitoring and Control. In *Glocalized Solutions for Sustainability in Manufacturing* (Vol. 82, Issue 3, pp. 341–346). Springer Berlin Heidelberg. https://doi.org/10.1007/978-3-642-19692-8_59

[41] Dietmair, A., & Verl, A. (2009). A generic energy consumption model for decision making and energy efficiency optimisation in manufacturing. *International Journal of Sustainable Engineering*, *2*(2), 123–133. https://doi.org/10.1080/19397030902947041

[42] Budinoff, H., Bhinge, R., & Dornfeld, D. (2016). A material-general energy prediction model for milling machine tools. *2016 International Symposium on Flexible Automation (ISFA)*, *7*, 161–164. https://doi.org/10.1109/ISFA.2016.7790153

[43] Deng, Z., Zhang, H., Fu, Y., Wan, L., & Liu, W. (2017). Optimization of process parameters for minimum energy consumption based on cutting specific energy consumption. *Journal of Cleaner Production*, *166*, 1407–1414. https://doi.org/10.1016/j.jclepro.2017.08.022

[44] Kara, S., & Li, W. (2011). Unit process energy consumption models for material removal processes. *CIRP Annals*, *60*(1), 37–40. https://doi.org/10.1016/j.cirp.2011.03.018

[45] Li, W., & Kara, S. (2011). An empirical model for predicting energy consumption of manufacturing processes: A case of turning process. *Proceedings of the Institution of Mechanical Engineers, Part B: Journal of Engineering Manufacture*, *225*(9), 1636–1646. https://doi.org/10.1177/2041297511398541

[46] Eisele, C., Schrems, S., & Abele, E. (2011). Energy-Efficient Machine Tools through Simulation in the Design Process. In J. Hesselbach & C. Herrmann (Eds.), *Glocalized Solutions for Sustainability in Manufacturing* (Vol. 82, Issue 3, pp. 258–262). Springer Berlin Heidelberg. https://doi.org/10.1007/978-3-642-19692-8_45

[47] Abele, E., Sielaff, T., Schiffler, A., & Rothenbücher, S. (2011). Analyzing Energy Consumption of Machine Tool Spindle Units and Identification of Potential for Improvements of Efficiency. In J. Hesselbach & C. Herrmann (Eds.), *Glocalized Solutions for Sustainability in Manufacturing* (pp. 280–285). Springer Berlin Heidelberg. https://doi.org/10.1007/978-3-642-19692-8_49

[48] Schudeleit, T., Züst, S., Weiss, L., & Wegener, K. (2016). Machine Tool Energy Efficiency – A Component Mapping-Based Approach. *International Journal of Automation Technology*, *10*(5), 717–726. https://doi.org/10.20965/ijat.2016.p0717

[49] NARITA, H., KAWAMURA, H., NORIHISA, T., CHEN, L., FUJIMOTO, H., & HASEBE, T. (2006). Development of Prediction System for Environmental Burden for Machine Tool Operation. *JSME International Journal Series C*, *49*(4), 1188–1195. https://doi.org/10.1299/jsmec.49.1188

[50] Bi, Z. M., & Wang, L. (2012). Energy modeling of machine tools for optimization of machine setups. *IEEE Transactions on Automation Science and Engineering*, *9*(3), 607–613. https://doi.org/10.1109/TASE.2012.2195173

[51] Flum, D., Sossenheimer, J., Stück, C., & Abele, E. (2019). Towards Energy-Efficient Machine Tools Through the Development of the Twin-Control Energy Efficiency Module. In M. Armendia, M. Ghassempouri, E. Ozturk, & F. Peysson (Eds.), *Twin-Control* (pp. 95–110). Springer International Publishing. https://doi.org/10.1007/978-3-030-02203-7_5

[52] Herrmann, C., Thiede, S., Zein, A., Ihlenfeldt, S., & Blau, P. (2009). Perspective Energy Efficiency of Machine Tools : Extending the Perspective. *Energy*.

[53] Xue, H., Kumar, V., & Sutherland, J. W. (2007). Material flows and environmental impacts of manufacturing systems via aggregated input-output models. *Journal of Cleaner Production*, *15*(13–14), 1349–1358. https://doi.org/10.1016/j.jclepro.2006.07.007

[54] Kuhrke, B., Schrems, S., Eisele, C., & Abele, E. (2010). Methodology to assess the energy consumption of cutting machine tools. In *Proceedings of the 17th CIRP International Conference on Life Cycle Engineering (LCE 2010)* (pp. 67–82).

[55] Götze, U., Koriath, H. J., Kolesnikov, A., Lindner, R., & Paetzold, J. (2012). Integrated methodology for the evaluation of the energy- and cost-effectiveness of machine tools. *CIRP Journal of Manufacturing Science and Technology*, *5*(3), 151–163. https://doi.org/10.1016/j.cirpj.2012.04.001

[56] Schmitt, R., Bittencourt, J. L., & Bonefeld, R. (2011). Modelling Machine Tools for Self-Optimisation of Energy Consumption. In *Glocalized Solutions for Sustainability in Manufacturing* (pp. 253–257). Springer Berlin Heidelberg. https://doi.org/10.1007/978-3-642-19692-8_44

[57] Wu, Z., Hobgood, M., & Wolf, M. (2016). Energy Mapping and Optimization in Rough Machining of Impellers. *Volume 3: Joint MSEC-NAMRC Symposia*, V003T08A020. https://doi.org/10.1115/MSEC2016-8719

[58] Kant, G., & Sangwan, K. S. (2015). Predictive modelling for energy consumption in machining using artificial neural network. *Procedia CIRP*, *37*, 205–210. https://doi.org/10.1016/j.procir.2015.08.081

[59] Avram, O., Stroud, I., & Xirouchakis, P. (2011). A multi-criteria decision method for sustainability assessment of the use phase of machine tool systems. *International Journal of Advanced Manufacturing Technology*, *53*(5–8), 811–828. https://doi.org/10.1007/s00170-010-2873-2

[60] Bhinge, R., Park, J., Law, K. H., Dornfeld, D. A., Helu, M., & Rachuri, S. (2016). Toward a Generalized Energy Prediction Model for Machine Tools. *Journal of Manufacturing Science and Engineering*, *139*(4), 041013. https://doi.org/10.1115/1.4034933

[61] Mohammadi, A., Züst, S., Mayr, J., Blaser, P., Sonne, M. R., Hattel, J. H., & Wegener, K. (2017). A methodology for online visualization of the energy flow in a machine tool. *CIRP Journal of Manufacturing Science and Technology*, *19*, 138–146. https://doi.org/10.1016/j.cirpj.2017.08.003

[62] Zampou, E., Plitsos, S., Karagiannaki, A., & Mourtos, I. (2014). Towards a framework for energy-aware information systems in manufacturing. *Computers in Industry*, *65*(3), 419–433. https://doi.org/10.1016/j.compind.2014.01.007

[63] Vijayaraghavan, A., & Dornfeld, D. (2010). Automated energy monitoring of machine tools. *CIRP Annals - Manufacturing Technology*, *59*(1), 21–24. https://doi.org/10.1016/j.cirp.2010.03.042

[64] Verl, A., Westkämper, E., Abele, E., Dietmair, A., Schlechtendahl, J., Friedrich, J., Haag, H., & Schrems, S. (2011). Architecture for Multilevel Monitoring and Control of Energy Consumption. In J. Hesselbach & C. Herrmann (Eds.), *Glocalized Solutions for Sustainability in Manufacturing: Proceedings of the 18th CIRP International Conference on Life Cycle Engineering, Technische Universit{ä}t Braunschweig, Braunschweig, Germany, May 2nd - 4th, 2011* (pp. 347–352). Springer Berlin Heidelberg. https://doi.org/10.1007/978-3-642-19692-8_60

[65] Seevers, J.-P., Jurczyk, K., Meschede, H., Hesselbach, J., & Sutherland, J. W. (2020). Automatic Detection of Manufacturing Equipment Cycles using Time Series. *Journal of Computing and Information Science in Engineering*, *20*(June), 1–43. https://doi.org/10.1115/1.4046208

[66] Debnath, S., Reddy, M. M., & Yi, Q. S. (2014). Environmental friendly cutting fluids and cooling techniques in machining: A review. *Journal of Cleaner Production*, *83*, 33–47. https://doi.org/10.1016/j.jclepro.2014.07.071

[67] Adler, D. P., Hii, W. W.-S., Michalek, D. J., & Sutherland, J. W. (2006). EXAMINING THE ROLE OF CUTTING FLUIDS IN MACHINING AND EFFORTS TO ADDRESS ASSOCIATED ENVIRONMENTAL/HEALTH CONCERNS. *Machining Science and Technology*, *10*(1), 23–58. https://doi.org/10.1080/10910340500534282

[68] Dimartino, R. (2018). *EXXONMOBIL LAUNCHES ENHANCED RANGE OF CUTTING FLUIDS, MOBILCUT™-NEW*. https://www.ien.eu/article/exxonmobil-launches-enhanced-range-of-cutting-fluids-mobilcuttm-new/

[69] Kemet. (2021). *Metal Working Lubricants & Equipment*. https://kemet-international.com/sg/products/minimum-quantity-lubrication

[70] Diaz, N., Choi, S., Helu, M., Chen, Y. Y., Jayanathan, S., Yasui, Y., Kong, D., Pavanaskar, S., & Dornfeld, D. (2010). Machine Tool Design and Operation Strategies for Green Manufacturing. *Proceedings of 4th CIRP International Conference on High Performance Cutting, 2010*, 271–276. http://www.escholarship.org/uc/item/5gz7j6rn

[71] Kong, D., Choi, S., Yasui, Y., Pavanaskar, S., Dornfeld, D., & Wright, P. (2011). Software-based tool path evaluation for environmental sustainability. *Journal of Manufacturing Systems*, *30*(4), 241–247. https://doi.org/10.1016/j.jmsy.2011.08.005

[72] Li, L., Deng, X., Zhao, J., Zhao, F., & Sutherland, J. W. (2018). Multi-objective optimization of tool path considering efficiency, energy-saving and carbon-emission for free-form surface milling. *Journal of Cleaner Production*, *172*, 3311–3322. https://doi.org/https://doi.org/10.1016/j.jclepro.2017.07.219

[73] Schlechtendahl, J., Eberspächer, P., Schraml, P., Verl, A., & Abele, E. (2016). Multi-level Energy Demand Optimizer System for Machine Tool Controls. *Procedia CIRP*, *41*, 783–788. https://doi.org/10.1016/j.procir.2015.12.030

[74] Fang, K., Uhan, N. A., Zhao, F., & Sutherland, J. W. (2013). Flow shop scheduling with peak power consumption constraints. *Annals of Operations Research*, *206*(1), 115–145. https://doi.org/10.1007/s10479-012-1294-z

[75] Zhang, H., Zhao, F., Fang, K., & Sutherland, J. W. (2014). Energy-conscious flow shop scheduling under time-of-use electricity tariffs. *CIRP Annals - Manufacturing Technology*, *63*(1), 37–40. https://doi.org/10.1016/j.cirp.2014.03.011

[76] Fang, K., Uhan, N. A., Zhao, F., & Sutherland, J. W. (2016). Scheduling on a single machine under time-of-use electricity tariffs. *Annals of Operations Research*, *238*(1–2), 199–227. https://doi.org/10.1007/s10479-015-2003-5

[77] Sharma, A., Zhao, F., & Sutherland, J. W. (2015). Econological scheduling of a manufacturing enterprise operating under a time-of-use electricity tariff. *Journal of Cleaner Production*, *108*, 256–270. https://doi.org/10.1016/j.jclepro.2015.06.002

[78] Yin, R., Cao, H., Li, H., & Sutherland, J. W. (2014). A process planning method for reduced carbon emissions. *International Journal of Computer Integrated Manufacturing*, *27*(12), 1175–1186. https://doi.org/10.1080/0951192X.2013.874585

[79] Liu, Q., Zhan, M., Chekem, F. O., Shao, X., Ying, B., & Sutherland, J. W. (2017). A hybrid fruit fly algorithm for solving flexible job-shop scheduling to reduce manufacturing carbon footprint. *Journal of Cleaner Production*, *168*, 668–678. https://doi.org/10.1016/j.jclepro.2017.09.037

[80] Dai, M., Tang, D., Giret, A., Salido, M. A., & Li, W. D. (2013). Energy-efficient scheduling for a flexible flow shop using an improved genetic-simulated annealing algorithm. *Robotics and Computer-Integrated Manufacturing*, *29*(5), 418–429. https://doi.org/10.1016/j.rcim.2013.04.001

[81] Morad, N., & Zalzala, A. (1999). Genetic algorithms in integrated process planning and scheduling. *Journal of Intelligent Manufacturing*, *10*(2), 169–179. https://doi.org/10.1023/A:1008976720878

[82] Biel, K., Zhao, F., Sutherland, J. W., & Glock, C. H. (2018). Flow shop scheduling with grid-integrated onsite wind power using stochastic MILP. *International Journal of Production Research*, *56*(5), 2076–2098. https://doi.org/10.1080/00207543.2017.1351638

[83] Li, Y., He, Y., Wang, Y., Tao, F., & Sutherland, J. W. (2020). An optimization method for energy-conscious production in flexible machining job shops with dynamic job arrivals and machine breakdowns. *Journal of Cleaner Production*, *254*, 120009. https://doi.org/10.1016/j.jclepro.2020.120009

[84] Rossi, A., & Dini, G. (2000). Dynamic scheduling of FMS using a real-time genetic algorithm. *International Journal of Production Research*, *38*(1), 1–20. https://doi.org/002075400189545

[85] Rai, R., Kameshwaran, S., & Tiwari, M. K. (2002). Machine-tool selection and operation allocation in FMS: Solving a fuzzy goal-programming model using a genetic algorithm. *International Journal of Production Research*, *40*(3), 641–665. https://doi.org/00207540110081515

[86] Bensmaine, A., Dahane, M., & Benyoucef, L. (2013). A non-dominated sorting genetic algorithm based approach for optimal machines selection in reconfigurable manufacturing environment. *Computers and Industrial Engineering*, *66*(3), 519–524. https://doi.org/10.1016/j.cie.2012.09.008

[87] Kumar, A., Prakash, Tiwari, M. K., Shankar, R., & Baveja, A. (2006). Solving machine-loading problem of a flexible manufacturing system with constraint-based genetic algorithm. *European Journal of Operational Research*, *175*(2), 1043–1069. https://doi.org/10.1016/j.ejor.2005.06.025

[88] He, Y., Li, Y., Wu, T., & Sutherland, J. W. (2015). An energy-responsive optimization method for machine tool selection and operation sequence in flexible machining job shops. *Journal of Cleaner Production*, *87*(C), 245–254. https://doi.org/10.1016/j.jclepro.2014.10.006

[89] Winter, M., Li, W., Kara, S., & Herrmann, C. (2014). Determining optimal process parameters to increase the eco-efficiency of grinding processes. *Journal of Cleaner Production*, *66*, 644–654. https://doi.org/10.1016/j.jclepro.2013.10.031

[90] Berkeley, U. C., Aachen, R., Berkeley, U. C., Diaz, N., Helu, M., Jarvis, A., Tönissen, S., Dornfeld, D., Schlosser, R., Aachen, R., Berkeley, U. C., Aachen, R., Berkeley, U. C., Diaz, N., Helu, M., Jarvis, A., Tönissen, S., Dornfeld, D., Schlosser, R., & Aachen, R. (2009). Strategies for Minimum Energy Operation for Precision Machining. *Laboratory for Manufacturing and Sustainability*. http://www.escholarship.org/uc/item/794866g5

[91] Jiang, Z., Zhou, F., Zhang, H., Wang, Y., & Sutherland, J. W. (2015). Optimization of machining parameters considering minimum cutting fluid consumption. *Journal of Cleaner Production*, *108*, 183–191. https://doi.org/10.1016/j.jclepro.2015.06.007

[92] Oda, Y., Mori, M., Ogawa, K., Nishida, S., Fujishima, M., & Kawamura, T. (2012). Study of optimal cutting condition for energy efficiency improvement in ball end milling with tool-workpiece inclination. *CIRP Annals - Manufacturing Technology*, *61*(1), 119–122. https://doi.org/10.1016/j.cirp.2012.03.034

[93] Oda, Y., Kawamura, Y., & Fujishima, M. (2012). Energy Consumption Reduction by Machining Process Improvement. *Procedia CIRP*, *4*, 120–124. https://doi.org/10.1016/j.procir.2012.10.022

[94] Yildiz, A. R. (2013). Cuckoo search algorithm for the selection of optimal machining parameters in milling operations. *International Journal of Advanced Manufacturing Technology*, *64*(1–4), 55–61. https://doi.org/10.1007/s00170-012-4013-7

[95] Suresh, P. V. S., Venkateswara Rao, P., & Deshmukh, S. G. (2002). A genetic algorithmic approach for optimization of surface roughness prediction model. *International Journal of Machine Tools and Manufacture*, *42*(6), 675–680. https://doi.org/10.1016/S0890-6955(02)00005-6

[96] Quiza Sardiñas, R., Rivas Santana, M., & Alfonso Brindis, E. (2006). Genetic algorithm-based multi-objective optimization of cutting parameters in turning processes. *Engineering Applications of Artificial Intelligence*, *19*(2), 127–133. https://doi.org/10.1016/j.engappai.2005.06.007

[97] Cus, F., Zuperl, U., & Gecevska, V. (2008). Cnc end milling optimization using evolutionary computation. *Annals of DAAAM and Proceedings of the International DAAAM Symposium*, *42*, 347–348.

[98] Oktem, H., Erzurumlu, T., & Erzincanli, F. (2006). Prediction of minimum surface roughness in end milling mold parts using neural network and genetic algorithm. *Materials and Design*, *27*(9), 735–744. https://doi.org/10.1016/j.matdes.2005.01.010

[99] Jiang, Z., Zhang, H., & Sutherland, J. W. (2011). Development of multi-criteria decision making model for remanufacturing technology portfolio selection. *Journal of Cleaner Production*, *19*(17–18), 1939–1945. https://doi.org/10.1016/j.jclepro.2011.07.010

[100] Du, Y., & Li, C. (2014). Implementing energy-saving and environmental-benign paradigm: Machine tool remanufacturing by OEMs in China. *Journal of Cleaner Production*, *66*, 272–279. https://doi.org/10.1016/j.jclepro.2013.10.033

[101] Du, Y., Cao, H., Liu, F., Li, C., & Chen, X. (2012). An integrated method for evaluating the remanufacturability of used machine tool. *Journal of Cleaner Production*, *20*(1), 82–91. https://doi.org/10.1016/j.jclepro.2011.08.016

[102] Gontarz, A. M., Hänni, F., Weiss, L. B., & Wegener, K. (2013). Machine tool optimization strategies for ecologic and economic efficiency. *Proceedings of the Institution of Mechanical Engineers, Part B: Journal of Engineering Manufacture*, *227*(1), 54–61. https://doi.org/10.1177/0954405412464932

[103] Cai, L. G., Li, K., Cheng, Q., Qi, Z., & Gu, P. H. (2014). Adaptable design methodology of heavy duty machine tool for green remanufacturing. *Applied Mechanics and Materials*, *496–500*, 2672–2678. https://doi.org/10.4028/www.scientific.net/AMM.496-500.2672

[104] Haapala, K. R., Zhao, F., Camelio, J., Sutherland, J. W., Skerlos, S. J., Dornfeld, D. A., Jawahir, I. S., Clarens, A. F., & Rickli, J. L. (2013). A Review of Engineering Research in Sustainable Manufacturing. *Journal of Manufacturing Science and Engineering*, *135*(4), 041013. https://doi.org/10.1115/1.4024040

[105] Yoon, H. S., Kim, E. S., Kim, M. S., Lee, J. Y., Lee, G. B., & Ahn, S. H. (2015). Towards greener machine tools - A review on energy saving strategies and technologies. *Renewable and Sustainable Energy Reviews*, *48*, 870–891. https://doi.org/10.1016/j.rser.2015.03.100

[106] Santos, J. P., Oliveira, M., Almeida, F. G., Pereira, J. P., & Reis, A. (2011). Improving the environmental performance of machine-tools: Influence of technology and throughput on the electrical energy consumption of a press-brake. *Journal of Cleaner Production*, *19*(4), 356–364. https://doi.org/10.1016/j.jclepro.2010.10.009

[107] Azevedo, M., Oliveira, M., Pereira, J. P., & Reis, A. (2011). Comparison of two LCA Methodologies in the Machine-Tools Environmental Performance Improvement Process. In *Glocalized Solutions for Sustainability in Manufacturing* (pp. 575–580). Springer Berlin Heidelberg. https://doi.org/10.1007/978-3-642-19692-8_100

[108] Weinert, K., Inasaki, I., Sutherland, J. W., & Wakabayashi, T. (2004). Dry Machining and Minimum Quantity Lubrication. *CIRP Annals - Manufacturing Technology*, *53*(2), 511–537. https://doi.org/10.1016/S0007-8506(07)60027-4

[109] Devoldere, T., Dewulf, W., Deprez, W., Willems, B., & Duflou, J. R. (2007). Improvement Potential for Energy Consumption in Discrete Part Production Machines. *Advances in Life Cycle Engineering for Sustainable Manufacturing Businesses*, 311–316. https://doi.org/10.1007/978-1-84628-935-4_54

[110] Neugebauer, R., Wabner, M., Rentzsch, H., & Ihlenfeldt, S. (2011). Structure principles of energy efficient machine tools. *CIRP Journal of Manufacturing Science and Technology*, *4*(2), 136–147. https://doi.org/10.1016/j.cirpj.2011.06.017

[111] Ramani, K., Ramanujan, D., Bernstein, W. Z. Z. W. Z., Zhao, F., Sutherland, J., Handwerker, C., Choi, J.-K. J.-K., Kim, H., & Thurston, D. (2010). Integrated sustainable life cycle design: A Review. *Journal of Mechanical Design*, *132*(9), 910041–9100415. https://doi.org/10.1115/1.4002308

[112] Umeda, Y., Takata, S., Kimura, F., Tomiyama, T., Sutherland, J. W., Kara, S., Herrmann, C., & Duflou, J. R. (2012). Toward integrated product and process life cycle planning - An environmental perspective. *CIRP Annals - Manufacturing Technology*, *61*(2), 681–702. https://doi.org/10.1016/j.cirp.2012.05.004

[113] Jayal, A. D., Badurdeen, F., Dillon, O. W., & Jawahir, I. S. (2010). Sustainable manufacturing: Modeling and optimization challenges at the product, process and system levels. *CIRP Journal of Manufacturing Science and Technology*, *2*(3), 144–152. https://doi.org/10.1016/j.cirpj.2010.03.006

[114] Seow, Y., Goffin, N., Rahimifard, S., & Woolley, E. (2016). A "Design for Energy Minimization" approach to reduce energy consumption during the manufacturing phase. *Energy*, *109*, 894–905. https://doi.org/10.1016/j.energy.2016.05.099

[115] Huang, H., Zhang, L., Liu, Z., & Sutherland, J. W. (2011). Multi-criteria decision making and uncertainty analysis for materials selection in environmentally conscious design. *International Journal of Advanced Manufacturing Technology*, *52*(5–8), 421–432. https://doi.org/10.1007/s00170-010-2745-9

[116] Saidur, R. (2010). A review on electrical motors energy use and energy savings. *Renewable and Sustainable Energy Reviews*, *14*(3), 877–898. https://doi.org/10.1016/j.rser.2009.10.018

[117] Capehart, B. L., Kennedy, W. J., & Turner, W. C. (2016). Guide to Energy Management. In *Fairmont Press, Inc.* (Issues 8th Edition-International Version). Fairmont Press, Inc. https://app.knovel.com/hotlink/toc/id:kpGEMIVE0U/guide-energy-management/guide-energy-management

[118] Hicks, C. (2004). A genetic algorithm tool for designing manufacturing facilities in the capital goods industry. *International Journal of Production Economics*, *90*(2), 199–211. https://doi.org/10.1016/S0925-5273(02)00467-X

[119] *Auto Lightweighting*. (2021). mscsoftware.com/auto-lightweighting

[120] Kroll, L., Blau, P., Wabner, M., Frieß, U., Eulitz, J., & Klärner, M. (2011). Lightweight components for energy-efficient machine tools. *CIRP Journal of Manufacturing Science and Technology*, *4*(2), 148–160. https://doi.org/10.1016/j.cirpj.2011.04.002

[121] Herrmann, C., Dewulf, W., Hauschild, M., Kaluza, A., Kara, S., & Skerlos, S. (2018). Life cycle engineering of lightweight structures. *CIRP Annals*, *67*(2), 651–672. https://doi.org/10.1016/j.cirp.2018.05.008

[122] Dietmair, A., Zulaika, J., Sulitka, M., Bustillo, A., & Verl, A. (2010). Lifecycle impact reduction and energy savings through light weight eco-design of machine tools. *Proceedings of the 17th CIRP Conference on Life Cycle Engineering*, 105–110.

[123] Aggogeri, F., Borboni, A., Merlo, A., Pellegrini, N., & Ricatto, R. (2017). Vibration damping analysis of lightweight structures in machine tools. *Materials*, *10*(3). https://doi.org/10.3390/ma10030297

[124] Li, B., Hong, J., & Liu, Z. (2014). Stiffness design of machine tool structures by a biologically inspired topology optimization method. *International Journal of Machine Tools and Manufacture*, *84*, 33–44. https://doi.org/10.1016/j.ijmachtools.2014.03.005

[125] Zhao, L., Chen, W.-Y., Ma, J.-F., & Yang, Y.-B. (2008). Structural Bionic Design and Experimental Verification of a Machine Tool Column. *Journal of Bionic Engineering*, *5*(SUPPL.), 46–52. https://doi.org/10.1016/S1672-6529(08)60071-2

[126] Triebe, M. J., Zhao, F., & Sutherland, J. W. (2019). Achieving Energy Efficient Machine Tools by Mass Reduction through Multi-Objective Optimization. *Procedia CIRP*, *80*, 73–78. https://doi.org/10.1016/j.procir.2019.01.085

[127] Zhao, L., Ma, J., Wang, T., & Xing, D. (2010). Lightweight design of mechanical structures based on structural bionic methodology. *Journal of Bionic Engineering*, *7*(SUPPL.), S224–S231. https://doi.org/10.1016/S1672-6529(09)60239-0

[128] Ciurana, J., Quintana, G., & Garcia-Romeu, M. L. (2008). Estimating the cost of vertical high-speed machining centres, a comparison between multiple regression analysis and the neural networks approach. *International Journal of Production Economics*, *115*(1), 171–178. https://doi.org/10.1016/j.ijpe.2008.05.009

[129] LLNL. (2020). *Energy, Water, and Carbon Informatics*. https://flowcharts.llnl.gov/

[130] Fortune Business Insights. (2020). *Vertical Milling Machine Market Size, Share and Industry Analysis, By Type (Turret Mills, Bed Mills, and Others), By Application (Automotive, General Machinery, Precision Engineering, Transport Machinery, and Others) and Regional Forecasts, 2019-2026*. https://www.fortunebusinessinsights.com/vertical-milling-machine-market-102655

[131] Triebe, M. J., Mendis, G. P., Zhao, F., & Sutherland, J. W. (2018). Understanding Energy Consumption in a Machine Tool through Energy Mapping. *Procedia CIRP*, *69*, 259–264. https://doi.org/https://doi.org/10.1016/j.procir.2017.11.041

[132] Deb, K., Pratap, A., Agarwal, S., & Meyarivan, T. (2002). A fast and elitist multiobjective genetic algorithm: NSGA-II. *IEEE Transactions on Evolutionary Computation*, *6*(2), 182–197. https://doi.org/10.1109/4235.996017

[133] Broek, C. Ten, Singh, H., & Hillebrecht, M. (2012). Lightweight Design for the Future Steel Vehicle. *Auto Tech Review*, *1*(11), 24–30. https://doi.org/10.1365/s40112-012-0171-0

[134] Bian, J., Mohrbacher, H., Zhang, J. S., Zhao, Y. T., Lu, H. Z., & Dong, H. (2015). Application potential of high performance steels for weight reduction and efficiency increase in commercial vehicles. *Advances in Manufacturing*, *3*(1), 27–36. https://doi.org/10.1007/s40436-015-0102-9

[135] Gokhale, A. A., Prasad, E. N., & Biswajit, B. (2019). *Light Weighting for Defense, Aerospace, and Transportation* (A. A. Gokhale, N. E. Prasad, & B. Basu (Eds.)). Springer Singapore. https://doi.org/10.1007/978-981-15-1263-6

[136] Hirsch, J. (2011). Aluminium in innovative light-weight car design. *Materials Transactions*, *52*(5), 818–824. https://doi.org/10.2320/matertrans.L-MZ201132

[137] Tharumarajah, A., & Koltun, P. (2007). Is there an environmental advantage of using magnesium components for light-weighting cars? *Journal of Cleaner Production*, *15*(11–12), 1007–1013. https://doi.org/10.1016/j.jclepro.2006.05.022

[138] Soutis, C. (2005). Fibre reinforced composites in aircraft construction. *Progress in Aerospace Sciences*, *41*(2), 143–151. https://doi.org/10.1016/j.paerosci.2005.02.004

[139] Merklein, M., Johannes, M., Lechner, M., & Kuppert, A. (2014). A review on tailored blanks - Production, applications and evaluation. *Journal of Materials Processing Technology*, *214*(2), 151–164. https://doi.org/10.1016/j.jmatprotec.2013.08.015

[140] Benjamin, L., & Wang, N. (2010). The Boeing 787 dreamliner designing an aircraft for the future. *Journal of Young Investigators*, 34. https://www.jyi.org/2010-august/2010/8/6/the-boeing-787-dreamliner-designing-an-aircraft-for-the-future

[141] Möhring, H. C. (2017). Composites in Production Machines. *Procedia CIRP*, *66*, 2–9. https://doi.org/10.1016/j.procir.2017.04.013

[142] Neugebauer, R., Wabner, M., Ihlenfeldt, S., Frieß, U., Schneider, F., & Schubert, F. (2012). Bionics based energy efficient machine tool design. *Procedia CIRP*, *3*(1), 561–566. https://doi.org/10.1016/j.procir.2012.07.096

[143] Merlo, A., Ricciardi, D., Aggogeri, J., Meo, F., & Lay, L. Le. (2008). Application of composite materials for lightweight and smart structures design of high performance milling machines. *Proceedings of the 13th European Conference on Composite Materials*.

[144] Li, B., Hong, J., Wang, Z., Wu, W., & Chen, Y. (2012). Optimal design of machine tool bed by load bearing topology identification with weight distribution criterion. *Procedia CIRP*, *3*(1), 626–631. https://doi.org/10.1016/j.procir.2012.07.107

[145] Capehart, B. L., Turner, W. C., & Kennedy, W. J. (2006). *Guide to energy management* (5th ed.). Fairmont Press ; Distributed by CRC/Taylor & Francis.

[146] Triebe, M. J., Zhao, F., & Sutherland, J. W. (2021). Genetic Optimization for the Design of a Machine Tool Slide Table for Reduced Energy Consumption. *Journal of Manufacturing Science and Engineering*, *143*(10), 1–13. https://doi.org/10.1115/1.4050551

[147] He, K., Tang, R., Zhang, Z., & Sun, W. (2016). Energy Consumption Prediction System of Mechanical Processes Based on Empirical Models and Computer-Aided Manufacturing. *Journal of Computing and Information Science in Engineering*, *16*(4), 1–9. https://doi.org/10.1115/1.4033921

[148] Gutowski, T., Murphy, C., Allen, D., Bauer, D., Bras, B., Piwonka, T., Sheng, P., Sutherland, J., Thurston, D., & Wolff, E. (2005). Environmentally benign manufacturing: Observations from Japan, Europe and the United States. *Journal of Cleaner Production*, *13*(1), 1–17. https://doi.org/10.1016/j.jclepro.2003.10.004

[149] Luan, X., Zhang, S., Chen, J., & Li, G. (2019). Energy modelling and energy saving strategy analysis of a machine tool during non-cutting status. *International Journal of Production Research*, *57*(14), 4451–4467. https://doi.org/10.1080/00207543.2018.1436787

[150] Balogun, V. A., & Mativenga, P. T. (2013). Modelling of direct energy requirements in mechanical machining processes. *Journal of Cleaner Production*, *41*, 179–186. https://doi.org/10.1016/j.jclepro.2012.10.015

[151] Larek, R., Brinksmeier, E., Meyer, D., Pawletta, T., & Hagendorf, O. (2011). A discrete-event simulation approach to predict power consumption in machining processes. *Production Engineering*, *5*(5), 575–579. https://doi.org/10.1007/s11740-011-0333-y

[152] Avram, O. I., & Xirouchakis, P. (2011). Evaluating the use phase energy requirements of a machine tool system. *Journal of Cleaner Production*, *19*(6–7), 699–711. https://doi.org/10.1016/j.jclepro.2010.10.010

[153] Ferreira, F. J. T. E., & De Almeida, A. T. (2016). Overview on energy saving opportunities in electric motor driven systems - Part 1: System efficiency improvement. *Conference Record - Industrial and Commercial Power Systems Technical Conference*, *2016-June*, 1–8. https://doi.org/10.1109/ICPS.2016.7490219

[154] Sutherland, J. W., & DeVor, R. E. (1986). An improved method for cutting force and surface error prediction in flexible end milling systems. *Journal of Manufacturing Science and Engineering, Transactions of the ASME*, *108*(4), 269–279. https://doi.org/10.1115/1.3187077

[155] *Machining data handbook* (3d ed.). (1980). MDC.

[156] Cook, N. H. (1966). *Manufacturing Analysis*. Addison-Wesley Pub.

[157] Pang, L., Hosseini, A., Hussein, H. M., Deiab, I., & Kishawy, H. A. (2015). Application of a new thick zone model to the cutting mechanics during end-milling. *International Journal of Mechanical Sciences*, *96–97*, 91–100. https://doi.org/10.1016/j.ijmecsci.2015.03.015

[158] Hughes, A., & Drury, B. (2019). *Electric Motors and Drives: Fundamentals, Types and Applications* (5th ed.). Elsevier. https://doi.org/10.1016/C2017-0-03226-3

[159] Siemens. (2006). *Sinamics S120 Synchronous Motor 1FK7* (p. 48). https://cache.industry.siemens.com/dl/files/106/28683106/att_110828/v1/PFK7S_1206_en.pdf

[160] Burt, C. M., Piao, X., Gaudi, F., Busch, B., & Taufik, N. F. (2008). Electric Motor Efficiency under Variable Frequencies and Loads. *Journal of Irrigation and Drainage Engineering*, *134*(2), 129–136. https://doi.org/10.1061/(ASCE)0733-9437(2008)134:2(129)

[161] *Yeong Chin Machinery Industries Co., LTD.* (2021). https://www.ycmcnc.com/en

[162] IEA. (2021). *Electricity*. https://www.iea.org/fuels-and-technologies/electricity

[163] Gibson, L. J., & Ashby, M. F. (1999). *Cellular solids: structure and properties* (2nd ed., 1). Cambridge University Press.

[164] Abuthakeer, S. S., Mohanram, P. V, & Kumar, G. M. (2011). Structural redesigning of a cnc lathe bed to improve its static and dynamic characteristics. *Annals of Faculty Engineering Hunedoara*, *9*(3), 389–394.

[165] Suh, J. Do, Chang, S. H., Lee, D. G., Choi, J. K., & Park, B. S. (2001). Damping characteristics of composite hybrid spindle covers for high speed machine tools. *Journal of Materials Processing Technology*, *113*(1–3), 178–183. https://doi.org/10.1016/S0924-0136(01)00699-9

[166] Venugopal, P. R., Kalayarasan, M., Thyla, P., Mohanram, P., Nataraj, M., Mohanraj, S., & Sonawane, H. (2019). Structural investigation of steel-reinforced epoxy granite machine tool column by finite element analysis. *Proceedings of the Institution of Mechanical Engineers, Part L: Journal of Materials: Design and Applications*, *233*(11), 2267–2279. https://doi.org/10.1177/1464420719840592

[167] US EIA. (2020). *How much electricity does an American home use?* https://www.eia.gov/tools/faqs/faq.php?id=97&t=3

[168] Hu, L., Liu, Y., Peng, C., Tang, W., Tang, R., & Tiwari, A. (2018). Minimising the energy consumption of tool change and tool path of machining by sequencing the features. *Energy*, *147*, 390–402. https://doi.org/10.1016/j.energy.2018.01.046

[169] Ben Jdidia, A., Hentati, T., Hassine, H., Khabou, M. T., & Haddar, M. (2022). Optimization of the Electrical Energy Consumed by a Machine Tool for a Coupled and Uncoupled Cutting System. In *Lecture Notes in Mechanical Engineering* (pp. 288–300). Springer International Publishing. https://doi.org/10.1007/978-3-030-84958-0_31

[170] Jain, A., & Bajpai, V. (2020). Introduction to high-speed machining (HSM). In *High Speed Machining* (pp. 1–25). Elsevier. https://doi.org/10.1016/B978-0-12-815020-7.00001-1

[171] Can, A., Thiele, G., Kruger, J., Fisch, J., & Klemm, C. (2019). A practical approach to reduce energy consumption in a serial production environment by shutting down subsystems of a machine tool. *Procedia Manufacturing*, *33*, 343–350. https://doi.org/10.1016/j.promfg.2019.04.042

[172] Mori, K., Bergmann, B., Kono, D., Denkena, B., & Matsubara, A. (2019). Energy efficiency improvement of machine tool spindle cooling system with on–off control. *CIRP Journal of Manufacturing Science and Technology*, *25*, 14–21. https://doi.org/10.1016/j.cirpj.2019.04.003

[173] Zhao, J., Li, L., Nie, H., Chen, X., Liu, J., & Shu, X. (2021). Multi-objective integrated optimization of tool geometry angles and cutting parameters for machining time and energy consumption in NC milling. *International Journal of Advanced Manufacturing Technology*, *117*(5–6), 1427–1444. https://doi.org/10.1007/s00170-021-07772-2

[174] Kalpakjian, S., & Schmid, S. R. (2000). *Manufacturing engineering and technology* (S. R. Schmid (Ed.); 4th ed.) [Book]. Prentice Hall.

[175] Ashby, M. F. (2012). *Materials and the environment eco-informed material choice* (2nd ed.) [Book]. Butterworth-Heinemann.

[176] Allen, A. J., & Swift, K. G. (1990). Manufacturing Process Selection and Costing. *Proceedings of the Institution of Mechanical Engineers, Part B: Journal of Engineering Manufacture*, *204*(2), 143–148. https://doi.org/10.1243/PIME_PROC_1990_204_057_02

[177] IEA. (2020). *Iron and Steel*. https://www.iea.org/reports/iron-and-steel

[178] IEA. (2020). *Tracking Industry 2020*. https://www.iea.org/reports/tracking-industry-2020

[179] Worldsteel Association. (2019). *Steel Statistical Yearbook 2019*. https://www.worldsteel.org/steel-by-topic/statistics/steel-statistical-yearbook.html

[180] Sherif, Y. S., & Kolarik, W. J. (1981). Life cycle costing: Concept and practice. *Omega*, *9*(3), 287–296. https://doi.org/10.1016/0305-0483(81)90035-9

[181] Bengtsson, M., & Kurdve, M. (2016). Machining Equipment Life Cycle Costing Model with Dynamic Maintenance Cost. *Procedia CIRP*, *48*, 102–107. https://doi.org/10.1016/j.procir.2016.03.110

[182] Saccani, N., Perona, M., & Bacchetti, A. (2017). The total cost of ownership of durable consumer goods: A conceptual model and an empirical application. *International Journal of Production Economics*, *183*(December 2012), 1–13. https://doi.org/10.1016/j.ijpe.2016.09.021

[183] Roda, I., Macchi, M., & Albanese, S. (2020). Building a Total Cost of Ownership model to support manufacturing asset lifecycle management. *Production Planning and Control*, *31*(1), 19–37. https://doi.org/10.1080/09537287.2019.1625079

[184] Heilala, J., Helin, K., & Montonen, J. (2006). Total cost of ownership analysis for modular final assembly systems. *International Journal of Production Research*, *44*(18–19), 3967–3988. https://doi.org/10.1080/00207540600806448

[185] Anderberg, S. E., Kara, S., & Beno, T. (2010). Impact of energy efficiency on computer numerically controlled machining. *Proceedings of the Institution of Mechanical Engineers, Part B: Journal of Engineering Manufacture*, *224*(4), 531–541. https://doi.org/10.1243/09544054JEM1712

[186] Wang, P., & Liang, M. (2005). An integrated approach to tolerance synthesis, process selection and machining parameter optimization problems. *International Journal of Production Research*, *43*(11), 2237–2262. https://doi.org/10.1080/00207540500050063

[187] Chen, S., & Keys, L. K. (2009). A cost analysis model for heavy equipment. *Computers and Industrial Engineering*, *56*(4), 1276–1288. https://doi.org/10.1016/j.cie.2008.07.015

[188] Thokala, P., Scanlan, J., & Chipperfield, A. (2010). Life cycle cost modelling as an aircraft design support tool. *Proceedings of the Institution of Mechanical Engineers, Part G: Journal of Aerospace Engineering*, *224*(4), 477–488. https://doi.org/10.1243/09544100JAERO574

[189] Roth, R., Clark, J., & Kelkar, A. (2001). Automobile bodies: Can aluminum be an economical alternative to steel? *Jom*, *53*(8), 28–32. https://doi.org/10.1007/s11837-001-0131-7

[190] *MetalsDepot*. (2021). https://www.metalsdepot.com

VITA

Matthew J. Triebe

EDUCATION

- **Doctor of Philosophy,** Environmental and Ecological Engineering December 2021
  Purdue University, West Lafayette, IN, USA
  Major Professors: Dr. John W. Sutherland & Dr. Fu Zhao
  Research Focus: Designing machine tools for reduced energy consumption via lightweighting

- **Master of Science,** Environmental and Ecological Engineering May 2020
  Purdue University, West Lafayette, IN, USA

- **Bachelor of Science,** Mechanical Engineering December 2010
  Purdue University, West Lafayette, IN, USA

INDUSTRY EXPERIENCE

Design Quality Engineer April 2014 to December 2015
Butler Aerospace & Defense, West Lafayette, IN

Airframe Design Engineer August 2012 to April 2014
Butler Aerospace & Defense, West Lafayette, IN

Project Engineer October 2013 to November 2013
Butler Aerospace & Defense, West Lafayette, IN

Transmission Engineer April 2012 to August 2012
Butler Aerospace & Defense, West Lafayette, IN

Supplier Support Engineer August 2011 to April 2012
Butler Aerospace & Defense, West Lafayette, IN

TEACHING/MENTORING EXPERIENCE

EEE 43000 Industrial Ecology and LCA Teaching Assistant January to April 2020/21
Purdue University, West Lafayette, IN

Summer Undergraduate Research Fellowship Mentor May to August 2020
Purdue University, West Lafayette, IN

LEADERSHIP EXPERIENCE

Environmental and Ecological Engineering Graduate Student Organization (EEEGSO)
Inaugural EEEGSO President August 2016 to July 2018
Purdue University, West Lafayette, IN

AWARDS/FELLOWSHIPS

COVID Relief Fellowship May 2021
Graduate School, Purdue University

Estus H. And Vashti L. Magoon Award for Excellence in Teaching March 2021
Purdue University

Italian Machine Tool Technology Award November 2019
Italian Trade Agency, Milan, Italy

Outstanding Service Scholarship April 2018
Purdue University

People's Choice Award March 2016
Science on Tap, Lafayette, IN

PUBLICATIONS

Li, L., Huang, H., Liu, Z., Li, X., **Triebe, M. J.**, and Zhao, F., "An energy-saving method to solve the mismatch between installed and demanded power in hydraulic press," *Journal of Cleaner Production,* 139, 2016, pp. 636-645.

Li, L., Huang, H., Zhao, F., **Triebe, M. J.**, and Liu, Z., "Analysis of a novel energy-efficient system with double-actuator for hydraulic press," *Mechatronics,* 47, 2017, pp. 77-87.

Triebe, M. J., Mendis, G. P., Zhao, F., and Sutherland, J. W., "Understanding energy consumption in a machine tool through energy mapping," *Proceedings of the 25th CIRP on Life Cycle Engineering,* Denmark, Apr 2018, pp. 259-264.

Ren, Y., Zhang, C., Zhao, F., **Triebe, M. J.**, and Meng, L., "An MCDM-Based Multiobjective General Variable Neighborhood Search Approach for Disassembly Line Balancing Problem," *IEEE Transactions on Systems, Man, and Cybernetics: Systems,* 2018, pp. 1-14.

Triebe, M. J., Zhao, F., and Sutherland, J. W., "Achieving Energy Efficient Machine Tools by Mass Reduction through Multi-Objective Optimization," *Proceedings of the 26th CIRP on Life Cycle Engineering,* Purdue University, May 2019, pp. 73-78.

Lee, W. J., Mendis, G. P., **Triebe, M.J.**, Sutherland, J. W., "Monitoring of a machining process using kernel principal component analysis and kernel density estimation," *Journal of Intelligent Manufacturing,* 31(5), 2019, pp. 1175-1189

Triebe, M. J., Zhao, F., Sutherland, J. W., "Genetic Optimization for the Design of a Machine Tool Slide Table for Reduced Energy Consumption," *Journal of Manufacturing Science and Engineering,* 143(10), 2021, pp. 101003-101012

Triebe, M. J., Zhao, F., Sutherland, J. W., "Development of a cost model for vertical milling machines cost to assess impact of lightweighting," *Journal of Manufacturing and Materials Processing,* 5(4), 2021, pp. 129

Triebe, M. J., Zhao, F., Sutherland, J. W., "Modelling the effect of slide table mass on machine tool energy consumption: the role of lightweighting," *Journal of Manufacturing Systems,* Under review